Wave Propagation in Relativistic Electron-Positron Plasmas

Caron Elizabeth Rooney B.Sc.

Thesis
submitted to the
University of Glasgow
for the degree
of Ph.D.

Department of Physics and Astronomy,
Kelvin Building,
Glasgow University,
Glasgow, G12 8QQ.

May 31, 1995

ProQuest LLC.
789 East Eisenhower Parkway
P.O. Box 1346
Ann Arbor, MI 48106 – 1346

To Mum, Dad and Saad

for all their

love and support

Oor universe is like an e'e
Turned in, man's benmaist hert to see,
And swamped in subjectivity.
But whether it can use its sicht
To bring what lies withoot to licht
The answer's still ayont my micht.
Hugh Macdiarmid

Abstract

The study of wave propagation in a plasma provides an invaluable insight into the plasma's fundamental behaviour and structure. In this thesis we study wave propagation in relativistic electron-positron plasmas. The effects of the mass symmetry of the two species on the plasma system are investigated in a regime where the energy of the plasma particles is of the same order of magnitude as their rest energy.

In chapter one we give a brief review of the field of modern plasma physics. We then introduce the concept of an equal-mass plasma, paying particular attention to the specific case of an electron-positron plasma, before giving an overview of the astrophysical situations where electron-positron plasmas are thought to play an important role.

Chapter two sets out the system of equations required to describe a plasma. Starting from a statistical description of every particle in the plasma, we derive the relativistic Vlasov equation; a kinetic equation which determines the behaviour of a particular species in the plasma in the absence of close particle collisions. Finally, we derive the components of the dielectric tensor for a general plasma system, using a relativistic analysis throughout.

The case of a cold, relativistically-streaming plasma system is studied in chapter three. Dispersion relations are determined for both counterstreaming electron-electron beams and electron-positron beams. For the case of waves propagating parallel to the equilibrium magnetic field, both longitudinal and transverse modes are investigated. We find that the longitudinal mode, which leads to the two-stream instability, is the same for both plasma systems but, for the transverse mode, there is an instability present in the electron-positron plasma that is completely absent in the electron-electron plasma.

In chapter four the case of a thermal plasma is considered. In equilibrium, the distribution function is given the form of a relativistic Maxwellian. We follow a similar procedure to that used in chapter three to obtain dispersion relations

for waves propagating perpendicularly to the equilibrium magnetic field. These dispersion equations, however, contain insoluble numerical expressions which require the use of numerical techniques to find the roots to the relations. The main body of work in this chapter involves setting out the techniques we use to find the roots of these dispersion relations. A review of the perpendicular wave modes which occur in non-relativistic Maxwellian plasmas is included before the results for the relativistic Maxwellian plasma are presented and compared with the non-relativistic case.

In chapter five we present a summary of our results along with some concluding remarks and a few suggestions for possible extensions to the work presented here.

The original work of this thesis is contained in chapters three and four.

Acknowledgments

The work carried out in this thesis was funded by a grant from the SERC (and latterly by the EPSRC) and I am grateful to the council for its financial support. During my studies I was a member of the Astronomy and Astrophysics Group in the Department of Physics and Astronomy here at the University of Glasgow. I would like to thank the group, and the department as a whole, for providing me with the facilities and support needed to complete my studies.

I am grateful to my supervisor Professor Ernest Laing for his help and guidance throughout my studies. I only hope that some of his knowledge of physics has rubbed off. My thanks also to Declan, Jack, Saad and David K for their many helpful discussions on the tricky subjects of plasmas and computers.

Thanks must also go to my office-mates David R, Jack, Saad and David K for not complaining *too* much about my endless computer runs, my untidy desk and my Extreme posters. Also to the remaining members of the Coffee Club: Graeme, Gary, Gerry, Brian, Luke, Andrew, Gordon, Douglas, Stephen, Paul and Susan and others: Carolyn, Christine, Kenneth and Alistair for their general good humour, witty conversations and terrible jokes. No thanks go to those people who always forgot to turn up to make coffee when they were supposed to - they know who they are!

A special thanks must go to my mum and dad for their support throughout all stages of my academic studies. I hope they think it was all worth it. Finally I would like to thank Saad for proofreading the thesis and for being there when I needed him.

Contents

1 Introduction **7**

1.1 Plasma Physics 7

1.2 Equal-mass Plasmas 9

1.3 Electron-Positron Plasmas 10

1.3.1 Electron-Positron Plasmas In Nature 10

1.3.2 Pair Annihilation and Creation 14

2 Derivation of the Kinetic Equations **17**

2.1 Phase Space Formalism and Liouville's Equation 17

2.2 Uncorrelated Particles 20

2.3 Validity of Vlasov Approximation 22

2.4 Relativistic Formulation of the Vlasov Equation 23

2.5 The Maxwell Equations 24

2.6 Derivation of the Dielectric Tensor 25

2.6.1 The System of Equations 26

2.6.2 Linear Analysis 27

3 Cold Relativistic Streaming Plasmas **32**

3.1 Introduction 32

3.2 Wave Propagation Parallel to the Magnetic Field 34

3.3 Specification of the Plasma System 35

3.4 The Longitudinal Mode 36

3.4.1 Electron-Electron Streams 37

3.4.2 Non-relativistic Beams 37
3.4.3 Electron-Positron Streams 38
3.5 The Transverse Mode 38
3.5.1 Electron-Electron Streams 38
3.5.2 Electron-Positron Streams 39
3.5.3 Investigation of the Dispersion Functions 40
3.5.4 Results 40

4 Wave Propagation in Relativistic Thermal Plasmas **65**
4.1 The Distribution Function 66
4.2 Wave Propagation Perpendicular to the Magnetic Field 67
4.3 Electron-Positron Plasmas 68
4.4 Singular Points 73
4.4.1 Case (i) : $\frac{n}{\tilde{\omega}} \geq 1$ 75
4.4.2 Case (ii) : $\frac{n}{\tilde{\omega}} < 1$ 83
4.5 Numerical Evaluation of the Integrals 84
4.5.1 Splitting The Range of Integration 85
4.5.2 Evaluation of the Bessel Functions 88
4.6 The Integration Code 89
4.7 Non-relativistic Thermal Plasmas 91
4.7.1 The Bernstein Modes 92
4.7.2 The Extraordinary Mode 94
4.7.3 The Ordinary Mode 94
4.8 Results for a Relativistic Thermal Plasma 95
4.9 Comparison with the Non-relativistic Case 96

5 Conclusions and Future Work **109**

A Bessel Function Identities **113**

B Contour Integration **115**
B.1 Landau's Contour 116

C Simpson's Rule 121

D Integration Code 123

List of Tables

3.1 Roots of $\hat{F}_{ee} = 0$ 42
3.2 Roots of $\hat{F}_{ep} = 0$ 43
3.3 The range of η values for which the instability is present for given $u\,\hat{k}$ values. 45

List of Figures

3.1 The function $f(b) = 1 + b^2 - (1 + 4\,b^2)^{1/2}$ plotted against b. 47

3.2 The function $f(\eta, k = 1)$ plotted as a function of η. 48

3.3 The function $f(\eta, k = 3)$ plotted as a function of η. 49

3.4 The function $\hat{F}(\hat{\omega})$ plotted against $\hat{\omega}$ for $u\,k = 0.5$ and $\eta = 15$. . . . 50

3.5 The function $\hat{F}(\hat{\omega})$ plotted against $\hat{\omega}$ for $u\,k = 0.5$ and $\eta = 1$. 51

3.6 The function $\hat{F}(\hat{\omega})$ plotted against $\hat{\omega}$ for $u\,k = 0.5$ and $\eta = 0.1$. . . . 52

3.7 The function $\hat{F}(\hat{\omega})$ plotted against $\hat{\omega}$ for $u\,k = 0.9$ and $\eta = 15$. . . . 53

3.8 The function $\hat{F}(\hat{\omega})$ plotted against $\hat{\omega}$ for $u\,k = 0.9$ and $\eta = 1$. 54

3.9 The function $\hat{F}(\hat{\omega})$ plotted against $\hat{\omega}$ for $u\,k = 0.9$ and $\eta = 0.1$. . . . 55

3.10 The function $\hat{F}(\hat{\omega})$ plotted against $\hat{\omega}$ for $u\,k = 1$ and $\eta = 15$. 56

3.11 The function $\hat{F}(\hat{\omega})$ plotted against $\hat{\omega}$ for $u\,k = 1$ and $\eta = 1$. 57

3.12 The function $\hat{F}(\hat{\omega})$ plotted against $\hat{\omega}$ for $u\,k = 1$ and $\eta = 0.1$. 58

3.13 The function $\hat{F}(\hat{\omega})$ plotted against $\hat{\omega}$ for $uk = 1.1$ and $\eta = 15$. 59

3.14 The function $\hat{F}(\hat{\omega})$ plotted against $\hat{\omega}$ for $uk = 1.1$ and $\eta = 1$. 60

3.15 The function $\hat{F}(\hat{\omega})$ plotted against $\hat{\omega}$ for $uk = 1.1$ and $\eta = 0.1$. . . . 61

3.16 The function $\hat{F}(\hat{\omega})$ plotted against $\hat{\omega}$ for $uk = 1.5$ and $\eta = 15$. 62

3.17 The function $\hat{F}(\hat{\omega})$ plotted against $\hat{\omega}$ for $uk = 1.5$ and $\eta = 1$. 63

3.18 The function $\hat{F}(\hat{\omega})$ plotted against $\hat{\omega}$ for $uk = 1.5$ and $\eta = 0.1$. . . . 64

4.1 The range of the $u_\perp$-integral split into its various sub-intervals for (a) m_{crit} odd and (b) m_{crit} even. 99

4.2 The range of the x-integral split into its various sub-intervals for (a) q_1 odd and (b) q_1 even. 100

4.3 The Bernstein modes for a non-relativistic electron-positron plasma with $\eta = 5^{1/2}$. 101
4.4 The relativistic dispersion curves for $a = 10$. 102
4.5 The relativistic dispersion curves for $a = 5$. 103
4.6 The relativistic dispersion curves for $a = 2$. 104
4.7 The relativistic dispersion curves for $a = 1$. 105
4.8 The relativistic dispersion curves for $a = 0.5$. 106
4.9 The relativistic dispersion curves for $a = 0.2$. 107
4.10 The relativistic dispersion curves for $a = 0.1$. 108

B.1 (a) represents a closed contour C over which the function f is integrated and (b) represents a similar curve which has a simple pole lying on the real axis. 119
B.2 The contours C_1 and C_2, where C_2 represents the Landau contour. . 120

Chapter 1

Introduction

> It is the great beauty of our science that advancement in it, whether in a degree great or small, instead of exhausting the subject of research, opens the doors to further and more abundant knowledge, overflowing with beauty and utility
> *Michael Faraday*

1.1 Plasma Physics

Plasma physics is the study of the behaviour and properties of ionised gases. It is a relatively new scientific discipline; the first detailed laboratory studies of plasmas were made only in the first half of this century. Over the last fifty years, however, our knowledge of the plasma state has increased immeasurably, mainly due to the effort put into harnessing nuclear fusion as a possible energy source.

Nuclear fusion is the process by which light atomic nuclei come together to form heavier nuclei, releasing large amounts of energy as they do so. It is the source of energy in the sun and other stars. Large experiments, such as JET, have been built to try and emulate the conditions inside these stars by producing plasmas at temperatures of $10^8 K$. They utilise immensely complicated magnetic confinement systems in an attempt to maintain the plasma long enough for fusion reactions to take place. Recent results with deuterium-tritium plasmas have been promising and the scientists involved are now looking forward to the next generation of bigger,

more *reactor-like* machines. A completely different approach in the search for nuclear fusion is that of inertial confinement. This involves the ablation of a small deuterium-tritium pellet by ultra-powerful laser beams. As the core of the pellet is compressed, the temperature may rise sufficiently to enable fusion to occur. Behind the more obvious technological advances made by these experiments, a vast amount of theoretical work has been carried out in an attempt to understand the behaviour of the plasmas contained in these machines. Without this understanding it would be impossible to predict or attempt to control the plasma behaviour.

In recent years, plasma physics in the laboratory has no longer been confined to fusion research. Many industrial applications have been found for plasmas, which can be grouped together under the heading *plasma processing*, a review of which is given by Johnson [1]. Key areas to benefit from plasma technology include modern industries like semiconductor fabrication, where plasmas are used to etch surfaces and deposit thin films in the manufacture of integrated circuits, traditional industries which make use of plasma arcs in the welding and cutting of metals and the novel use of plasmas in waste management. Here plasmas can be used to treat the emissions of nitrogen and sulphur dioxide from power stations as well as solid refuse, both household and potentially hazardous industrial waste, decreasing the impact of such waste on the environment. Plasma processes, in addition to being cleaner, are mainly more effective than their traditional, chemical-based counterparts and if the problem of higher costs can be overcome should prove to be an increasingly important tool in certain industrial applications.

The plasmas which exist on earth are almost exclusively man-made (the most notable exception is lightning), and out of the four states of matter plasma is the least common. For this reason the earth, along with the other planets in the solar system, is rather exceptional, as it is now commonly accepted that over 99.9% of the observable universe is in the plasma state. Plasma physics must therefore play an important role in our understanding of the universe, from the workings of an individual star to the formation of the universe as a whole. Plasmas exist over all length scales: from the magnitude of the solar wind and the earth's magnetosphere to the far-reaching effects of the intergalactic plasma. The subject of astrophysical

plasmas will be dealt with in more detail in Section 1.3.1.

1.2 Equal-mass Plasmas

An equal-mass plasma is one in which the two species are made up of particles of equal mass and charge that is equal in magnitude but opposite in sign. These plasmas are far removed from the usual electron-ion plasmas in which $m_e << m_i$, leading to the electron and ion dynamics having quite distinct properties. One species will usually dominate over the other, eg in the high-frequency regime the ions are assumed to form a static uniform background and only the electron motion is important and in the low-frequency regime the electrons are thought of as a uniform massless frictionless fluid and the ion motion dominates. For an equal-mass plasma the symmetry of the components ensures that each species is equally important and must be included for all frequency regimes; the problem can thus no longer be simplified to a one-component plasma. The mass symmetry, however, should introduce simplifications of its own. Earlier work in this relatively unexplored field includes Stewart & Laing [2], who have shown that phenomena like Faraday rotation and whistler modes are not seen in equal-mass plasmas, and Abdul-Rassak & Laing [3], who have found that several transport coefficients indeed vanish due to the symmetry present.

Plasmas that contain positive and negative ions which differ in mass only by a very small amount can be approximated to equal-mass. One such example is an $H^- - H^+$ plasma, where the mass difference is just two electron masses. This type of plasma was first considered by Imshennik et al. [4] whose analysis of beams of positive and negative ions of the same mass was backed up with experiments on positive and negative hydrogen ion beams. In a more recent experiment, a laser was used to irradiate a uranium target producing UO_2^+ and UO_3^- ions. As the mass difference is small compared to the ion masses, this too can be approximated to an equal-mass plasma.

An exact equal-mass plasma has a very specific form, that of a particle / anti-particle plasma. Here the mass ratio of the species is exactly unity. In this thesis we

will deal almost exclusively with one particular example of an equal-mass plasma, namely that of an electron-positron plasma. These will be described more fully in the next section.

1.3 Electron-Positron Plasmas

Due to their rather exotic nature, electron-positron plasmas are only found in energetic surroundings. Such environments do not exist in the vicinity of the earth, although some suitable astrophysical applications have been put forward. To study these plasmas at close hand would require the manufacture of electrons and positrons in the laboratory . As there were no obvious commercial applications associated with electron-positron plasmas this has been a rather neglected area of research in past years. It is only recently that scientists have started to explore the possibility of producing and storing positrons in the laboratory to examine their plasma properties. It is envisaged that experiments could be set up to inject an electron beam into a positron plasma to investigate the electron-positron beam-plasma instability as discussed by Surko [5]. More advanced experiments might hope to maintain actual electron-positron plasmas long enough for their behaviour to be studied.

1.3.1 Electron-Positron Plasmas In Nature

Before the recent laboratory experiments, scientists had to look further afield in their search for electron-positron plasmas. As a result, the subject has received far more attention from astrophysicists than from the plasma physics community and it is thought to play an important role in several astrophysical situations. When electrons and positrons occur together in sufficient numbers, it is likely that many pairs will annihilate to form $\gamma-$rays at an energy of $0.511\ MeV$, which is equivalent to the rest-mass energy of an electron (and positron). So, if an emission line at this energy is observed it would be a clear indication that electrons and positrons are present. If the source of the emissions could be identified then an attempt could be made to study their nature, in particular to see whether or not the particles are exhibiting any plasma-like behaviour.

On some occasions astrophysical models are put forward which require the existence of electron-positron pairs, which are likely to be acting like a plasma, despite no observational evidence to this effect.

A brief review of electron-positron plasmas in astrophysical contexts follows, including examples illustrating both of the above points.

The Galactic Centre

A radiation line at $0.511 MeV$ has been discovered in the direction of the galactic centre [6]. If the radiation emanates from the centre itself, it could suggest the presence of a massive black hole. An alternative proposal is that the source of the radiation could be a supernova lying along our line of sight. Scientists at the moment are unsure which is the more likely solution but whichever model is correct, there is a strong likelihood that electron-positron pairs are present in the vicinity of the source of the radiation. Annihilation radiation has also been observed from gamma-ray bursters. However, the energy of this radiation is less than the rest-mass energy of an electron. If these gamma-ray bursters are assumed to be some sort of compact objects, like neutron stars at large astronomical distances from the earth, then the energy could have been lowered by a gravitational red-shift.

Black Holes and Extragalactic Jets

Quantum mechanics tells us that a vacuum is made up of a complex array of virtual particles; continuously being created, they interact and annihilate over very short timescales. If the vacuum sits in a large external electric or magnetic field then it is possible that some of these virtual particles *borrow* enough energy from the field to become real (or long-lived).

The creation of particles from vacuum by an external field is thought to occur in the vicinity of a black hole, as discussed in Novikov & Frolov [7]. One natural product of this particle creation is electron-positron pairs. These pairs are thought to play an important role in the large parsec-scale jets which are observed to flow out from the centre of active galaxies, which themselves are thought to contain supermassive black holes.

Some of the pairs created will obviously just annihilate again but others will survive for longer periods of time. The annihilation rate depends not just on the particle density but also on the conditions in the area surrounding the black hole and the energy of the particles; if the pairs are relativistic then the annihilation cross-section is smaller than if they had been non-relativistic. So, given enough energy, it is likely that many of the pairs will survive long enough to be forced into the outflowing jets, probably by radiation pressure. More details of this model are given in Ghisellini [8].

Observations of these jets indicate that they are highly polarised. This result causes problems for models that take the main constituents of the jets to be electrons and protons because linearly polarised waves travelling through these plasmas undergo Faraday rotation. This corresponds to a rotation in space of their plane of polarisation and leads to a depolarisation of the waves. If we thus assume that the jets are dominated by electron-proton plasmas, then the high degree of polarisation observed puts a strong constraint on the maximum particle density in the plasmas to minimise the effects of the Faraday rotation. However, as already mentioned above, Stewart & Laing [2] have proven that Faraday rotation does not occur in electron-positron plasmas . So a dominance of electron-positron pairs in the jets should prove to be more consistent with the observational data.

Plasma instabilities in the electron-positron beams present in extragalactic jets have also merited some attention. Achatz & Schlickeiser [9] have investigated the stability of such plasmas for electromagnetic wave propagation. They assume a cold electron-positron beam moving with a relativistic velocity through a cold electron-proton background plasma. They obtain the dispersion relation for electromagnetic waves and carry out a stability analysis. Their results indicate that the electron-positron beam is unstable only for small beam densities. At these weak densities there is little interaction between the electrons and positrons but each species can instigate a separate instability. The analysis carried out is similar in some respects to that carried out in Chapter 3. There we use the same cold-stream description to specify the form of the plasma. Our plasma configuration, however, is different; it consists of counterstreaming electron and positron beams without the presence of a

background plasma rather than the single beam described above.

Pulsars

In some astrophysical situations electrons and positrons are thought to exist together, even though there is no evidence of a $0.511\ MeV$ emission line. One example of this is a pulsar. Pulsars are thought to be one of the most likely environments for finding electron-positron plasmas. Although there is no direct evidence for this hypothesis, the indirect evidence is quite substantial.

Ruderman and Sutherland [10] were amongst the first authors to postulate the existence of electron-positron plasmas in this context. A pulsar is a rapidly spinning neutron star, thought to be the remnant of a supernova explosion. Due to conservation of magnetic flux during the star's collapse the pulsar will possess an extremely large magnetic field of the order of $10^8 - 10^{12}\,T$. Since the magnetic field corotates with the star, a correspondingly large electric field, $\mathbf{v} \times \mathbf{B}$, is induced in the star's magnetosphere. The fields present are strong enough to pull electrons off the surface of the star. These electrons are then accelerated along the curved magnetic field lines; any motion normal to the magnetic field is quickly damped because of the huge energy losses through synchrotron radiation. Since the field lines are curved the electrons emit radiation in the form of γ-rays that are energetic enough for pair creation. This radiation is known as curvature radiation and is similar to synchrotron radiation. The resulting pairs will also start to move along the field lines and the process is repeated. This should result in an abundance of electron-positron pairs being present in the pulsar's magnetosphere. A considerable amount of work has been done on the study of electron-positron pairs in super-strong magnetic fields, with direct relevance to the likely conditions in pulsar magnetospheres, including the work by Arons & Barnard [11] and Ray & Benford [12].

The intensity of the radio emissions observed from pulsars suggests that the radiation was produced in a coherent manner. This would be possible if the electrons (and similarly the positrons) were bunched together, which points to the likelihood of the particles behaving like a plasma in so far as several plasma instabilities result in a bunching together of the plasma particles. Due to the remoteness of the pulsars,

accurate details of the plasma systems are scarce and many different models for the plasma instabilities involved have been put forward without any real consensus on which is the most likely. Ruderman & Sutherland [10] put forward the proposition that the particle bunching is the result of a two-stream instability caused by a highly relativistic stream of positrons passing through a less relativistic pair plasma. Cheng & Ruderman [13] and Asseo et al [14], on the other hand, have both put forward the proposal that the most important process is the two-stream instability resulting from the relative motion of the electrons and positrons in the neutral pair plasma along the field lines. In most of the papers produced on this subject, there seemed to be a lack of detailed plasma-based analysis in the models and this was one of our main motivations in trying to establish a solid analytical base for our investigations into relativistic electron-positron plasmas.

1.3.2 Pair Annihilation and Creation

One of the most immediately striking aspects of an electron-positron plasma is the existence of particle / anti-particle pairs. A great deal of effort has been put into studying the effects of particle collisions on the equilibrium state of such plasmas. In fact, the particle nature of electron-positron plasmas has received just as much, or even more, attention than their *plasma behaviour.*

Lightman & Band [15] investigated radiation mechanisms in relativistic thermal plasmas to find in which temperature regimes processes like particle creation or annihilation are important. If these reactions prove to be significant then they could seriously affect the number of pairs present in the plasma. In two subsequent papers ([16] and [17]), Lightman went on to study the possible equilibria which can exist in relativistic thermal pair plasmas. The timescales of important creation and annihilation reactions were compared to various plasma timescales to investigate whether or not the plasmas have a chance to establish themselves or if it is the particle behaviour which dominates. The creation and annihilation reactions which were considered include:

$$\text{pair production} \quad - \qquad \gamma\,\gamma \rightarrow e^{+}\,e^{-} \qquad \text{(in the presence of a nucleus)}$$

$$\gamma\, e^{\pm} \rightarrow e^{\pm}\, e^{+}\, e^{-}$$
$$e^{\pm}\, e^{\pm} \rightarrow e^{\pm}\, e^{\pm}\, e^{+}\, e^{-}$$

pair annihilation - $e^{+}\, e^{-} \rightarrow \gamma\, \gamma$

Pair creation depends intrinsically on the presence of energetic γ-rays. So the additional photon production mechanisms were also studied:

bremsstrahlung - $e^{\pm}\, e^{\pm} \rightarrow e^{\pm}\, e^{\pm}\, \gamma$

double Compton - $e^{\pm}\, \gamma \rightarrow e^{\pm}\, \gamma\, \gamma$

synchrotron - $e^{\pm} \rightarrow e^{\pm}\, \gamma$ (in the presence of a magnetic field)

where γ denotes a photon, e^{+} and e^{-} denote a positron and electron respectively and $e^{\pm}$ may be either a positron or electron.

Taking all of these reactions into account it was discovered that the pair equilibria are temperature dependent; above a maximum temperature the pair production rate starts to outstrip the annihilation rate and the resulting imbalance of particles destroys the equilibrium. Takahara & Kusunose [18] have extended this work to investigate the effect of magnetic field strength on the equilibrium conditions. As the magnetic field gets stronger one important effect is the significant decrease in the maximum temperature attainable while still maintaining equilibrium.

The above references all concentrate on the nature of individual particles; investigating inter-particle or particle-photon collisions. The work , in general, does not include any basic plasma analysis, which involves looking at the overall system and treating it as a medium for wave propagation and collective particle effects. Amongst the first authors to consider the plasma properties of electrons and positrons were Holcomb & Tajima [19] who carried out a linear analysis of electron-positron plasmas within the frame work of general relativity. This work is relevant to studies of the early universe (from $t = 10^{-2}$ to $t = 1\, s$) where the matter is in the plasma state and electrons and positrons are the most abundant particles. Collisional effects, including creation and annihilation, are neglected which is a valid assumption provided the plasma frequency is far greater than the frequency of the collisions. Tajima

& Taniuti [20] went on to consider the nonlinear interaction of such a general-relativistic electron-positron plasma with electromagnetic waves. Again collisions were neglected and the plasma assumed to be unmagnetised.

The early universe is another example of an astrophysical application where electron-positron plasmas are thought to play an important role and could be included in the list of likely occurrences given in Section 1.3.1.

Chapter 2

Derivation of the Kinetic Equations

> Mathematics may be defined as the subject in which we never know what we are talking about, nor whether what we are saying is true.
> *Bertrand Russell*

2.1 Phase Space Formalism and Liouville's Equation

Following the analysis in Clemmow & Dougherty [21] and Krall & Trivelpiece [22], we would like to present a brief outline of how the kinetic equations used to define the plasma are derived. An exact description of a plasma requires that the position $\mathbf{x}$ and velocity $\mathbf{v}$ of every particle in the plasma are known at time t, for all t. So, if there are N particles present in the plasma, there will be $3N$ equations of motion to solve in $6N$ variables. The exact state of the plasma , therefore, is described by a point moving through a $6N$- dimensional phase space (known as Γ-space). The method of trying to solve the equations of motion of every particle simultaneously is clearly intractable. We shall use instead a statistical mechanics formalism which provides a more practical approach to the analysis.

Consider then a probability density $\rho(X_1, X_2, \ldots, X_N, t)$, where $X_i = (\mathbf{x}_i, \mathbf{v}_i)$

specifies the position and velocity of particle i, such that

$$\rho\,(X_1,\ldots,X_N,t)\,dX_1\ldots dX_N \tag{2.1}$$

is the probability of finding the plasma system in the state $[(X_1, X_1+dX_1),\ldots,(X_N, X_N+dX_N)]$ at time t. The distribution ρ will be assumed to be symmetric under the interchange of like particles. Normalisation requires that

$$\int\int\ldots\int \rho\, dX_1\ldots dX_N = 1 \tag{2.2}$$

The probability density ρ satisfies Liouville's equation

$$\frac{\partial\rho}{\partial t}+\sum_{j=1}^{N}\frac{\partial}{\partial \mathbf{x}_j}\cdot(\rho\,\mathbf{v}_j)+\sum_{j=1}^{N}\frac{\partial}{\partial \mathbf{v}_j}\cdot(\rho\,\mathbf{a}_j)=0, \tag{2.3}$$

where $\mathbf{a}_j$ is the acceleration of particle j, which states that the system conserves volume in Γ-space.

If the acceleration depends on the velocity only through a term of the form $\mathbf{v}\times\mathbf{B}$, then we may write Liouville's equation as

$$\frac{\partial\rho}{\partial t}+\sum_{j=1}^{N}\mathbf{v}_j\cdot\frac{\partial\rho}{\partial \mathbf{x}_j}+\sum_{j=1}^{N}\mathbf{a}_j\cdot\frac{\partial\rho}{\partial \mathbf{v}_j}=0, \tag{2.4}$$

Solving this equation still requires a detailed knowledge of all particles in the plasma. To proceed further we shall write Liouville's equation in terms of the one-particle distribution function. The exact one-particle distribution function is defined as

$$F\,(\mathbf{x},\mathbf{v},t)=\sum_i \delta\,[X-X_i\,(t)], \tag{2.5}$$

for a gas in a given state $X_1\,(t), X_2\,(t),\ldots$, where $X=(\mathbf{x},\mathbf{v})$ is a typical point of μ-space, which is the 6-dimensional phase space of a single particle.

The function F gives the density of the plasma in μ-space and is exact except for the identity of the particles. A more useful definition is that of the average one-particle distribution function

$$f_1\,(\mathbf{x},\mathbf{v},t)=<F\,(\mathbf{x},\mathbf{v},t)>, \tag{2.6}$$

where the expectation value ($<\ldots>$) is defined as follows

$$<F\,(\mathbf{x},\mathbf{v},t)>\equiv\int\int\ldots\int\rho\,(X_1,\ldots,X_N,t)\;F\,(\mathbf{x},\mathbf{v},t)\,dX_1\ldots dX_N. \tag{2.7}$$

Using the definition of $F(\mathbf{x},\mathbf{v},t)$, we have

$$f_1(\mathbf{x},\mathbf{v},t) = \int\dots\int \rho\,(X_1,\dots,X_N,t) \times \sum_{i=1}^{N} \delta\,[X - X_i(t)]\,dX_1\dots dX_N \tag{2.8}$$

$$= N\int\dots\int \rho\,(X_1,X_2,\dots,X_N,t)\,dX_2\dots dX_N, \tag{2.9}$$

since all terms in the summation are equal.

We can define $f_1(\mathbf{x},\mathbf{v},t)\,d^3x\,d^3v$ to be the probability of a particle occupying the volume element $d^3x\,d^3v$ at time t. Alternatively, if we multiply this expression by n_0 which represents an average number density, we can interpret it to be the mean number of particles occupying the volume element $d^3x\,d^3v$ around the point (**x**,**v**). This latter definition requires the volume element to be large enough to contain a large number of particles.

We can extend this analysis to s points $X, X', \dots, X^{(s)}$, where the average s-particle distribution is

$$f_s\left(X,X',\dots,X^{(s)},t\right) = \frac{N!}{(N-s)!}\int\dots\int \rho(X,X',\dots,X^{(s)}, X_{s+1},\dots,X_N,t)\,dX_{s+1}\dots dX_N. \tag{2.10}$$

This represents the probability of finding particles simultaneously at X, X', $\dots, X^{(s)}$ provided all the points are distinct and there is no overlap.

We will now return to Liouville's equation. Multiply through by $\frac{N!}{(N-s)!}$ and integrate with respect to the variables $X_{s+1},\dots,X_N$. The result is

$$\frac{\partial f_s}{\partial t} + \sum_{j=1}^{s} \mathbf{v}_j \cdot \frac{\partial f_s}{\partial \mathbf{x}_j} + \sum_{j=1}^{s}\sum_{1=0}^{s} \mathbf{a}_j^{(i)} \cdot \frac{\partial f_s}{\partial \mathbf{v}_j} + \sum_{j=1}^{s}\int \mathbf{a}_j^{(s+1)} \cdot \frac{\partial f_{s+1}}{\partial \mathbf{v}_j}\,dX_{s+1} = 0. \tag{2.11}$$

Here the acceleration is written as

$$\mathbf{a}_j = \sum_{i=0}^{N} \mathbf{a}_j^{(i)} \tag{2.12}$$

which, for $i \neq 0$, is the acceleration of particle j due to the presence of particle i and where $\mathbf{a}_j^{(0)}$ is the acceleration due to any external fields. The first three terms represent a Liouville equation for s particles, whereas the last term represents the forces due to the remaining $N - s$ particles. For a fixed value of j the terms for

$s+1 \leq j \leq N$ are all the same, by the symmetry of ρ, and we can represent each term in this sum by the term for $i = s+1$. For the other two sums in the equation all the contributions for $s+1 \leq j \leq N$ are zero due to the boundary conditions that $\rho \to 0$ as $\mathbf{x} \to \infty$ and as $\mathbf{v} \to \infty$ respectively.

The set of equations (2.11), for $s = 1, 2, \ldots, N$, is known as the BBGKY chain after Bogliubov, Born, Green, Kirkwood and Yvon, who were responsible for its development. As it stands the set is open: s equations in $s+1$ unknowns. To close the set we must be able to write f_{s+1} in terms of the functions $f_1, \ldots, f_s$. Again it is impractical to attempt to solve this chain of equations. Instead we must find a suitable way of truncating the series.

2.2 Uncorrelated Particles

Consider the case where there is no interaction between the particles. The acceleration experienced by each particle will then reduce to the acceleration due only to the external fields, ie $\mathbf{a}_j = \mathbf{a}_j^{(0)}$. The integral term in (2.11) vanishes and one solution of Liouville's equation is

$$\rho\left(X_1, X_2, \ldots, X_N, t\right) = N^{-N} \prod_{j=1}^{N} f_1\left(X_j, t\right), \tag{2.13}$$

(ie ρ is a product of N identical one-particle distributions) and the s-particle distribution can be written as

$$f_s = \prod_{j=1}^{s} f_1\left(X_j, t\right), \tag{2.14}$$

which says that the particles are uncorrelated.

In a plasma we cannot expect the particles to be non-interacting. We may, however, try to find some circumstances when it would be reasonable to take the approximation of uncorrelated particles. Consider a particle of charge q and mass m in external electric and magnetic fields $\mathbf{E}_0$ and $\mathbf{B}_0$ respectively. The acceleration of the particle due to these external fields is

$$\mathbf{a}_j^{(0)} = \frac{q}{m}\left[\mathbf{E}_0 + \mathbf{v} \times \mathbf{B}_0\right] \tag{2.15}$$

and the acceleration due to the presence of particle i is

$$\mathbf{a}_j^{(i)} = \frac{q}{m}\left[\mathbf{E}_j^{(i)} + \mathbf{v}_j \times \mathbf{B}_j^{(i)}\right], \tag{2.16}$$

where $\mathbf{E}_j^{(i)}$ and $\mathbf{B}_j^{(i)}$ are the electric and magnetic fields caused by particle i at the position of particle j. Using the Coulomb and Biot-Savart laws respectively, we can express these fields as

$$\mathbf{E}_j^{(i)} = \frac{q}{4\pi\epsilon_0}\frac{\mathbf{x}_j - \mathbf{x}_i}{|\mathbf{x}_j - \mathbf{x}_i|^3}, \tag{2.17}$$

$$\mathbf{B}_j^{(i)} = \frac{\mu_0 q}{4\pi}\frac{\mathbf{v}_i \times (\mathbf{x}_j - \mathbf{x}_i)}{|\mathbf{x}_j - \mathbf{x}_i|^3}. \tag{2.18}$$

These field definitions are not strictly accurate. To be completely rigorous we should use retarded potentials which take into account the fact that the field at time t due to a particle a distance r away should be calculated with regard to the state of the particle at time $t - r/c$. If we neglect this effect we can only consider plasmas where this transit time r/c is much smaller than the plasma timescales involved.

We suppose that the number of particles, N, and the volume, V, of the plasma are both very large, with the average number density given by $n_0 = N/V$. We now 'pulverise' the particles by taking the limit $n_0 \to \infty$, but with $e \to 0$ and $m \to 0$ so that $n_0\, e$, $n_0\, m$ and e/m remain constant. In this limit, we have $f_s = O(n_0^s)$, $\mathbf{a}_j^{(0)}$ is constant and $\mathbf{a}_j^{(i)} = O(n_0^{-1})$ for $i \neq 0$. So returning to (2.11), we see that with the exception of $i = 0$, the third term is one order of magnitude less than the other terms and may be neglected. The set of equations then reduces to

$$\frac{\partial f_s}{\partial t} + \sum_{j=1}^{s} \mathbf{v}_j \cdot \frac{\partial f_s}{\partial \mathbf{x}_j} + \sum_{j=1}^{s} \mathbf{a}_j^{(0)} \cdot \frac{\partial f_s}{\partial \mathbf{v}_j} + \sum_{j=1}^{s} \int \mathbf{a}_j^{(s+1)} \cdot \frac{\partial f_{s+1}}{\partial \mathbf{v}_j}\, dX_{j+1} = 0. \tag{2.19}$$

Consider the case of uncorrelated particles. Look for solutions of the type (2.13), with f_s given by (2.14), which satisfy equations (2.19) provided

$$\frac{\partial f_1(X_1,t)}{\partial t} + \mathbf{v}_1 \cdot \frac{\partial f_1(X_1,t)}{\partial \mathbf{x}_1} + \left[\mathbf{a}_1^{(0)} + \int \mathbf{a}_1^{(2)} f_1(X_2,t)\, dX_2\right] \cdot \frac{\partial f_1(X_1,t)}{\partial \mathbf{v}_1} = 0 \tag{2.20}$$

which becomes

$$\frac{\partial f}{\partial t} + \mathbf{v} \cdot \frac{\partial f}{\partial \mathbf{x}} + \mathbf{a} \cdot \frac{\partial f}{\partial \mathbf{v}} = 0 \tag{2.21}$$

when we drop the suffices. Here **a** is the acceleration due to external fields as well as the self-consistent internal fields, ie

$$\mathbf{a} = \frac{q}{m}\left[\mathbf{E}_0 + \mathbf{v} \times \mathbf{B}_0\right] + \int \frac{q}{m}\left[\mathbf{E} + \mathbf{v} \times \mathbf{B}\right] f_1(\mathbf{x}, \mathbf{v})\, d^3x\, d^3v. \tag{2.22}$$

Equation (2.21) is known as the collisionless Boltzmann, or Vlasov equation. It is valid only for particles of a single species; for a complete description of the plasma, we require a Vlasov equation for each species present. The force acting on an individual particle is due to all the other particles in the plasma. In the Vlasov approximation it has been assumed that we can *smooth* these interactions into a continuous, slowly-varying function in space. This viewpoint neglects the effect of particles close to the one under consideration, whose fields may be changing rapidly over this small region. In effect, it assumes that there are no *collisions* taking place in the plasma. To take account of these close interactions a collision term $(\frac{\partial f}{\partial t})_c$, which represents the rate of change of f due to these collisions must be included on the right-hand side of the Boltzmann equation (2.21).

2.3 Validity of Vlasov Approximation

The Vlasov equation was obtained by assuming that the electrons were smoothed out to form a continuous fluid. We would now like to return to the set of equations (2.11) and express them in dimensionless variables to investigate the significance of taking this limit.

The mean density n_0 is taken to be very large with e and m both small enough to ensure $n_0\, e^2/m$ and $f_s\, n_0^{-s}$ are always finite. We choose ω_p^{-1}, where ω_p is the plasma frequency $n_0\, e^2/\epsilon_0\, m$, to be the characteristic timescale, $(\kappa T/m)^{1/2}$, where T is the mean temperature, as a characteristic speed and the Debye length, $\lambda = (\epsilon_0\, \kappa T/n_0\, e^2)^{1/2}$, as a characteristic length. We can now define the following normalised variables:

$$\mathbf{v} = \lambda\, \omega_p\, \overline{\mathbf{v}}, \quad \mathbf{x} = \lambda\, \overline{\mathbf{x}}, \quad t = \frac{\overline{t}}{\omega_p}, \quad dX = \lambda^6\, \omega_p^3\, d\overline{X}, \tag{2.23}$$

$$n_0^s\ f_s = (\lambda\, \omega_p)^{-3s}\, \overline{f}_s\ ,\ \mathbf{a}^{(0)} = \lambda\, \omega_p^2\, \overline{\mathbf{a}}^{(0)}\ ,\ \mathbf{a}_j^{(i)} = \frac{\omega_p^2}{n_0\, \lambda^2}\, \overline{\mathbf{a}}_j^{(i)}, \tag{2.24}$$

where the last dimensionless acceleration term is

$$\overline{\mathbf{a}}_j^{(i)} = \frac{1}{4\pi}\frac{\overline{\mathbf{x}}_j - \overline{\mathbf{x}}_i}{|\overline{\mathbf{x}}_j - \overline{\mathbf{x}}_i|^3} + \frac{1}{4\pi\,\overline{c}^2}\overline{\mathbf{v}}_j \times \left[\overline{\mathbf{v}}_i \times \frac{\overline{\mathbf{x}}_j - \overline{\mathbf{x}}_i}{|\overline{\mathbf{x}}_j - \overline{\mathbf{x}}_i|^3}\right] \tag{2.25}$$

Note that the speed of light, c, has also been normalised: $c = \lambda\,\omega_p\,\overline{c}$. The BBGKY chain of equations, written in terms of these normalised variables, become

$$\frac{\partial \overline{f}_s}{\partial \overline{t}} + \sum_{j=1}^{s} \overline{\mathbf{v}}_j \cdot \frac{\partial \overline{f}_s}{\partial \overline{\mathbf{x}}_j} + \sum_{j=1}^{s} \overline{\mathbf{a}}_j^{(0)} \cdot \frac{\partial \overline{f}_s}{\partial \overline{\mathbf{v}}_j} + \frac{1}{n\,\lambda^3} \sum_{i=1}^{s}\sum_{j=1}^{s} \overline{\mathbf{a}}_j^{(i)} \cdot \frac{\partial \overline{f}_s}{\partial \overline{\mathbf{v}}_j}$$
$$+ \sum_{j=1}^{s} \int \overline{\mathbf{a}}_j^{(s+1)} \cdot \frac{\partial \overline{f}_{s+1}}{\partial \overline{\mathbf{v}}_j}\, d\overline{X}_{s+1} = 0. \tag{2.26}$$

Apart from the additional factor $(n_0\,\lambda^3)^{-1}$ in the fourth term, this equation has essentially the same form as eqn. (2.11). The expression $n_0\,\lambda^3$ represents the number of particles per cubic Debye length. In the Vlasov approximation this number is taken to be very large (in the limit of completely 'smoothed-out' particles, it tends to ∞) which allows us to neglect the term in this limit. A large number of particles in the Debye cube is an essential requirement that must be satisfied before the system can be considered to be a plasma.

2.4 Relativistic Formulation of the Vlasov Equation

We have seen that in the standard non-relativistic analysis carried out in the previous sections the distribution functions are all defined to be functions of position, velocity and time. In a relativistic analysis, however, it is more convenient to express the distribution function in terms of momentum rather than velocity, ie $f = f(\mathbf{x}, \mathbf{p}, t)$, so that macroscopic quantities are obtained by integrating over all momentum space. The reason for this will become clear presently. The mean number of particles of a given species in the phase space volume element $d^3x\,d^3p$ at time t is $n_0\,f(\mathbf{x}, \mathbf{p}, t)\,d^3x\,d^3p$ which gives the probable number density to be

$$n(\mathbf{x}, t) = n_0 \int f(\mathbf{x}, \mathbf{p}, t)\, d^3p. \tag{2.27}$$

Consider a single particle of charge q and rest mass m in an electric field $\mathbf{E}$ and magnetic field $\mathbf{B}$. The relativistic equation of motion for this particle is

$$\frac{\partial \mathbf{p}}{\partial t} = q\,(\mathbf{E} + \mathbf{v} \times \mathbf{B}) \equiv \mathbf{G}, \tag{2.28}$$

where the relativistic momentum is $\mathbf{p} = \gamma m \mathbf{v}$ and the Lorentz factor has its usual definition: $\gamma = (1 + \frac{p^2}{m^2 c^2})^{1/2}$. The quantity $\mathbf{G}$ represents the force on the particle.

Return now to the particles in the phase space element $d^3x\, d^3p$ about the point $(\mathbf{x}, \mathbf{p})$. In a time δt, the particles will have moved to the point $\mathbf{x} + \mathbf{v}\,\delta t, \mathbf{p} + \mathbf{G}\,\delta t$. If we assume that a single particle does not significantly disturb the $\mathbf{E}$ and $\mathbf{B}$ fields, then the volume element $d^3x\, d^3p$ will remain invariant in time δt and if we make the further assumption that close collisions may be neglected we have

$$n_0 \left[f(\mathbf{x} + \mathbf{v}\,\delta t, \mathbf{p} + \mathbf{G}\,\delta t, t + \delta t) - f(\mathbf{x}, \mathbf{p}, t) \right] d^3x\, d^3p = 0 \tag{2.29}$$

which gives

$$\frac{\partial f}{\partial t} + \mathbf{v} \cdot \frac{\partial f}{\partial \mathbf{x}} + \mathbf{G} \cdot \frac{\partial f}{\partial \mathbf{p}} = 0. \tag{2.30}$$

This is the relativistic form of the Vlasov equation; it is invariant under a Lorentz transformation.

For comparison, we shall transform the Vlasov equation (2.30) from $(\mathbf{x}, \mathbf{p})$−space to $(\mathbf{x}, \mathbf{v})$−space. We can write

$$\frac{\partial}{\partial \mathbf{p}} \mathbf{v} = \frac{1}{m\gamma} (\underline{\underline{1}} - \frac{\mathbf{v}\,\mathbf{v}}{c^2}), \tag{2.31}$$

where $\underline{\underline{1}}$ is the unit tensor. The Jacobian of the transformation is

$$\left| \frac{\partial(\mathbf{p})}{\partial(\mathbf{v})} \right| = m^3 \gamma^5. \tag{2.32}$$

Define a new distribution function

$$F(\mathbf{x}, \mathbf{v}, t) = f(\mathbf{x}, \mathbf{p}, t) \left| \frac{\partial(\mathbf{p})}{\partial(\mathbf{v})} \right| \tag{2.33}$$

so that the number density is defined as $n(\mathbf{x}, t) = n_0 \int F(\mathbf{x}, \mathbf{v}, t)\, d^3v$. Multiply equation (2.30) by $m^3 \gamma^5$ to give

$$\frac{\partial F}{\partial t} + \mathbf{v} \cdot \frac{\partial F}{\partial \mathbf{x}} + \gamma^5 \left(\mathbf{G} \cdot \frac{\partial}{\partial \mathbf{p}} \mathbf{v} \right) \cdot \frac{\partial}{\partial \mathbf{v}} \left(\frac{F}{\gamma^5} \right) = 0. \tag{2.34}$$

Substituting (2.31) into the last term and differentiating the last bracket, allows us to write the Vlasov equation as

$$\frac{\partial F}{\partial t} + \mathbf{v} \cdot \frac{\partial F}{\partial \mathbf{x}} + \frac{\partial}{\partial \mathbf{v}} \cdot (\mathbf{g} F) = 0, \tag{2.35}$$

where $\mathbf{g} = \frac{1}{m\gamma} [\mathbf{G} - \frac{1}{c^2} \mathbf{v} (\mathbf{v} \cdot \mathbf{G})]$. This form of the equation is obviously less convenient than (2.30) above, which is written in terms of the momentum.

2.5 The Maxwell Equations

The electromagnetic fields in the plasma are described by the Maxwell equations (as given in Lorrain & Corson [23])

$$\nabla \times \mathbf{E} = -\frac{\partial \mathbf{B}}{\partial t} \tag{2.36}$$

$$\nabla \times \mathbf{H} = \mathbf{j}_f - \frac{\partial \mathbf{D}}{\partial t} \tag{2.37}$$

$$\nabla \cdot \mathbf{D} = \rho_f \tag{2.38}$$

$$\nabla \cdot \mathbf{B} = 0. \tag{2.39}$$

Here $\mathbf{E}$ is the electric field intensity and $\mathbf{B}$ the magnetic induction, as introduced previously, $\mathbf{D}$ is the electric displacement , $\mathbf{H}$ is the magnetic field intensity, ρ_f is the free charge density, $\mathbf{j}_f$ is the corresponding free current density and $\partial \mathbf{D}/\partial t$ is the displacement current density.

Formally, $\mathbf{D}$ is defined to be

$$\mathbf{D} = \epsilon \mathbf{E} + \mathbf{P}, \tag{2.40}$$

where $\mathbf{P}$ is the electric polarisation, which can be expressed in terms of the bound charge density by the equation $\rho_b = -\nabla \cdot \mathbf{P}$, and $\mathbf{H}$ is given by

$$\mathbf{H} = \frac{1}{\mu_0} \mathbf{B} - \mathbf{M}, \tag{2.41}$$

where $\mathbf{M}$ is the magnetisation.

Expressing the Maxwell equations only in terms of $\mathbf{E}$ and $\mathbf{B}$ gives, with the assumption that both $\mathbf{P}$ and $\mathbf{M}$ may be set equal to zero,

$$\nabla \cdot \mathbf{E} = \frac{\rho}{\epsilon_0}, \tag{2.42}$$

$$\nabla \cdot \mathbf{B} = 0 \tag{2.43}$$

$$\nabla \times \mathbf{E} = -\frac{\partial \mathbf{B}}{\partial t} \tag{2.44}$$

$$\nabla \times \mathbf{B} = \mu_0 \mathbf{j} + \frac{1}{c^2} \frac{\partial \mathbf{E}}{\partial t}. \tag{2.45}$$

In terms of the distribution function f, the charge and current densities are defined to be

$$\rho = \sum_s n_0 q_s \int f_s(\mathbf{x}, \mathbf{p}, t)\, d^3p \tag{2.46}$$

$$\mathbf{j} = \sum_s \frac{n_0 q_s}{m_s} \int f_s(\mathbf{x}, \mathbf{p}, t) \frac{\mathbf{p}}{\gamma_s} d^3p, \tag{2.47}$$

where we sum over each plasma species s.

2.6 Derivation of the Dielectric Tensor

We will now use a linear analysis to derive a general expression for the dielectric tensor $\underline{\underline{\mathbf{R}}}$ from the relativistic Vlasov-Maxwell system of equations. A linear analysis assumes that the plasma is initially in an equilibrium state and undergoes only small perturbations about this equilibrium position. This allows us to neglect second order (and higher) terms in the perturbed quantities. In an attempt to solve this system of equations we will perform a Fourier-Laplace transform on the equations, following the analysis in Montgomery & Tidman [24], and use the resulting expressions to obtain the components of $\underline{\underline{\mathbf{R}}}$. From these expressions we can derive dispersion relations for the waves that may exist in the plasma.

2.6.1 The System of Equations

Combining the expressions in sections 2.4 and 2.5, the relativistic Vlasov-Maxwell system of equations can be written as

$$\frac{\partial f}{\partial t} + \mathbf{v} \cdot \frac{\partial f}{\partial \mathbf{x}} + \mathbf{G} \cdot \frac{\partial f}{\partial \mathbf{p}} = 0. \tag{2.48}$$

$$\nabla \times \mathbf{E} = -\frac{\partial \mathbf{B}}{\partial t} \tag{2.49}$$

$$\nabla \times \mathbf{B} = \mu_0 \mathbf{j} + \frac{1}{c^2} \frac{\partial \mathbf{E}}{\partial t}. \tag{2.50}$$

where the remaining two Maxwell equations are taken to be initial conditions.

We assume that the plasma is in an equilibrium state and apply a small perturbation. Since a linear analysis is being used, all terms greater than first order are ignored and the physical quantities of the system can thus be written as

$$f(\mathbf{x}, \mathbf{p}, t) = f_0(\mathbf{p}) + f_1(\mathbf{x}, \mathbf{p}, t)\ ,\ \mathbf{E}(\mathbf{x}, t) = \mathbf{E}_1(\mathbf{x}, t)\ ,\ \mathbf{B}(\mathbf{x}, t) = \mathbf{B}_0 + \mathbf{B}_1(\mathbf{x}, t) \tag{2.51}$$

where we have assumed that in the equilibrium state the distribution function f_0 depends only on momentum, the electric field is zero and the magnetic field is uniform and along the $z-$direction.

Zero-order Equations

In the equilibrium state, the above system of equations reduces to

$$\frac{q}{m}\mathbf{v}\times\mathbf{B}_0\cdot\nabla_p f_0 = 0 \tag{2.52}$$

$$\nabla\times\mathbf{B}_0 = \mu_0\mathbf{j}_0 \tag{2.53}$$

Writing $\mathbf{v} = \mathbf{p}/(m\gamma)$, the Vlasov equation has the form $\mathbf{p}\times\mathbf{B}_0\cdot\nabla_p f_0 = 0$. If we express the momentum in cylindrical polar coordinates $(p_\perp, \phi, p_{||})$ this equation reduces to the form

$$-B_0\frac{\partial f_0}{\partial\phi} = 0. \tag{2.54}$$

Thus the equilibrium distribution function f_0 depends only on $p_\perp$ and $p_{||}$ and we choose to write it as $f_0 = f_0\left(p_\perp^2, p_{||}\right)$. This is the most general form of solution to the zero-order Vlasov equation which is isotropic in the plane perpendicular to $\mathbf{B}_0$.

First-Order Equations

The first order Vlasov - Maxwell system of equations, which will form the basis of our analysis, can be written as

$$\frac{\partial f_1}{\partial t} + \mathbf{v}\cdot\frac{\partial f_1}{\partial\mathbf{x}} + q\left(\mathbf{E}_1 + \mathbf{v}\times\mathbf{B}_1\right)\cdot\frac{\partial f_0}{\partial\mathbf{p}} + q\,\mathbf{v}\times\mathbf{B}_0\cdot\frac{\partial f_1}{\partial\mathbf{p}} = 0, \tag{2.55}$$

$$\nabla\times\mathbf{E}_1 = -\frac{\partial\mathbf{B}_1}{\partial t} \tag{2.56}$$

$$\nabla\times\mathbf{B}_1 = \mu_0\mathbf{j}_1 + \frac{1}{c^2}\frac{\partial\mathbf{E}_1}{\partial t} \tag{2.57}$$

2.6.2 Linear Analysis

To proceed we apply a Fourier transform to the space variable $\mathbf{x}$ and a Laplace transform to the time variable t in each of the above equations. The Fourier transform

of f_1 with respect to $\mathbf{x}$ is

$$f_k(\mathbf{k},\mathbf{p},t) = \frac{1}{(2\pi)^{3/2}} \int_{-\infty}^{\infty} d\mathbf{x}\, e^{-i\mathbf{k}\cdot\mathbf{x}} f_1(\mathbf{x},\mathbf{p},t) \tag{2.58}$$

and if we then take the Laplace transform of f_k, the resulting variable is

$$f(\mathbf{k},\mathbf{p},s) = \int_0^{\infty} dt\, e^{-s\,t} f_k(\mathbf{k},\mathbf{p},t), \tag{2.59}$$

where s is the Laplace transform variable. The distribution function thus undergoes the transformation $f_1(\mathbf{x},\mathbf{p},t) \mapsto f(\mathbf{k},\mathbf{p},s)$. The electromagnetic fields $\mathbf{E}_1$ and $\mathbf{B}_1$ undergo equivalent transformations.

Firstly, we take the Fourier transform in $\mathbf{x}$. Multiply the Vlasov equation (2.55) by $e^{-i\mathbf{k}\cdot\mathbf{x}}/(2\pi)^{3/2}$ and integrate each term over the integral $(-\infty,\infty)$ to give

$$\frac{\partial f_k}{\partial t} + i\,\mathbf{k}\cdot\mathbf{v}\, f_k + q\,(\mathbf{E}_k + \mathbf{v}\times\mathbf{B}_k)\cdot\frac{\partial f_0}{\partial \mathbf{p}} + q\,\mathbf{v}\times\mathbf{B}_0\cdot\frac{\partial f_k}{\partial \mathbf{p}} = 0. \tag{2.60}$$

We now apply the Laplace transform in t. All the expressions transform in a straightforward manner with the exception of the first term which contains a derivative with respect to time. Here we have to use the rule

$$LT\left(\dot{f}_k\right) = s\,LT\,(f_k) - f_k(t=0), \tag{2.61}$$

where LT denotes the Laplace transform. The transformed Vlasov equation is thus

$$(s + i\,\mathbf{k}\cdot\mathbf{v})\,f + q\,\mathbf{v}\times\mathbf{B}_0\cdot\frac{\partial f}{\partial \mathbf{p}} + q\,(\mathbf{E}+\mathbf{v}\times\mathbf{B})\cdot\frac{\partial f_0}{\partial \mathbf{p}} = f_k(t=0), \tag{2.62}$$

where

$$f_k(t=0) = \frac{1}{(2\pi)^{3/2}} \int_{-\infty}^{\infty} d\mathbf{x}\, e^{-i\mathbf{k}\cdot\mathbf{x}} f_1(\mathbf{x},\mathbf{p},t=0). \tag{2.63}$$

Following the same procedure as for the Vlasov equation, we can obtain the transformed Maxwell equations

$$i\,\mathbf{k}\times\mathbf{E} = -s\,\mathbf{B} + \mathbf{B}_k(t=0) \tag{2.64}$$

$$i\,\mathbf{k}\times\mathbf{B} = \mu_0\,\mathbf{j} + \frac{s}{c^2}\,\mathbf{E} - \frac{1}{c^2}\,\mathbf{E}_k(t=0). \tag{2.65}$$

We can combine equations (2.64) and (2.65) into one equation which does not depend on $\mathbf{B}$. The transformed Vlasov-Maxwell equations can then be written as:

$$\begin{aligned}(s + i\,\mathbf{k}\cdot\mathbf{v})\,f + q\,\mathbf{v} \times \mathbf{B}_0\cdot\frac{\partial f}{\partial \mathbf{p}} + q\left[\mathbf{E} - \frac{i}{s}\,\mathbf{v}\times(\mathbf{k}\times\mathbf{E})\right]\cdot\frac{\partial f_0}{\partial \mathbf{p}} \\ = f_k(t=0) - \frac{q}{s}\,\mathbf{v}\times\mathbf{B}_k(t=0)\cdot\frac{\partial f_0}{\partial \mathbf{p}}\end{aligned} \tag{2.66}$$

$$(s^2 + c^2\,k^2)\,\mathbf{E} - c^2\,(\mathbf{k}\cdot\mathbf{E})\,\mathbf{k} = -\frac{s}{\epsilon_0}\mathbf{j} + s\,\mathbf{E}_k\,(t=0) + i\,c^2\,\mathbf{k}\times\mathbf{B}_k\,(t=0). \quad (2.67)$$

Using cylindrical polar coordinates $\left(p_\perp, \phi, p_{||}\right)$ we can write equation (2.66) as

$$\frac{\partial f}{\partial \phi} - \frac{(s + i\,\mathbf{k}\cdot\mathbf{v})}{\Omega} f = \frac{\Phi\,(\phi)}{\Omega}, \quad (2.68)$$

where the relativistic cyclotron frequency is defined to be

$$\Omega \equiv \frac{q\,B_0}{\gamma\,m}\left(= \frac{\Omega_0}{\gamma}\right) \quad (2.69)$$

and Ω_0 is the more usual non-relativistic cyclotron frequency. The function Φ is defined to be

$$\begin{aligned}\Phi\,(\phi) \;=\; & q\left[\mathbf{E} - \frac{i}{s}\mathbf{v}\times(\mathbf{k}\times\mathbf{E})\right]\cdot\frac{\partial f_0}{\partial \mathbf{p}} - f_k\,(t=0) \\ & + \frac{q}{s}\,\mathbf{v}\times\mathbf{B}_k\,(t=0)\cdot\frac{\partial f_0}{\partial \mathbf{p}}. \end{aligned} \quad (2.70)$$

Introducing the integrating factor

$$G\,(\phi') = \exp\frac{1}{\Omega}\left[(s + i\,k_{||}\,v_{||})\,(\phi - \phi') - i\,k_\perp\,v_\perp\,(\sin\phi' - \sin\phi)\right] \quad (2.71)$$

allows us to solve equation (2.68) for f, giving

$$f = \frac{1}{\Omega}\int_0^\phi G\,(\phi')\,\Phi\,(\phi')\,d\phi', \quad (2.72)$$

which is then substituted into the second equation along with the explicit integral form for $\mathbf{j}$:

$$\begin{aligned}&(s^2 + c^2\,k^2)\,\mathbf{E} - c^2\,(\mathbf{k}\cdot\mathbf{E})\,\mathbf{k} + \frac{s}{\epsilon_0}\sum\frac{n_0\,q^2}{m\,\Omega_0}\times \\ &\qquad \int d\mathbf{p}\,\mathbf{p}\int_\infty^\phi d\phi'\,G\,(\phi')\left[\mathbf{E} - \frac{i}{s}\mathbf{v}'\times(\mathbf{k}\times\mathbf{E})\right]\cdot\frac{\partial f_0}{\partial \mathbf{p}'} = \mathbf{I}, \end{aligned} \quad (2.73)$$

where all the initial conditions have been gathered into the vector $\mathbf{I}$:

$$\begin{aligned}\mathbf{I} \;=\; & s\,\mathbf{E}_k\,(t=0) + i\,c^2\,\mathbf{k}\times\mathbf{B}_k\,(t=0) + \frac{s}{\epsilon_0}\sum\frac{n_0\,q^2}{m\,\Omega_0}\times \\ & \int d\mathbf{p}\,\mathbf{p}\int_\infty^\phi d\phi'\,G\,(\phi')\left[f_k\,(t=0) - \frac{q}{s}\mathbf{v}'\times\mathbf{B}_k\,(t=0)\cdot\frac{\partial f_0}{\partial \mathbf{p}'}\right]. \end{aligned} \quad (2.74)$$

We define the conductivity tensor $\underline{\underline{\sigma}}$ so that the last term on the left hand side of equation (2.73) can be written as $\underline{\underline{\sigma}}\cdot\mathbf{E}$ and the equation becomes

$$\left(s^2 + c^2\,k^2\right)\mathbf{E} - c^2\,\mathbf{k}\,(\mathbf{k}\cdot\mathbf{E}) + \frac{s}{\epsilon_0}\underline{\underline{\sigma}}\cdot\mathbf{E} = \mathbf{I}. \quad (2.75)$$

This can be written more compactly as

$$\underline{\underline{\mathbf{R}}} \cdot \mathbf{E} = \mathbf{I}, \tag{2.76}$$

where $\underline{\underline{\mathbf{R}}}$ is the dielectric tensor.

For the specific case of an isotropic equilibrium state, ie $f_0 = f_0\left(\left|\underline{p}\right|\right)$, we can carry out two of the four integrations involved in the components of $\underline{\underline{\mathbf{R}}}$. We can write the integrals in the $\underline{\underline{\sigma}} \cdot \mathbf{E}$ term as follows

$$\begin{aligned} -s \sum \frac{\omega^2}{\Omega_0} \int_{-\infty}^{\infty} dp_{\|} \int_0^{\infty} dp_\perp \, p_\perp \int_0^{2\pi} d\phi \, (p_\perp \cos\phi, p_\perp \sin\phi, p_{\|}) \times \\ \int_{-\infty}^{0} d\alpha \exp \frac{1}{\Omega} \left[(s + i\, k_{\|} v_{\|})\, \alpha - i\, k_\perp v_\perp (\sin(\phi - \alpha) - \sin\phi) \right] \\ \times \left\{ [E_x \cos(\phi - \alpha) + E_y \sin(\phi - \alpha)] \cdot \frac{\partial f_0}{\partial p_\perp} + E_z \frac{\partial f_0}{\partial p_{\|}} \right\}, \end{aligned} \tag{2.77}$$

where we have changed the integration variable from ϕ' to $\alpha = \phi - \phi'$. Bessel function identities, which are summarised in Appendix A can be used to write the ϕ - integrations in terms of sums of Bessel functions. We can then carry out the α - integrals so that the components of $\underline{\underline{\mathbf{R}}}$ can be written as

$$\begin{aligned} R_{xx} &= s^2 + c^2 k_{\|}^2 - 2\, s\, \pi \sum \frac{\omega_p^2}{\Omega_0} \sum_n \int_{-\infty}^{\infty} dp_{\|} \\ &\qquad \int_0^{\infty} dp_\perp \, p_\perp^2 \, \frac{n^2 \, \Omega^3 \, J_n^2 \, (\partial f_0 / \partial p_\perp)}{k_\perp^2 \, v_\perp^2 \, (s + i\, k_{\|} \, v_{\|} + i\, n\, \Omega)} \end{aligned} \tag{2.78}$$

$$\begin{aligned} R_{xy} &= -R_{yx} = -2\, i\, s\, \pi \sum \frac{\omega_p^2}{\Omega_0} \sum_n \int_{-\infty}^{\infty} dp_{\|} \\ &\qquad \int_0^{\infty} dp_\perp \, p_\perp^2 \, \frac{n \, \Omega^2 \, J_n \, J_n' \, (\partial f_0 / \partial p_\perp)}{k_\perp \, v_\perp \, (s + i\, k_{\|} \, v_{\|} + i\, n\, \Omega)} \end{aligned} \tag{2.79}$$

$$\begin{aligned} R_{xz} &= -c^2 \, k_\perp \, k_{\|} - 2\, s\, \pi \sum \frac{\omega_p^2}{\Omega_0} \sum_n \int_{-\infty}^{\infty} dp_{\|} \\ &\qquad \int_0^{\infty} dp_\perp \, p_\perp^2 \, \frac{n \, \Omega^2 \, J_n^2 \left(\partial f_0 / \partial p_{\|} \right)}{k_\perp \, v_\perp \, (s + i\, k_{\|} \, v_{\|} + i\, n\, \Omega)} \end{aligned} \tag{2.80}$$

$$R_{yy} = s^2 + c^2 \, k^2 - 2\, s\, \pi \sum \frac{\omega_p^2}{\Omega_0} \sum_n \int_{-\infty}^{\infty} dp_{\|}$$

$$\int_0^\infty dp_\perp\, p_\perp^2\, \frac{\Omega\,(J_n')^2\,(\partial f_0/\partial p_\perp)}{(s + i\,k_{||}\,v_{||} + i\,n\,\Omega)} \tag{2.81}$$

$$R_{yz} = 2\,i\,s\,\pi \sum \frac{\omega_p^2}{\Omega_0} \sum_n \int_{-\infty}^\infty dp_{||} \int_0^\infty dp_\perp\, p_\perp^2\, \frac{\Omega\, J_n\, J_n' \left(\partial f_0/\partial p_{||}\right)}{(s + i\,k_{||}\,v_{||} + i\,n\,\Omega)} \tag{2.82}$$

$$R_{zx} = -c^2\,k_{||}\,k_\perp - 2\,s\,\pi \sum \frac{\omega_p^2}{\Omega_0} \sum_n \int_{-\infty}^\infty dp_{||}\, p_{||} \int_0^\infty dp_\perp\, p_\perp\, \frac{n\,\Omega^2\, J_n^2\,(\partial f_0/\partial p_\perp)}{k_\perp\, v_\perp\,(s + i\,k_{||}\,v_{||} + i\,n\,\Omega)} \tag{2.83}$$

$$R_{zy} = -2\,i\,s\,\pi \sum \frac{\omega_p^2}{\Omega_0} \sum_n \int_{-\infty}^\infty dp_{||}\, p_{||} \int_0^\infty dp_\perp\, p_\perp\, \frac{\Omega\, J_n\, J_n'\,(\partial f_0/\partial p_\perp)}{(s + i\,k_{||}\,v_{||} + i\,n\,\Omega)} \tag{2.84}$$

$$R_{zz} = s^2 + c^2\,k_\perp^2 - 2\,s\,\pi \sum \frac{\omega_p^2}{\Omega_0} \sum_n \int_{-\infty}^\infty dp_{||}\, p_{||} \int_0^\infty dp_\perp\, p_\perp\, \frac{\Omega\, J_n^2 \left(\partial f_0/\partial p_{||}\right)}{(s + i\,k_{||}\,v_{||} + i\,n\,\Omega)} \tag{2.85}$$

The above integrals are defined for $\Re(s) > 0$ and the argument of the Bessel functions is

$$z = \frac{k_\perp\, v_\perp}{\Omega}. \tag{2.86}$$

To investigate the form of $\underline{\underline{\mathbf{R}}}$ for a specific plasma we must specify a form for the appropriate equilibrium distribution function f_0. In the following chapters we will study two distinct cases, namely that of cold streaming plasmas and plasmas with relativistic Maxwellian distributions.

Chapter 3

Cold Relativistic Streaming Plasmas

> One thing I have learnt in a long life: that all our science, measured against reality is primitive and childlike - and yet it is the most precious thing we have
> *Albert Einstein*

3.1 Introduction

Streaming electron plasmas are one of the most fundamental plasma systems to have been studied by plasma physicists and have merited a great deal of attention over the last several decades (see, for example, Briggs [25]). Our first task in this chapter is to rewrite the basic system of equations in a relativistic format. We will look at the specific case of two counterstreaming electron beams travelling with velocities $+v_0$ and $-v_0$ respectively, where $|v_0|$ is taken to be a significant proportion of the speed of light. A uniform magnetic field B_0 is assumed to exist along the direction of the positive-velocity stream and we will investigate wave propagation parallel to this magnetic field. Our aim is then to replace one of the electron streams with a positron stream and compare the results of the two systems.

Throughout this chapter we make the assumption that the plasma streams are

completely cold, that is there is no thermal spread within each stream (ie every particle in the v_0 stream travels with exactly this velocity). In this zero temperature limit, the streaming distribution function for plasma species ν is

$$f_{0\nu} = \frac{1}{\pi\, p_\perp}\, \delta\,(p_\perp)\, \delta\,(p_{||} - p_{0\nu}), \tag{3.1}$$

where the particles in species ν are taken to be streaming along the direction of the equilibrium magnetic field $\mathbf{B_0}$ with momentum $p_{0\nu}\,(=\gamma_\nu\, m_\nu\, v_{0\nu})$. The delta function is defined so that

$$\int_0^\infty \delta\,(p_\perp)\, dp_\perp = \frac{1}{2}. \tag{3.2}$$

When we substitute this form of distribution function into the components of $\underline{\underline{\mathbf{R}}}$ given by (2.73) and carry out the integrations we obtain the following expressions for the dielectric tensor components:

$$R_{xx} = s^2 + c^2\, k_{||}^2 + \sum_\nu \omega_{p\nu}^2\, \frac{(s + i\, k_{||}\, v_{0\nu})^2}{\Omega_\nu^2 + (s + i\, k_{||}\, v_{0\nu})^2} \tag{3.3}$$

$$R_{xy} = -R_{yx} = \sum_\nu \omega_{p\nu}^2\, \frac{\Omega_\nu\,(s + i\, k_{||}\, v_{0\nu})}{\Omega_\nu^2 + (s + i\, k_{||}\, v_{0\nu})^2} \tag{3.4}$$

$$R_{xz} = R_{zx} = -c^2\, k_\perp\, k_{||} - i \sum_\nu \omega_{p\nu}^2\, \frac{k_\perp\, v_{0\nu}\,(s + i\, k_{||}\, v_{0\nu})}{\Omega_\nu^2 + (s + i\, k_{||}\, v_{0\nu})^2} \tag{3.5}$$

$$R_{yy} = s^2 + c^2\, k^2 + \sum_\nu \omega_{p\nu}^2\, \frac{(s + i\, k_{||}\, v_{0\nu})^2}{\Omega_\nu^2 + (s + i\, k_{||}\, v_{0\nu})^2} \tag{3.6}$$

$$R_{yz} = -R_{zy} = i \sum_\nu \omega_{p\nu}^2\, \frac{k_\perp\, v_{0\nu}\, \Omega_\nu}{\Omega_\nu^2 + (s + i\, k_{||}\, v_{0\nu})^2} \tag{3.7}$$

$$R_{zz} = s^2 + c^2\, k_\perp^2 + \sum_\nu \omega_{p\,\nu}^2\, \frac{s^2}{(s + i\, k_{||}\, v_{0\,\nu})^2} \tag{3.8}$$

$$- \sum_\nu \frac{\omega_{p\nu}^2}{\gamma^2}\, \frac{k_\perp^2\, v_{0\nu}^2}{\Omega_\nu^2 + (s + i\, k_{||}\, v_{0\nu})^2} \tag{3.9}$$

where, you may recall,

$$\Omega_\nu = \frac{q_\nu\, B_0}{\gamma_\nu\, m_\nu} \tag{3.10}$$

is the relativistic cyclotron frequency for species ν and $\omega_{p\nu}$, defined to be

$$\frac{n_{0\nu}\, q_\nu^2}{\epsilon_0\, \gamma_\nu\, m_\nu}, \tag{3.11}$$

is the relativistic plasma frequency for species ν. The total plasma frequency for the whole system is equal to the sum of the individual plasma frequencies, ie

$$\omega_p^2 = \sum_\nu \omega_{p\nu}^2. \tag{3.12}$$

3.2 Wave Propagation Parallel to the Magnetic Field

The case of wave propagation at oblique angles to the magnetic field requires extensive analysis. To simplify the working, we will consider instead waves propagating parallel to the equilibrium magnetic field $\mathbf{B}_0$ (ie $k_{||} = k$, $k_\perp = 0$). The dielectric tensor then reduces to the form

$$\underline{\underline{\mathbf{R}}} = \begin{bmatrix} R_{xx} & R_{xy} & 0 \\ -R_{xy} & R_{yy} & 0 \\ 0 & 0 & R_{zz} \end{bmatrix}. \tag{3.13}$$

The normal modes of the plasma correspond to the solutions of the expression

$$R = det\left(\underline{\underline{\mathbf{R}}}\right) = 0. \tag{3.14}$$

With the form of $\underline{\underline{\mathbf{R}}}$ given above, this results in the following two relations:

$$R_{zz} = 0 \quad \text{and} \quad R_{xx}R_{yy} + R_{xy}^2 = 0, \tag{3.15}$$

which represent the longitudinal and transverse wave modes respectively. We shall investigate each of these modes in turn for both counterstreaming electron-electron and electron-positron beams.

Since our primary interest in this analysis is the study of wave propagation in our plasma systems, we will write the Laplace transform variable in terms of the wave frequency: $s = -i\omega$. The waves would then have a time-dependence of $e^{-i\omega t}$ and the behaviour of the waves would depends on the nature of ω as follows :

ω purely real $\rightarrow$ waves propagate undamped

ω purely imaginary $\rightarrow$ $\omega < 0$: no wave propagation, purely evanescent

$\omega > 0$: waves grow exponentially, instability

ω complex $\rightarrow$ waves propagate, but are either damped or growing

If we now write the components of $\underline{\underline{\mathbf{R}}}$ in terms of ω instead of s, we have the following expressions:

$$R_{xx} = R_{yy} = -\omega^2 + c^2 k_{||}^2 - \sum_{\nu} \omega_{p\nu}^2 \frac{(\omega - k_{||} v_{0\nu})^2}{\Omega_\nu^2 - (\omega - k_{||} v_{0\nu})^2} \tag{3.16}$$

$$R_{xy} = -R_{yx} = -i \sum_{\nu} \omega_{p\nu}^2 \frac{\Omega_\nu (\omega - k_{||} v_{0\nu})}{\Omega_\nu^2 - (\omega - k_{||} v_{0\nu})^2} \tag{3.17}$$

$$R_{zz} = -\omega^2 + \sum_{\nu} \frac{\omega_{p\nu}^2}{\gamma^2} \frac{\omega^2}{(\omega - k_{||} v_{0\nu})^2} \tag{3.18}$$

3.3 Specification of the Plasma System

As stated previously, two distinct plasma systems will be under investigation; namely

(i) counterstreaming electron beams with velocities $\pm v_0$ (with static ions)

(ii) a positron stream with velocity v_0 and an electron stream with velocity $-v_0$.

In the following analysis we will use a subscript e to denote electron quantities and p to denote positron ones.

We will assume that all the plasma streams under consideration have the same number density n_0. Then, since $q_e = -e$, $q_p = e$ and $m_e = m_p = m$, the plasma frequency, by definition, must be the same for both species. (The Lorentz factors of the different streams are the same since they depend only on the square of the velocities.) We can also define

$$\Omega_p = \frac{e B_0}{\gamma m} \equiv \Omega, \tag{3.19}$$

so that

$$\Omega_e = \frac{-e B_0}{\gamma m} \equiv -\Omega. \tag{3.20}$$

In the equilibrium state, the current density is defined to be

$$\mathbf{j}_0 = \sum_{\nu} \frac{n_{0\nu} q_\nu}{m_\nu} \int \frac{\mathbf{p}}{\gamma_\nu} f_{0\nu}(\mathbf{p})\, d\mathbf{p}, \tag{3.21}$$

which reduces to

$$j_{0z} = \sum_{\nu} n_{0\nu}\, q_\nu\, v_{0\nu} \tag{3.22}$$

for the particular distribution function defined by (3.1).

For the counterstreaming electron beams we have $j_{0z} = 0$ so there is no net current flowing in the equilibrium state. For the electron-positron case, however, we have $j_{0z} = 2\, n_0\, e\, v_0$. This non-zero current density will result in an azimuthal contribution to the magnetic field.

Consider Amperé's circuital law, which states that the line integral of $\mathbf{B} \cdot d\mathbf{l}$ around a closed curve C is equal to μ_0 times the current linking C, ie

$$\oint_C \mathbf{B} \cdot d\mathbf{l} = \mu_0 \int_A \mathbf{j} \cdot d\mathbf{A}. \tag{3.23}$$

For the electron-positron case, we have

$$B_\phi = \frac{\mu_0\, j_{0z}\, R}{2} = \mu_0\, n_0\, e\, v_0\, R \tag{3.24}$$

at a distance R from the centre of the stream, assuming that the curve C is contained within the diameter of the stream. If, however, C is outwith the dimensions of the stream, the magnetic field intensity would then be

$$B_\phi = \frac{\mu_0\, n_0\, e\, v_0\, r_s^2}{R} \tag{3.25}$$

where the distance R is greater than the stream radius r_s.

In an attempt to simplify the analysis we will assume that $B_\phi << B_0$ and can be neglected. This allows us to treat the electron-positron case in the same way as the electron-electron case although it will put some restrictions on the allowed values of some of the plasma parameters. Looking at the expression for B_ϕ, it would seem to suggest that there would have to be an upper limit on the density of the streams.

We will now investigate wave propagation in these two plasma systems, looking firstly at the longitudinal mode and then at the transverse modes.

3.4 The Longitudinal Mode

Longitudinal waves are defined as having their electric field parallel to the wave vector, ie $\mathbf{E} \parallel \mathbf{k}$. As $\mathbf{k}$ has already been specified as being in the direction of $\mathbf{B}_0$, we

must have $\mathbf{E} = (0, 0, E_{||})$ for these waves and thus $R_{zz} = 0$. The general dispersion relation for longitudinal waves is then given by

$$1 - \sum_{\nu} \omega_{p\nu}^2 \frac{1}{\gamma_\nu^2 (\omega - k_{||} v_{0\nu})^2} = 0. \tag{3.26}$$

We will now specify each of the plasma systems in turn.

3.4.1 Electron-Electron Streams

The dispersion relation for counterstreaming electron beams is

$$1 - \frac{\omega_p^2}{\gamma^2} \left\{ \frac{1}{(\omega - k_{||} v_0)^2} + \frac{1}{(\omega + k_{||} v_0)^2} \right\} = 0. \tag{3.27}$$

Compare this with the non-relativistic case.

3.4.2 Non-relativistic Beams

The non-relativistic counterpart of the contrastreaming electron beams, described in the previous section has been studied extensively and the associated two-stream instability is well documented in most standard plasma physics texts. The dispersion relation for two counterstreaming electron beams travelling with non-relativistic velocities $\pm v_{nr}$, as given in Sturrock [26], is

$$1 - \frac{\omega_{pnr}^2}{(\omega - v_{nr}\, k)^2} - \frac{\omega_{pnr}^2}{(\omega + v_{nr}\, k)^2}, \tag{3.28}$$

where $\omega_{p_{nr}} = \sqrt{n\, e^2 / \epsilon_0\, m}$ is the usual non-relativistic plasma frequency.

Solving this equation for ω^2 gives the result

$$\omega^2 = \omega_{pnr}^2 + v_{nr}^2\, k^2 \pm \omega_{p_{nr}} \sqrt{\omega_{pnr}^2 + 4\, v_{nr}^2\, k^2}. \tag{3.29}$$

If we now let $v_{nr}\, k = b\, \omega_{p_{nr}}$, where b is a positive quantity, then the roots reduce to the form

$$\omega^2 = \left[1 + b^2 \pm \sqrt{1 + 4\, b^2} \right] \omega_{p_{nr}}^2. \tag{3.30}$$

For the positive sign, the function within the square brackets will always be greater than zero and ω will be a real quantity. The negative sign, however, can result in more interesting behaviour. The plot of the function $f(b) = 1 + b^2 - \sqrt{1 + 4\, b^2}$

against ω is shown in Fig 3.1. We can see that for $b < \sqrt{2}$, the function f, and therefore ω^2, will be negative which means that there will be two imaginary roots. One of these roots corresponds to a growing wave. We can therefore say that the two-stream instability exists for $v_{nr}\, k < \sqrt{2}\,\omega_{p_{nr}}$.

If we now return to the relativistic dispersion relation (3.27), we find that the equivalent roots of this expression are

$$\omega^2 = \frac{1}{\gamma^2}\left\{\gamma^2 k_{||}^2 v_0^2 + \omega_p^2 \pm \omega_p \sqrt{\omega_p^2 + 4\,\gamma^2 k_{||}^2 v_0^2}\right\}. \tag{3.31}$$

If we set $\gamma\, k_{||}\, v_0 = b\,\omega_p$, we can follow the same analysis as above to find the range of wave numbers for which the waves are unstable. In this case, we find that the waves are unstable for $k_{||}\, v_0 < \sqrt{2}\,\omega_p/\gamma$.

3.4.3 Electron-Positron Streams

For the case of counterstreaming relativistic electron-positron beams, the dispersion relation is

$$1 - \frac{\omega_p^2}{\gamma^2}\left\{\frac{1}{(\omega - k_{||}\, v_0)^2} + \frac{1}{(\omega + k_{||}\, v_0)^2}\right\} = 0. \tag{3.32}$$

This is exactly equal to the dispersion relation for the counterstreaming electron beams (3.27). Therefore, the two-stream instability exists in the electron-positron plasma under exactly the same conditions as for the electron-electron plasma. So replacing one of the electron streams with a positron stream seems to have no effect on the physical behaviour of the longitudinal waves.

3.5 The Transverse Mode

For transverse waves, the electric field is normal to the wave vector. So, for the system we defined above, this requires $E_z = 0$, $E_x, E_y \neq 0$ and the dispersion relation of interest is

$$R_{xx}\, R_{yy} + R_{xy}^2 = 0. \tag{3.33}$$

Since the electric field is perpendicular to the magnetic field these are electromagnetic waves. Looking back to the components of $\underline{\underline{\mathbf{R}}}$, given by (3.16) - (3.18), we can see that this expression is rather more involved than the dispersion relation for

longitudinal waves. Again, we will specify the relation for the two plasma systems under investigation.

3.5.1 Electron-Electron Streams

After some straightforward manipulation, the dispersion relation can be written as

$$\begin{aligned} F_{ee}(\omega) &= \left[\omega^2 - c^2 k_{||}^2 - \omega_p^2 \left\{ \frac{\omega - k_{||} v_0}{\omega - k_{||} v_0 + \Omega} + \frac{\omega + k_{||} v_0}{\omega + k_{||} v_0 + \Omega} \right\}\right] \\ &\times \left[\omega^2 - c^2 k_{||}^2 - \omega_p^2 \left\{ \frac{\omega - k_{||} v_0}{\omega - k_{||} v_0 - \Omega} + \frac{\omega + k_{||} v_0}{\omega + k_{||} v_0 - \Omega} \right\}\right] \\ &= 0 \end{aligned} \tag{3.34}$$

We would like to express the function F_{ee} in terms of dimensionless variables. To this end, we will introduce the following quantities:

$$\hat{\omega} = \frac{\omega}{\Omega}, \qquad \hat{k} = \frac{c\, k_{||}}{\Omega}, \qquad \eta = \frac{\omega_p}{\Omega}, \qquad u = \frac{v_0}{c}. \tag{3.35}$$

In terms of these non-dimensional variables, the function F_{ee} becomes

$$\begin{aligned} F_{ee}(\hat{\omega}) &= \Omega^4 \left[\hat{\omega}^2 - \hat{k}^2 - \eta^2 \left\{ \frac{\hat{\omega} - u\hat{k}}{\hat{\omega} - u\hat{k} + 1} + \frac{\hat{\omega} + u\hat{k}}{\hat{\omega} + u\hat{k} + 1} \right\}\right] \\ &\times \left[\hat{\omega}^2 - \hat{k}^2 - \eta^2 \left\{ \frac{\hat{\omega} - u\hat{k}}{\hat{\omega} - u\hat{k} - 1} + \frac{\hat{\omega} + u\hat{k}}{\hat{\omega} + u\hat{k} - 1} \right\}\right] \end{aligned} \tag{3.36}$$

which we will write as

$$F_{ee}(\hat{\omega}) \equiv \Omega^4 \hat{F}_{ee}(\hat{\omega}). \tag{3.37}$$

3.5.2 Electron-Positron Streams

When we repeat the analysis of the last section for the case of counterstreaming electron-positron beams, we obtain the dispersion relation

$$\begin{aligned} F_{ep}(\omega) &= \left[\omega^2 - c^2 k_{||}^2 - \omega_p^2 \left\{ \frac{\omega - k_{||} v_0}{\omega - k_{||} v_0 - \Omega} + \frac{\omega + k_{||} v_0}{\omega + k_{||} v_0 + \Omega} \right\}\right] \\ &\times \left[\omega^2 - c^2 k_{||}^2 - \omega_p^2 \left\{ \frac{\omega - k_{||} v_0}{\omega - k_{||} v_0 + \Omega} + \frac{\omega + k_{||} v_0}{\omega + k_{||} v_0 - \Omega} \right\}\right] \\ &= 0. \end{aligned} \tag{3.38}$$

Scaling the equation in the same way as before, we get

$$F_{ep}(\omega) \equiv \Omega^4 \hat{F}_{ep}(\hat{\omega}) \tag{3.39}$$

where

$$\hat{F}_{ep}(\hat{\omega}) = \left[\hat{\omega}^2 - \hat{k}^2 - \eta^2 \left\{ \frac{\hat{\omega} - u\hat{k}}{\hat{\omega} - u\hat{k} - 1} + \frac{\hat{\omega} + u\hat{k}}{\hat{\omega} + u\hat{k} + 1} \right\}\right] \times \left[\hat{\omega}^2 - \hat{k}^2 - \eta^2 \left\{ \frac{\hat{\omega} - u\hat{k}}{\hat{\omega} - u\hat{k} + 1} + \frac{\hat{\omega} + u\hat{k}}{\hat{\omega} + u\hat{k} - 1} \right\}\right]. \quad (3.40)$$

When we compare the functions $\hat{F}_{ee}$ and $\hat{F}_{ep}$ ((3.36 and (3.40) respectively) we see that there is very little difference between the two expressions and the question we have to ask is: do these small differences result in a significant difference in the physical behaviour of the two systems?

We will now try to answer this question.

3.5.3 Investigation of the Dispersion Functions

The dispersion functions $\hat{F}_{ee}$ and $\hat{F}_{ep}$ are both eighth order polynomials in the variable $\hat{\omega}$. By investigating the form of these functions, we can determine the nature of the wave propagation through the respective plasma systems.

The transverse modes are given by the roots of the equations $\hat{F}_{ee} = 0$ and $\hat{F}_{ep} = 0$. Finding these roots analytically can only be attempted with the aid of a computer algebra package like MAPLEV or REDUCE and even then the results are made up of so many pages of algebra that no useful information can be gained from them. Instead we shall proceed by investigating the nature of the roots numerically.

For all of the results given, u has been set equal to $0.5\,c$ and the corresponding frequency term $u\hat{k}$ has been taken in the range

$$0.5 < u\hat{k} < 1.5. \quad (3.41)$$

The parameter η was specified to have the values: 15, 1, 0.1.

Specifying values for the above quantities reduces $\hat{F}_{ee}$ and $\hat{F}_{ep}$ to functions of $\hat{\omega}$ alone. We can then easily find the roots of these functions using a computer algebra package. Recall that the waves in the plasma have an $e^{-i\hat{\omega}t}$ dependence and their nature depends on whether the root $\hat{\omega}$ is real, imaginary or fully complex.

3.5.4 Results

The functions $\hat{F}_{ee}$ and $\hat{F}_{ep}$ were plotted against $\hat{\omega}$ for all the different parameter values stated above and the resulting graphs are shown in Figs 3.4-3.18. In some cases, not all the zeros are shown: $\hat{\omega}$ was restricted to the range $[-3, 3]$ to emphasize the behaviour of the functions around the asymptotes.

The graphs illustrate some interesting features of the behaviour of the two dispersion functions. Figs 3.13-3.18 show the functions for the frequencies $u\,\hat{k} = 1.1$ and $u\,\hat{k} = 1.5$, for all values of η. In each of these graphs, it is clear that the functions $\hat{F}_{ee}$ and $\hat{F}_{ep}$ are very similar; the two curves have exactly the same shape and, more significantly, all their roots are real. As there are no imaginary roots, there can be no unstable modes present in either of the two systems for these frequency values.

For $u\,\hat{k} = 0.5$, the behaviour of the functions $\hat{F}_{ee}$ and $\hat{F}_{ep}$ depends on the value of η. The functions for $\eta = 15$ are shown in Fig 3.4. The shape of the two functions is very similar, the only difference is that the portion of the $\hat{F}_{ep}$ curve in the interval $[-0.5, 0.5]$ is entirely negative whereas the corresponding part of the $\hat{F}_{ee}$ curve crosses the axis twice. This indicates that $\hat{F}_{ep}$ has two less real roots than $\hat{F}_{ee}$, and thus must have two imaginary roots instead. For $\eta = 1$, shown in Fig 3.5, $\hat{F}_{ep}$ also has two imaginary roots but here the shapes of the curves are different throughout the range. Fig 3.6 shows the curves for $\eta = 0.1$ and here the behaviour is the same as that described above for frequencies $u\,\hat{k} > 1$: the roots of $\hat{F}_{ee}$ and $\hat{F}_{ep}$ are all real and the curves have the same shape. Therefore $\hat{F}_{ep}$ cannot have any imaginary roots.

The situation for $u\,\hat{k} = 0.9$ is similar to that for $u\,\hat{k} = 0.5$; the relative behaviour of the two functions depends on the value of η. For $\eta = 15$, the shapes of the curves are quite different and $\hat{F}_{ep}$ has two less real roots than $\hat{F}_{ee}$, indicating the presence of an unstable mode. This behaviour is repeated for $\eta = 1$. There are no unstable modes for $\eta = 0.1$ however. For this case, the two curves arevery similar in shape and the roots of both functions are all real.

One of the most striking differences between $\hat{F}_{ee}$ and $\hat{F}_{ep}$ occurs for $u\,\hat{k} = 1$. Here $\hat{F}_{ee}$ has an asymptote at $\hat{\omega} = 0$ which is absent in $\hat{F}_{ep}$. $\hat{F}_{ee}$ also has two more real roots than $\hat{F}_{ep}$ for all values of η. However, $\hat{F}_{ep}$ reduces to a sixth order polynomial

when $u\,\hat{k} = 1$ and so its roots are still all real.

To investigate the roots more thoroughly we used the MAPLEV computer algebra package to evaluate the roots of the functions for all the $u\,\hat{k}$ and η values under consideration. The roots of $\hat{F}_{ee}$ are given in Table 3. 1 and those of $\hat{F}_{ep}$ in Table 3. 2.

For the electron-electron plasma we can see that, in all cases, $\hat{F}_{ee} = 0$ has eight real roots. The electron-positron plasma, on the other hand, has only six real roots plus a complex conjugate pair in four of the cases looked at. In each of these cases the positive imaginary root $i\,\hat{\omega}_i$ corresponds to an unstable mode, as the wave would then have a time-dependence of $e^{\hat{\omega}_i}$, where $\hat{\omega}_i$ is positive. From Table 3. 2, we can see that these instabilities occur for values of $u\,\hat{k} < 1$ and $\eta \geq 1$.

First impressions suggest that there may be a change of behaviour at $u\,\hat{k} = 1$. We will now investigate the form of the roots of $\hat{F}_{ep}$ more closely. By retaining $u\,\hat{k}$ and η as unspecified variables, the roots we obtain for the dispersion relation are general expressions in these quantities. To simplify the algebra we will, as before, set $u = 0.5$. The roots will then depend on $\hat{k}$ and η. By specifying numerical values for these quantities, the roots just reduce to the results presented in the Tables 3. 1 and 3. 2. If we do this we find that the imaginary roots obtained above all descend from the same pair of general roots given by

$$\pm\ \frac{1}{4}\left[10\,\hat{k}^2 - 8\,\hat{k} + 8 + 16\,\eta^2 - 2\left(9\,\hat{k}^4 + 24\,\hat{k}^3 - 8\,\hat{k}^2 + 48\,\eta^2\,\hat{k}^2 - 32\,\hat{k} + 16 + 64\,\eta^2 + 64\,\eta^4\right)^{1/2}\right]^{1/2}. \tag{3.42}$$

Denote the expression contained in the square brackets by $f(\eta, \hat{k})$. If $f(\eta, \hat{k}) < 0$ then the roots will be imaginary. As it stands, $f(\eta, \hat{k})$ is rather difficult to analyse, any manipulation we try will only result in an involved and unhelpful expression in η and $\hat{k}$. We will attempt to simplify the situation by specifying a value for $\hat{k}$ and reducing f to a function of η only. By investigating the behaviour of this function we will determine over what range of η values the unstable modes exist. Let $\hat{k} = 1$ (which means $u\,\hat{k} = 0.5$), so that

$$f(\eta, 1) = 10 + 16\,\eta^2 - 2\left(64\,\eta^4 + 112\,\eta^2 + 9\right)^{1/2} \tag{3.43}$$

η $u\,\hat{k}$	15	1	0.1
0.5	± 21.742 ± 20.744 ± 1.207 ± 0.205	± 2.226 ± 1.468 ± 1.177 ± 0.065	± 1.508 ± 1.010 ± 1.005 ± 0.487
0.9	± 21.793 ± 20.798 ± 1.530 ± 0.525	± 2.642 ± 2.132 ± 1.601 ± 0.111	± 1.923 ± 1.803 ± 1.783 ± 0.097
1.0	± 21.810 ± 20.817 ± 1.619 ± 0.612	± 2.768 ± 2.310 ± 1.723 ± 0.182	± 2.053 ± 2.003 ± 1.953 ± 0.002
1.1	± 21.829 ± 20.837 ± 1.710 ± 0.702	± 2.902 ± 2.491 ± 1.846 ± 0.257	± 2.224 ± 2.203 ± 2.081 ± 0.102
1.5	± 21.923 ± 20.938 ± 2.085 ± 1.070	± 3.500 ± 3.234 ± 2.331 ± 0.597	± 3.007 ± 3.002 ± 2.496 ± 0.501

Table 3.1: Roots of $\hat{F}_{ee} = 0$

η $u\hat{k}$	15	1	0.1
0.5	$\pm$ 21.272 $\pm$ 21.248 $\pm$ 0.867 $\pm$ 0.499 i	$\pm$ 2.097 $\pm$ 1.824 $\pm$ 0.923 $\pm$ 0.274 i	$\pm$ 1.508 $\pm$ 1.016 $\pm$ 0.998 $\pm$ 0.487
0.9	$\pm$ 21.334 $\pm$ 21.292 $\pm$ 1.310 $\pm$ 0.299 i	$\pm$ 2.557 $\pm$ 2.297 $\pm$ 1.521 $\pm$ 0.167 i	$\pm$ 1.923 $\pm$ 1.806 $\pm$ 1.781 $\pm$ 0.097
1.0	$\pm$ 21.354 $\pm$ 21.307 $\pm$ 1.417	$\pm$ 2.690 $\pm$ 2.449 $\pm$ 1.663	$\pm$ 2.052 $\pm$ 2.005 $\pm$ 1.952
1.1	$\pm$ 21.376 $\pm$ 21.325 $\pm$ 1.524 $\pm$ 0.330	$\pm$ 2.830 $\pm$ 2.610 $\pm$ 1.801 $\pm$ 0.199	$\pm$ 2.222 $\pm$ 2.204 $\pm$ 2.081 $\pm$ 0.102
1.5	$\pm$ 21.481 $\pm$ 21.413 $\pm$ 1.944 $\pm$ 0.861	$\pm$ 3.448 $\pm$ 3.302 $\pm$ 2.316 $\pm$ 0.586	$\pm$ 3.006 $\pm$ 3.003 $\pm$ 2.496 $\pm$ 0.501

Table 3.2: Roots of $\hat{F}_{ep} = 0$

and specifying $f(\eta, 1) < 0$ leads to the condition

$$\eta > \sqrt{0.5} = 0.707. \tag{3.44}$$

Thus, the roots will have the form of a complex conjugate pair, with one root leading to instability, for $\eta > 0.707$. Fig 3.2 shows the function $F(\eta, 1)$ plotted as a function of η. The graph agrees with the result obtained here as it shows that the function $f(\eta, 1)$ is negative for the range $|\eta| > 0.707$.

The function $f(\eta, \hat{k})$ has a similar form for all values of $u\hat{k} < 1$. So each will have a comparable instability condition, although the zeros of $f(\eta, \hat{k})$ will necessarily change because of their dependence on $\hat{k}$.

If $u\hat{k} \geq 1$ then the corresponding function $f(\eta)$ has a completely different shape from that obtained above. Fig 3.3 shows $f(\eta)$ plotted against η for $u\hat{k} = 1.5$. Here we can see that the function f has no zeros and is always positive. Therefore, for this value of $u\hat{k}$ the roots are always real and there is no instability. This is in agreement with the results shown in Table 3. 2. Similar graphs will exist for all $u\hat{k}$ values greater than unity.

Returning to the $u\hat{k} < 1$ case, we want to compare the range of η values for which the instability is present for several different $u\hat{k}$ values. This is shown in Table 3. 3 below.

$u\hat{k}$	unstable when $\eta >$
0.5	0.707
0.9	0.424
0.95	0.308
0.97	0.241
0.99	0.141
0.999	0.045

Table 3.3: The range of η values for which the instability is present for given $u\hat{k}$ values.

These values clearly indicate that as $u\hat{k}$ approaches unity, the unstable mode

is present for all values of η. The instability, though, is completely absent when $u\hat{k} = 1$. If we set $u\hat{k} = 1$ (ie let $\hat{k} = 2$ in the expression for f) then we find $f(\eta, 2) = 0$ for all values of η. This value of $u\hat{k}$ seems to separate two different types of behaviour which can be summarised as follows:

$$0 \leq u\hat{k} < 1 \quad : \quad \text{roots are a complex conjugate pair.} \tag{3.45}$$

$$u\hat{k} \geq 1 \quad : \quad \text{roots are real} \tag{3.46}$$

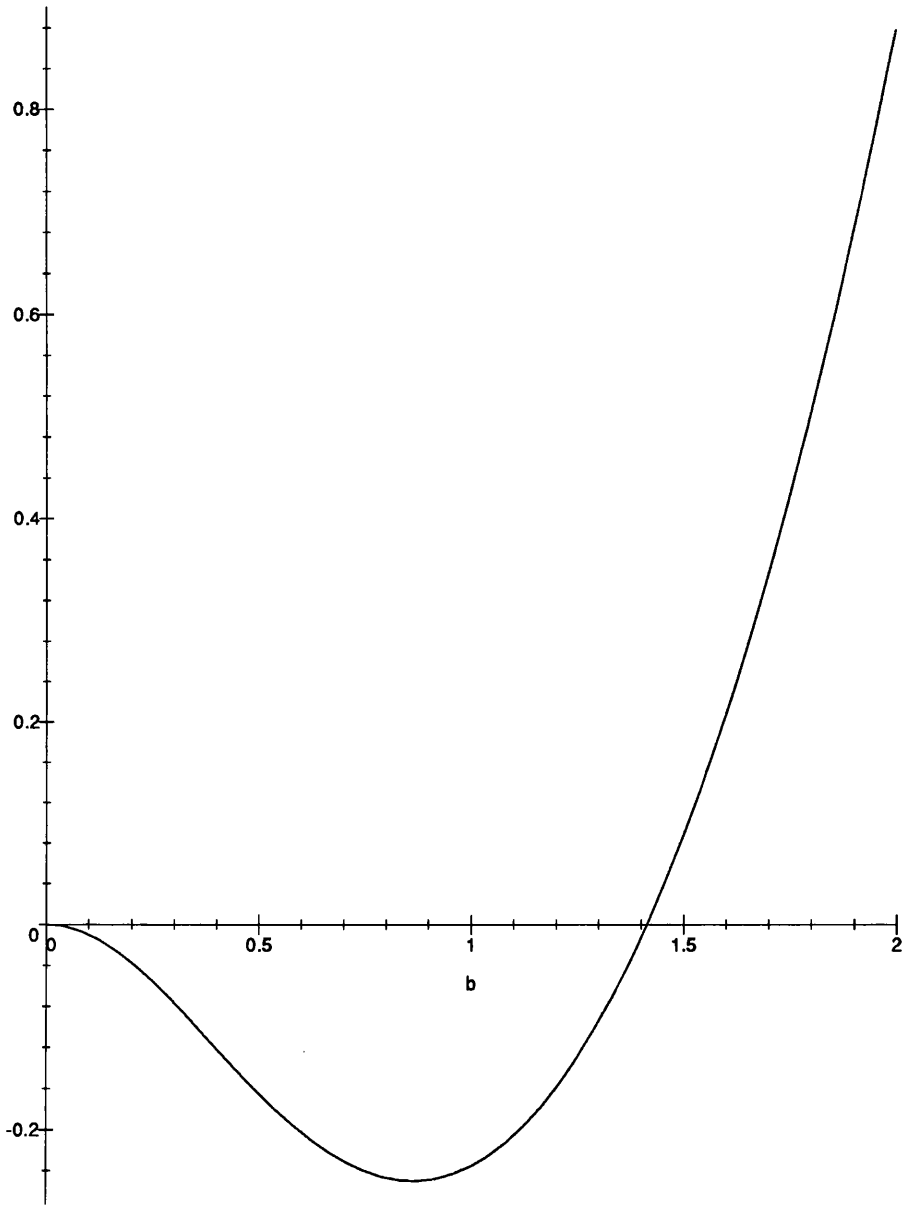

Figure 3.1: The function $f(b) = 1 + b^2 - (1 + 4\,b^2)^{1/2}$ plotted against b.

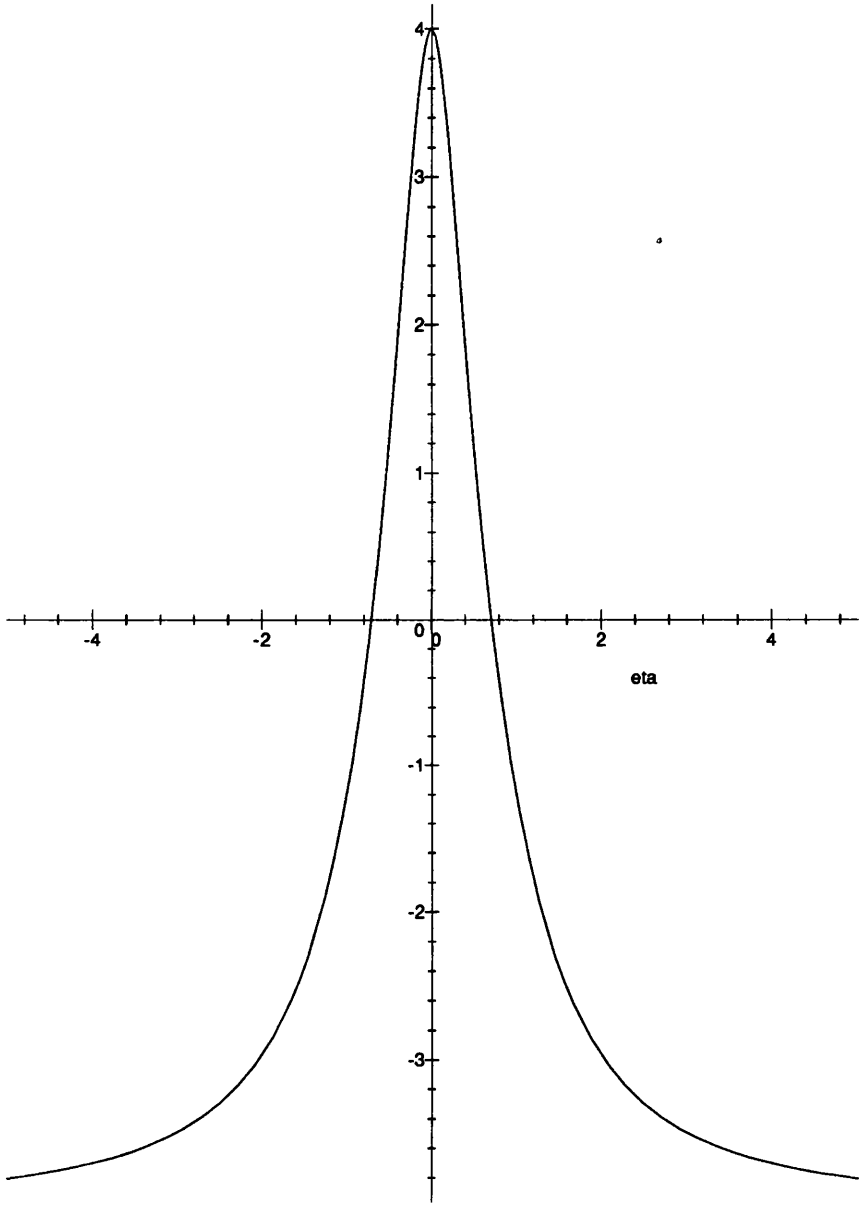

Figure 3.2: The function $f(\eta, k = 1)$ plotted as a function of η.

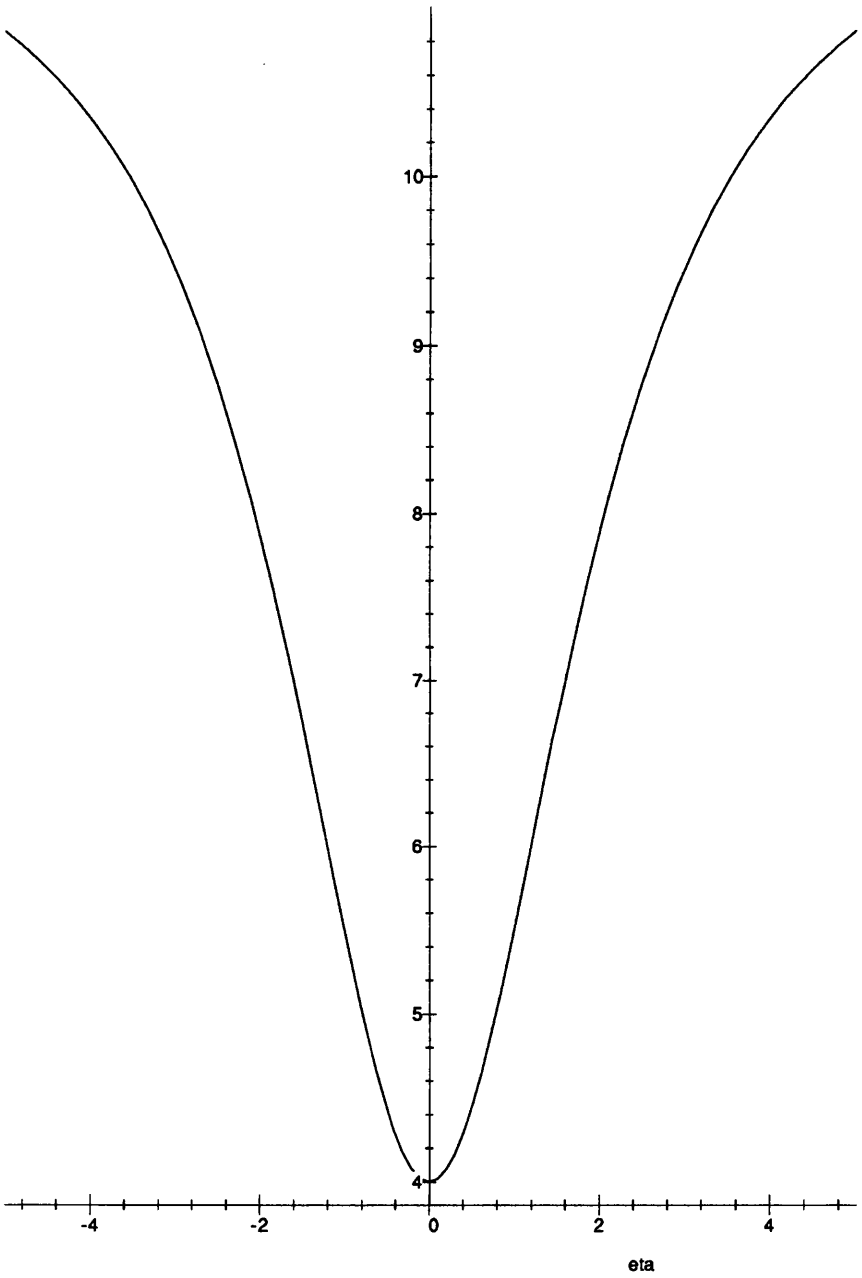

Figure 3.3: The function $f(\eta, k = 3)$ plotted as a function of η.

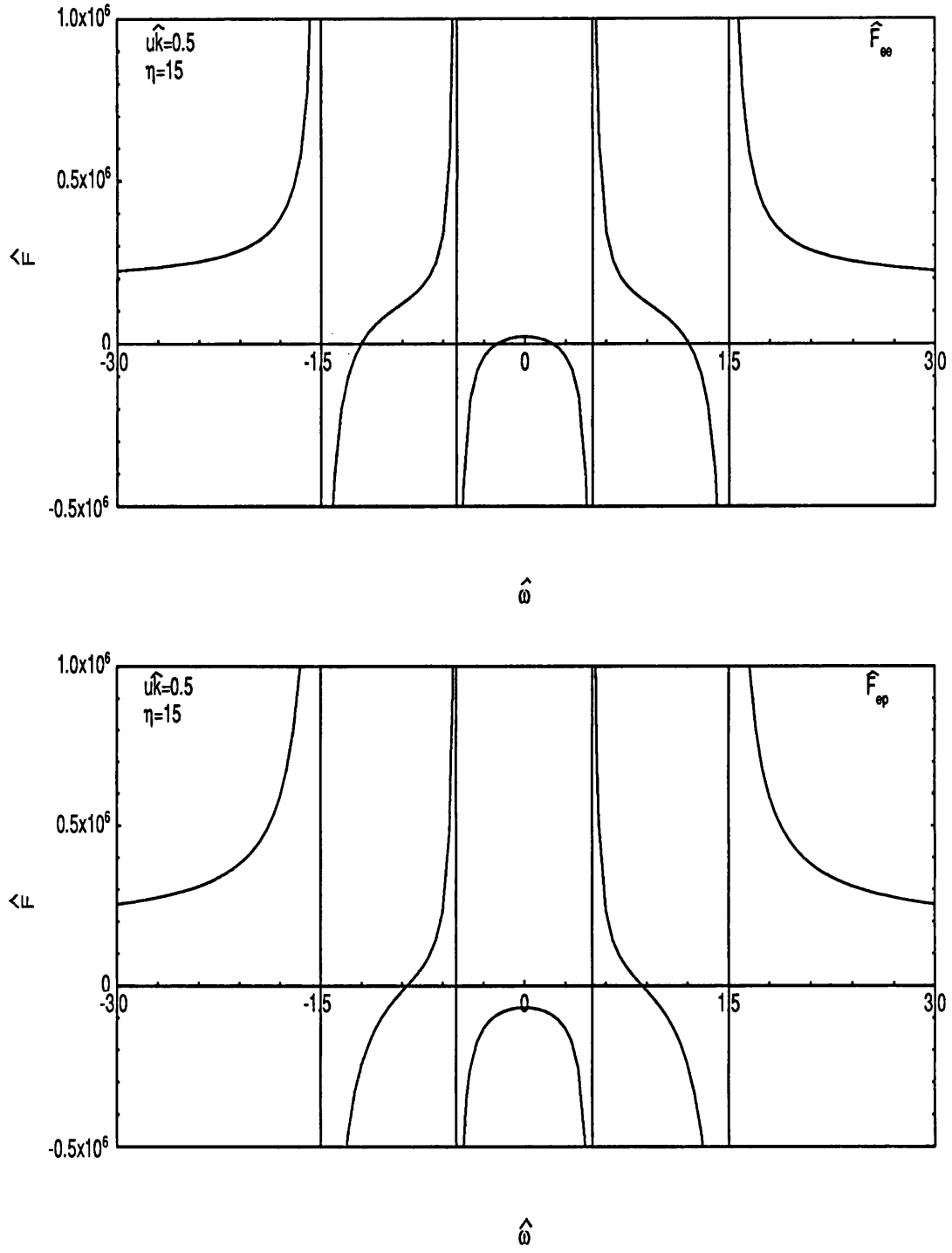

Figure 3.4: The function $\hat{F}(\hat{\omega})$ plotted against $\hat{\omega}$ for $u\hat{k} = 0.5$ and $\eta = 15$.

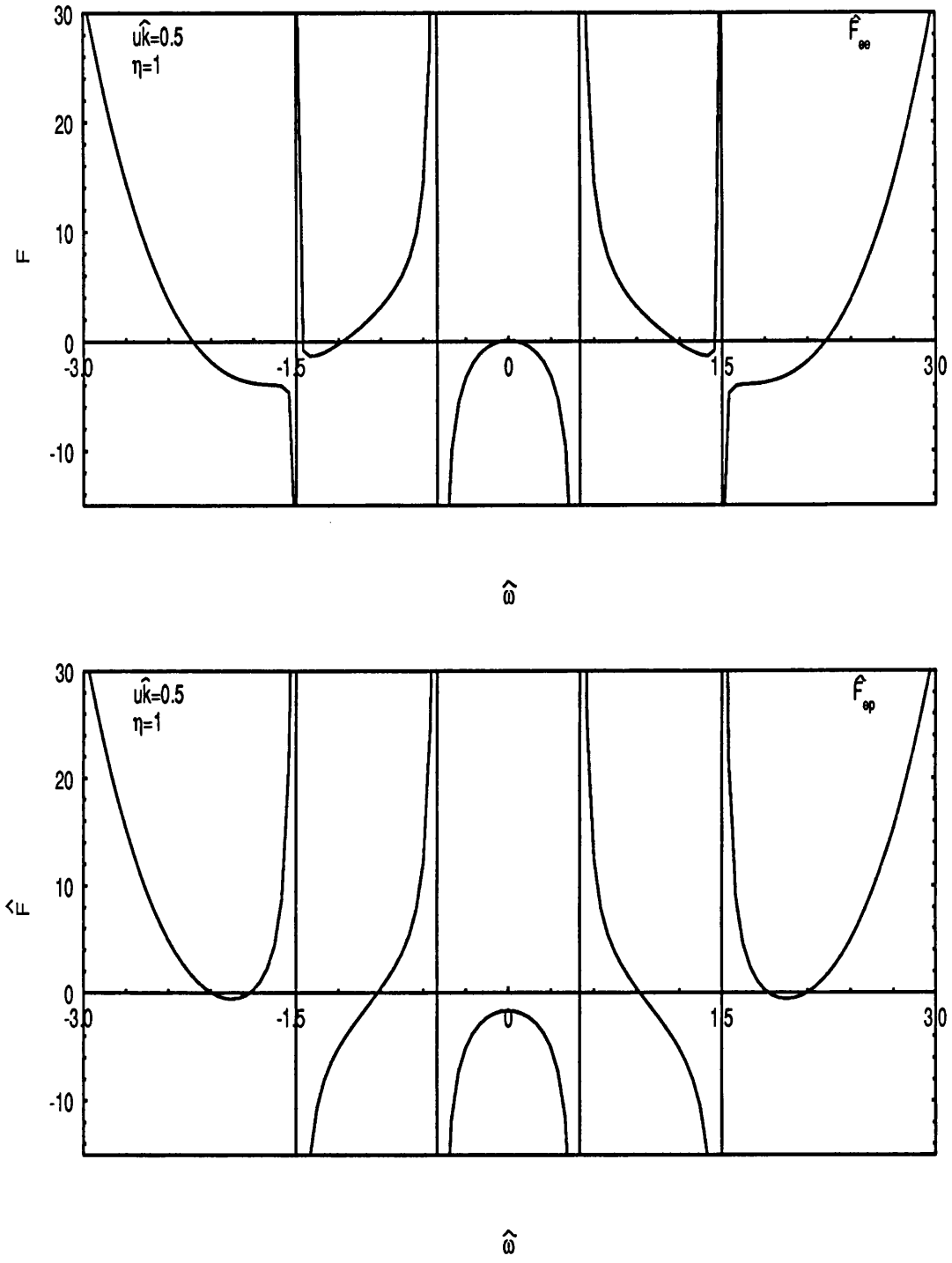

Figure 3.5: The function $\hat{F}(\hat{\omega})$ plotted against $\hat{\omega}$ for $u\hat{k} = 0.5$ and $\eta = 1$.

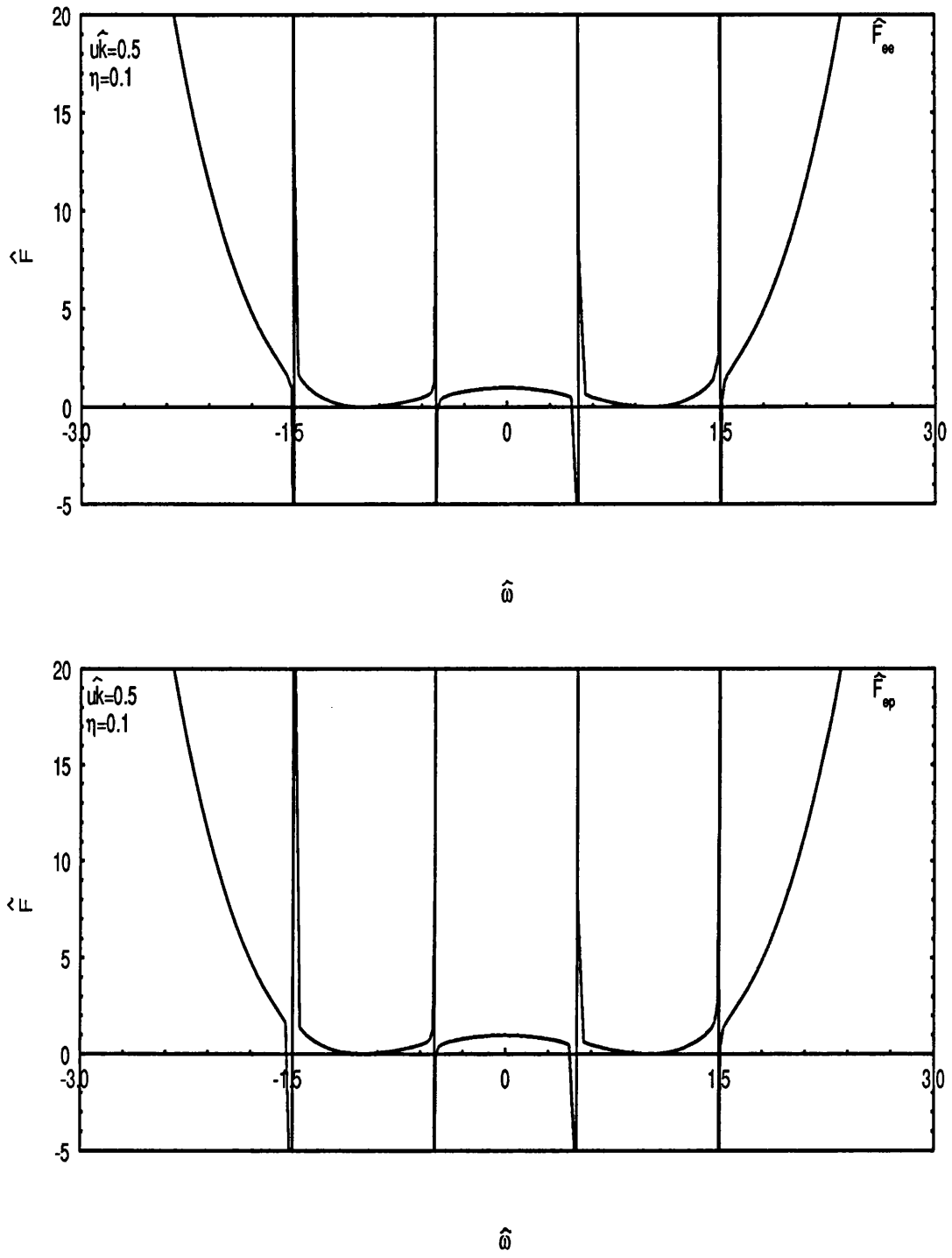

Figure 3.6: The function $\hat{F}(\hat{\omega})$ plotted against $\hat{\omega}$ for $u\hat{k} = 0.5$ and $\eta = 0.1$.

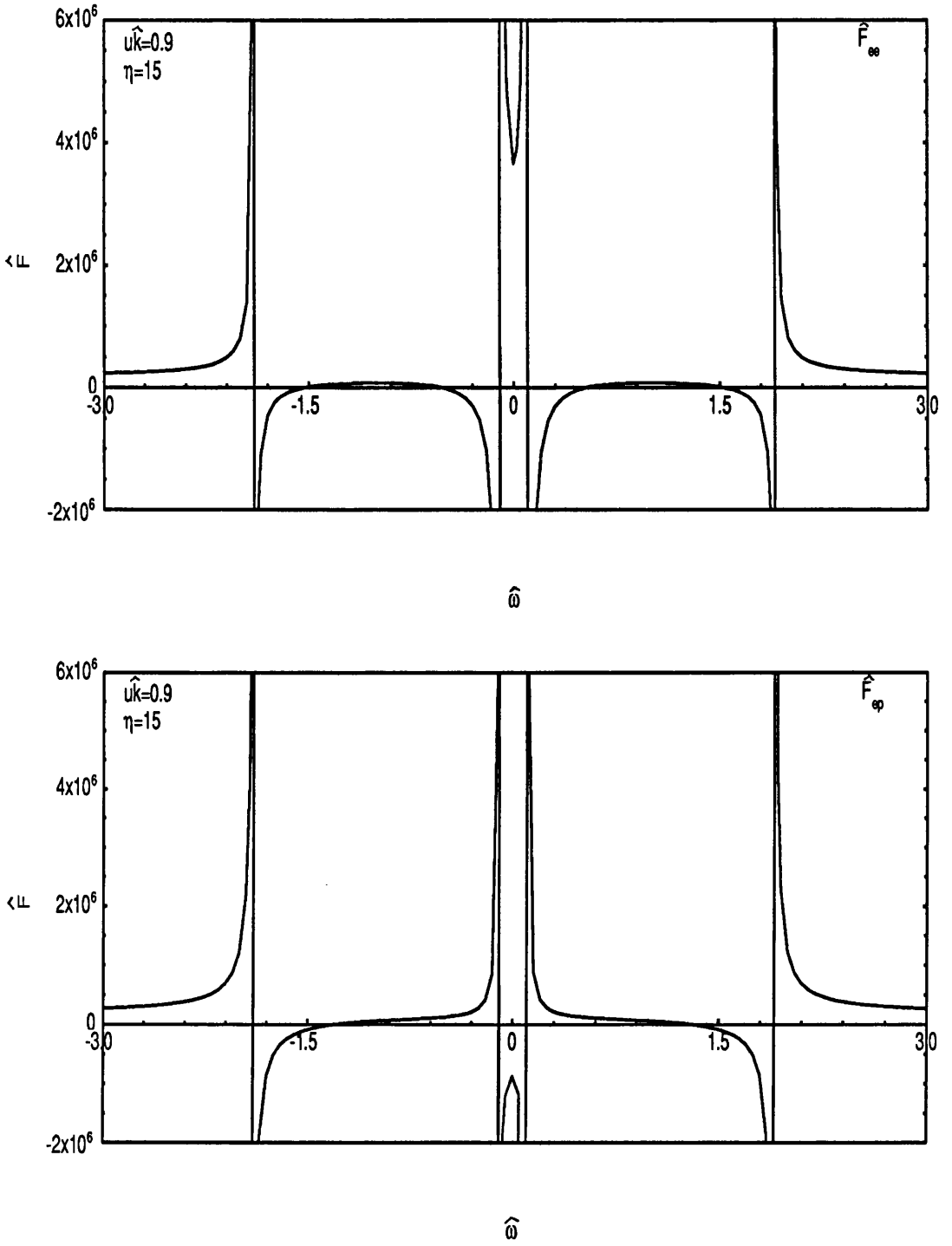

Figure 3.7: The function $\hat{F}(\hat{\omega})$ plotted against $\hat{\omega}$ for $u\hat{k} = 0.9$ and $\eta = 15$.

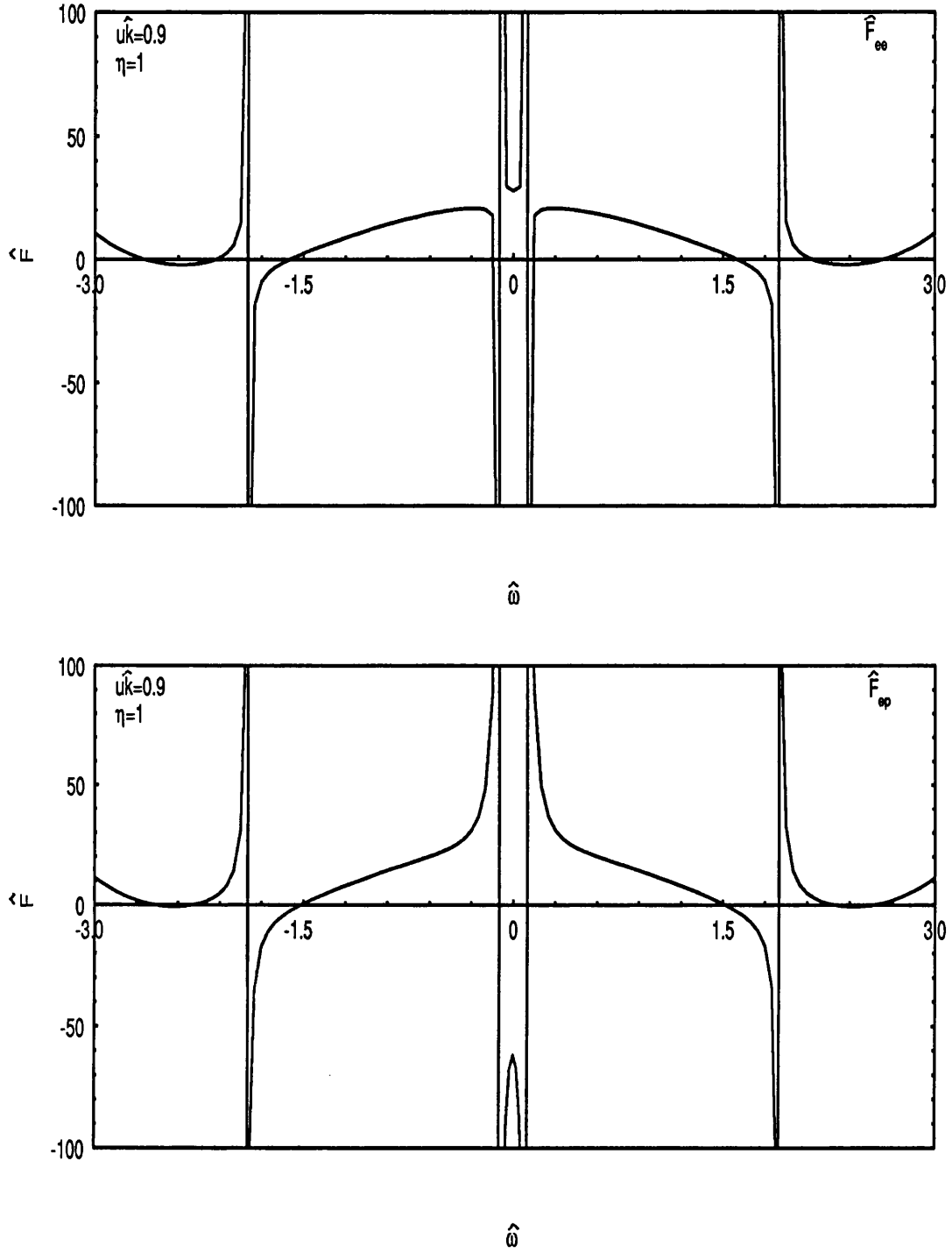

Figure 3.8: The function $\hat{F}(\hat{\omega})$ plotted against $\hat{\omega}$ for $u\hat{k} = 0.9$ and $\eta = 1$.

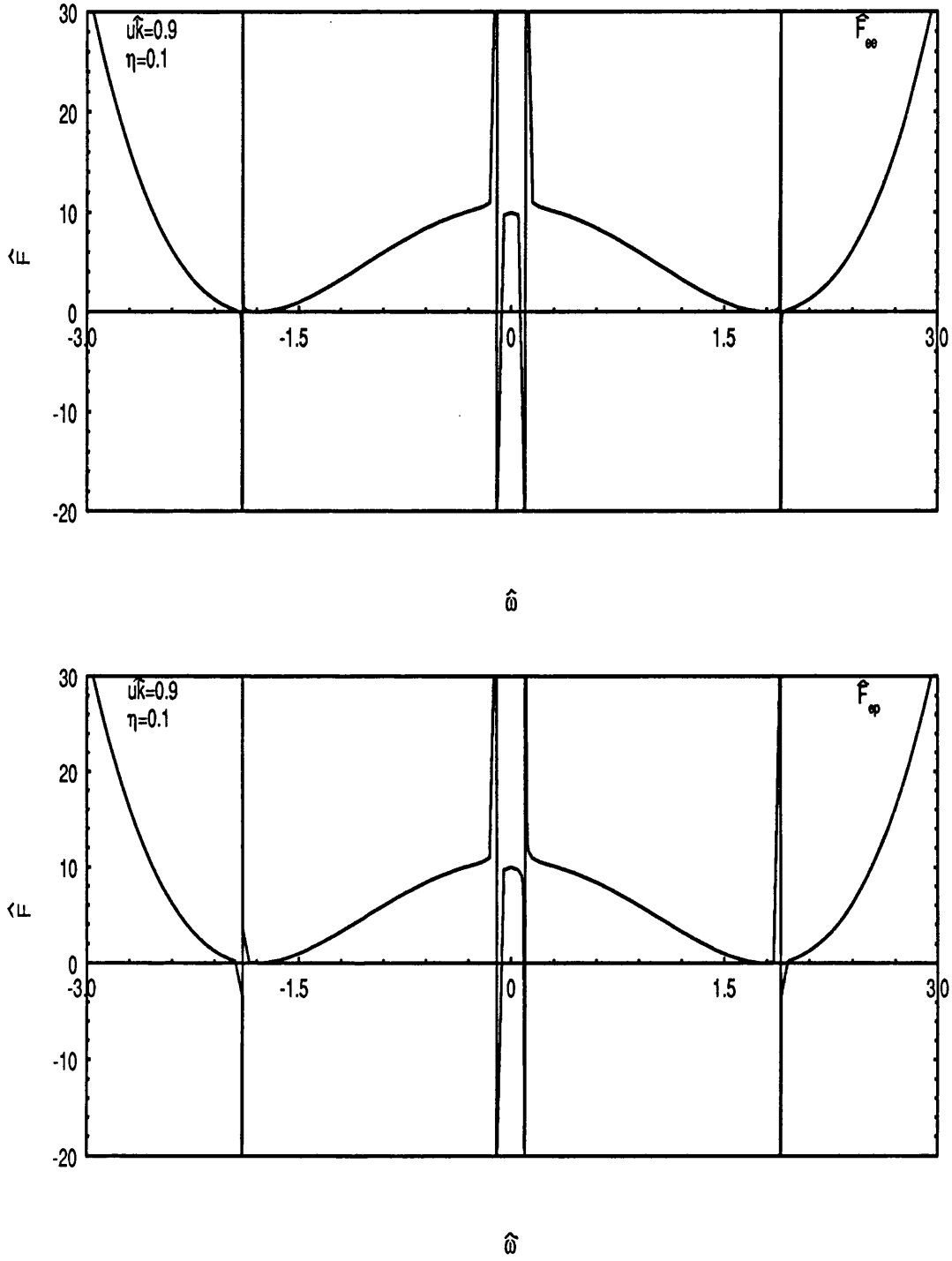

Figure 3.9: The function $\hat{F}(\hat{\omega})$ plotted against $\hat{\omega}$ for $u\hat{k} = 0.9$ and $\eta = 0.1$.

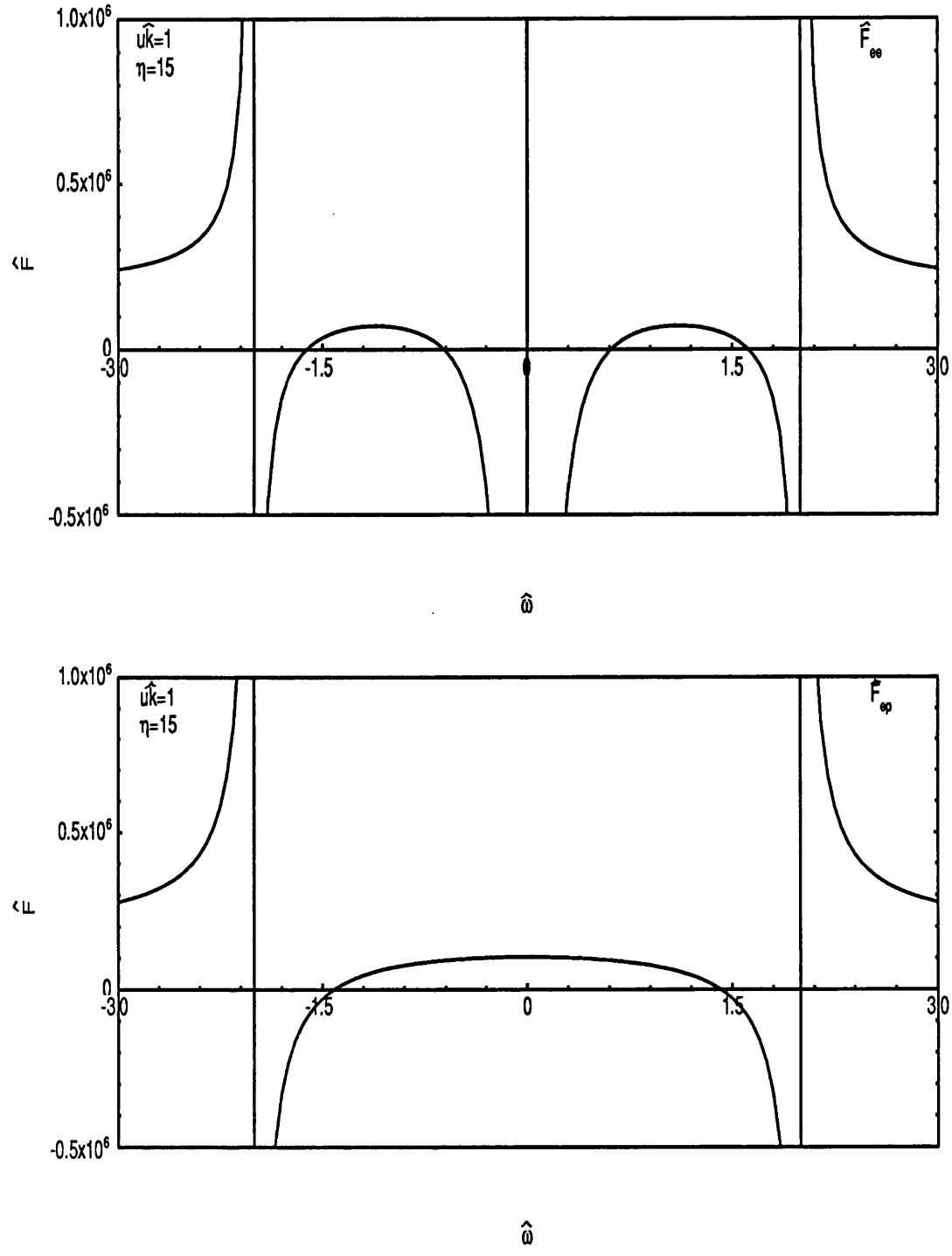

Figure 3.10: The function $\hat{F}(\hat{\omega})$ plotted against $\hat{\omega}$ for $u\hat{k} = 1$ and $\eta = 15$.

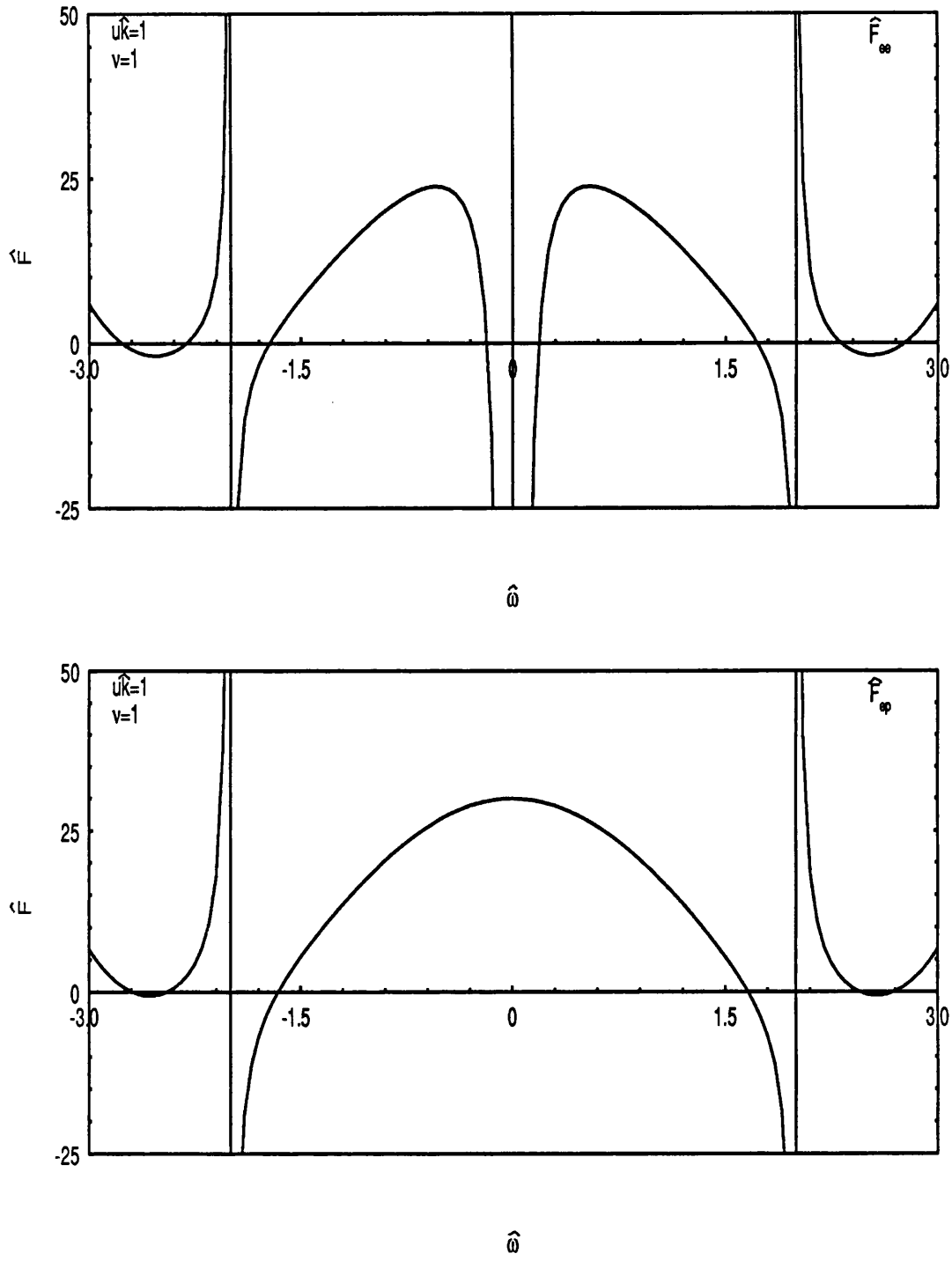

Figure 3.11: The function $\hat{F}(\hat{\omega})$ plotted against $\hat{\omega}$ for $u\hat{k} = 1$ and $\eta = 1$.

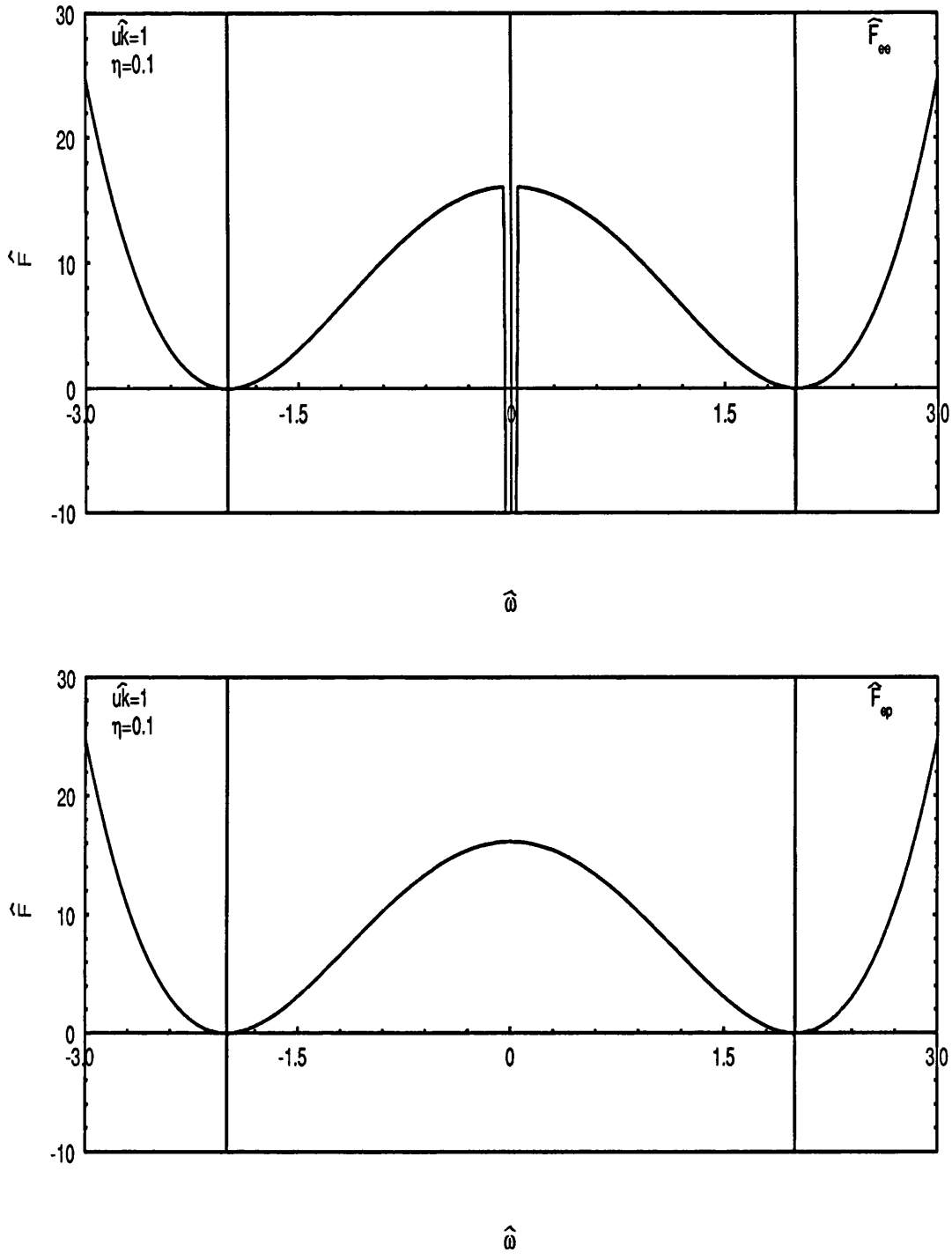

Figure 3.12: The function $\hat{F}(\hat{\omega})$ plotted against $\hat{\omega}$ for $\hat{u}\,\hat{k} = 1$ and $\eta = 0.1$.

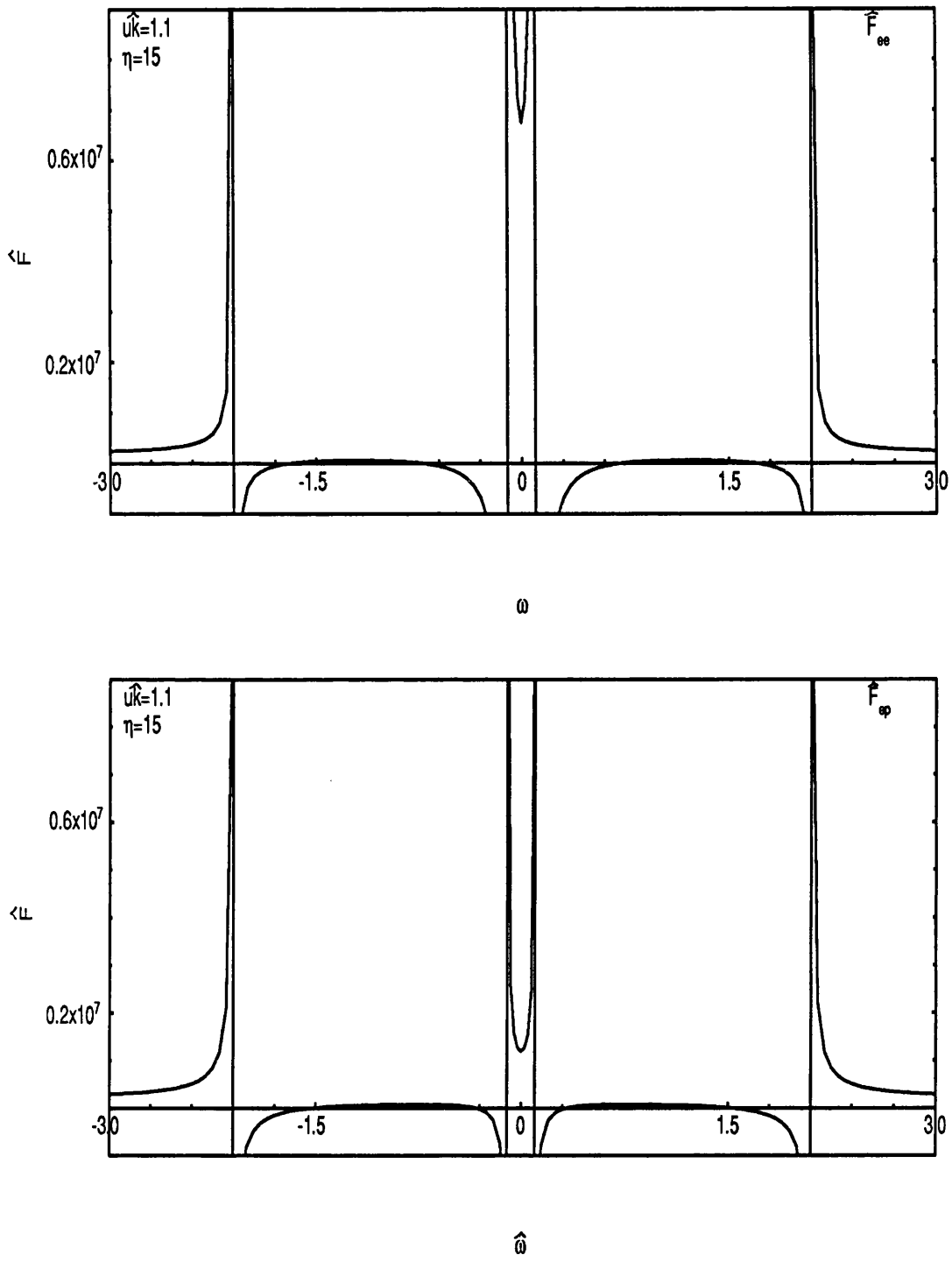

Figure 3.13: The function $\hat{F}(\hat{\omega})$ plotted against $\hat{\omega}$ for $u\hat{k} = 1.1$ and $\eta = 15$.

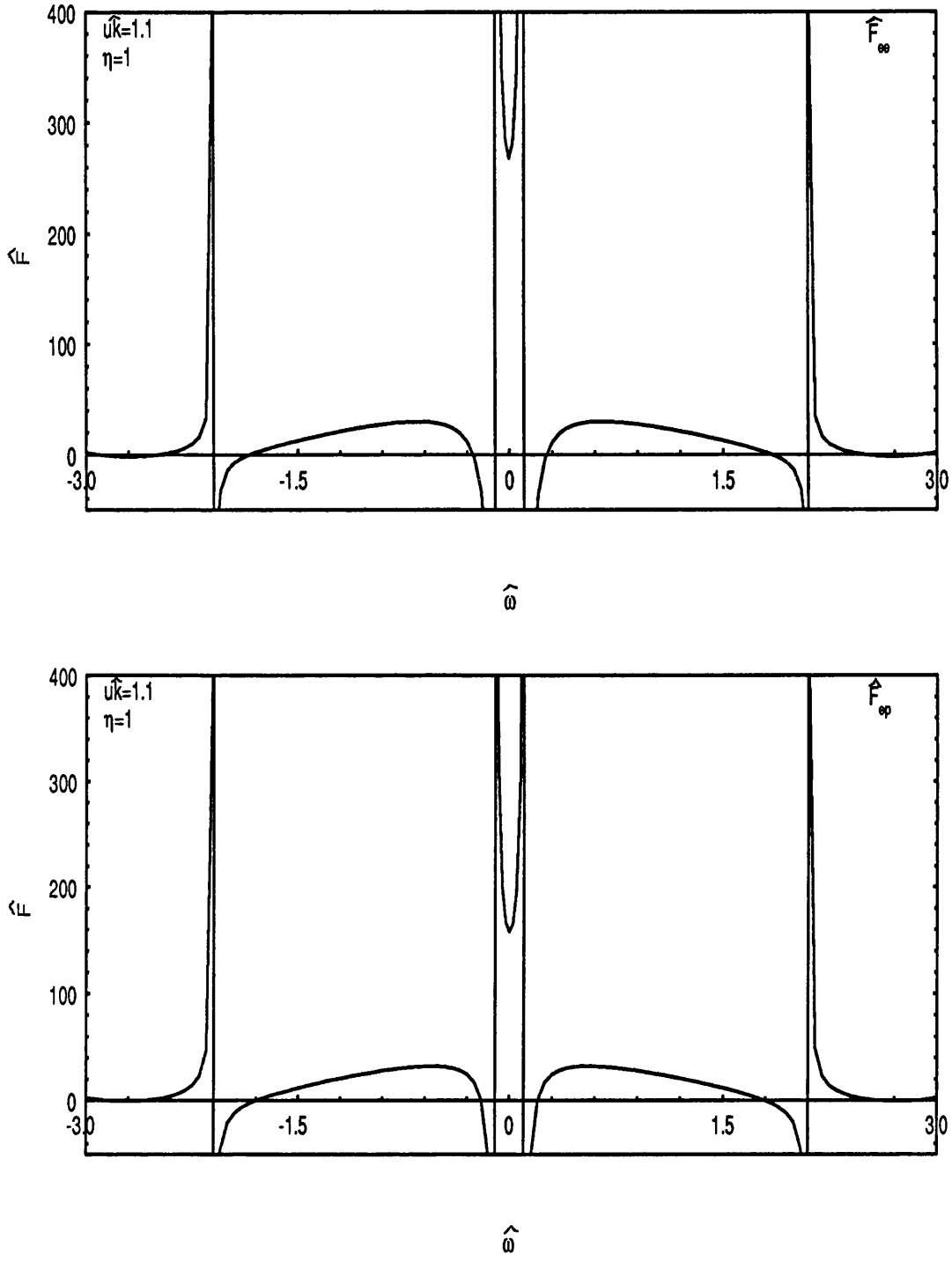

Figure 3.14: The function $\hat{F}(\hat{\omega})$ plotted against $\hat{\omega}$ for $u\hat{k} = 1.1$ and $\eta = 1$.

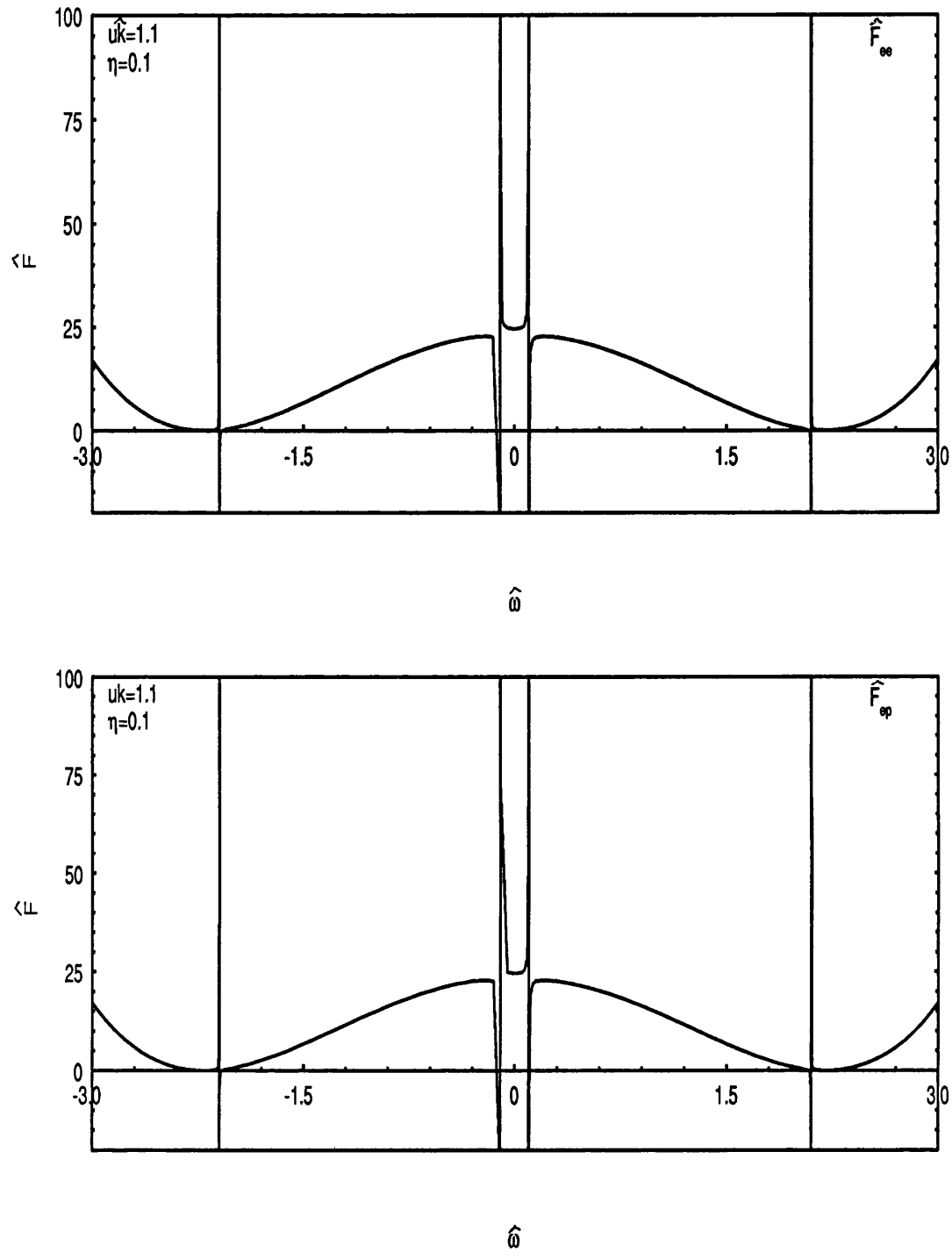

Figure 3.15: The function $\hat{F}(\hat{\omega})$ plotted against $\hat{\omega}$ for $\widehat{uk} = 1.1$ and $\eta = 0.1$.

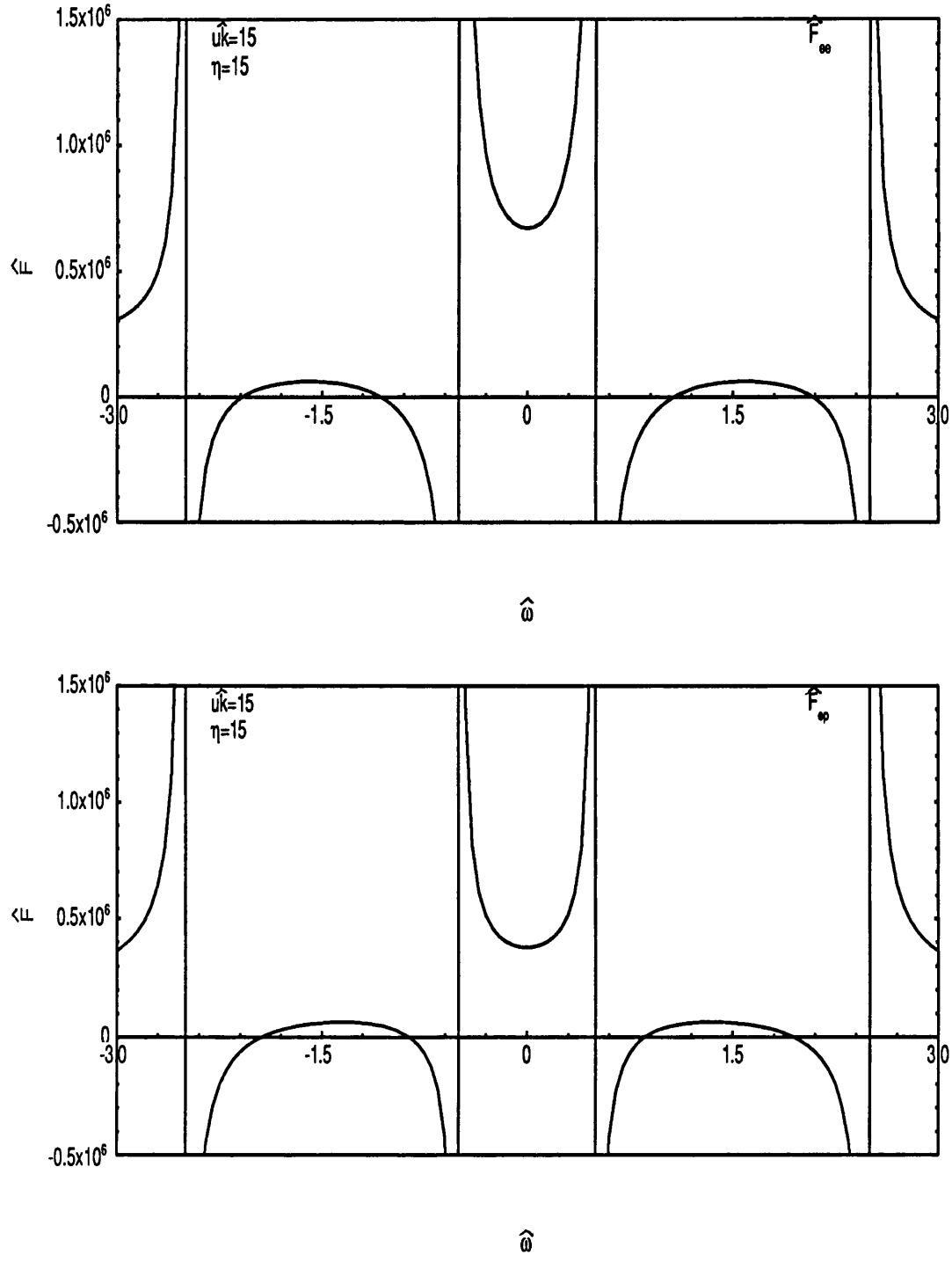

Figure 3.16: The function $\hat{F}(\hat{\omega})$ plotted against $\hat{\omega}$ for $\hat{uk} = 1.5$ and $\eta = 15$.

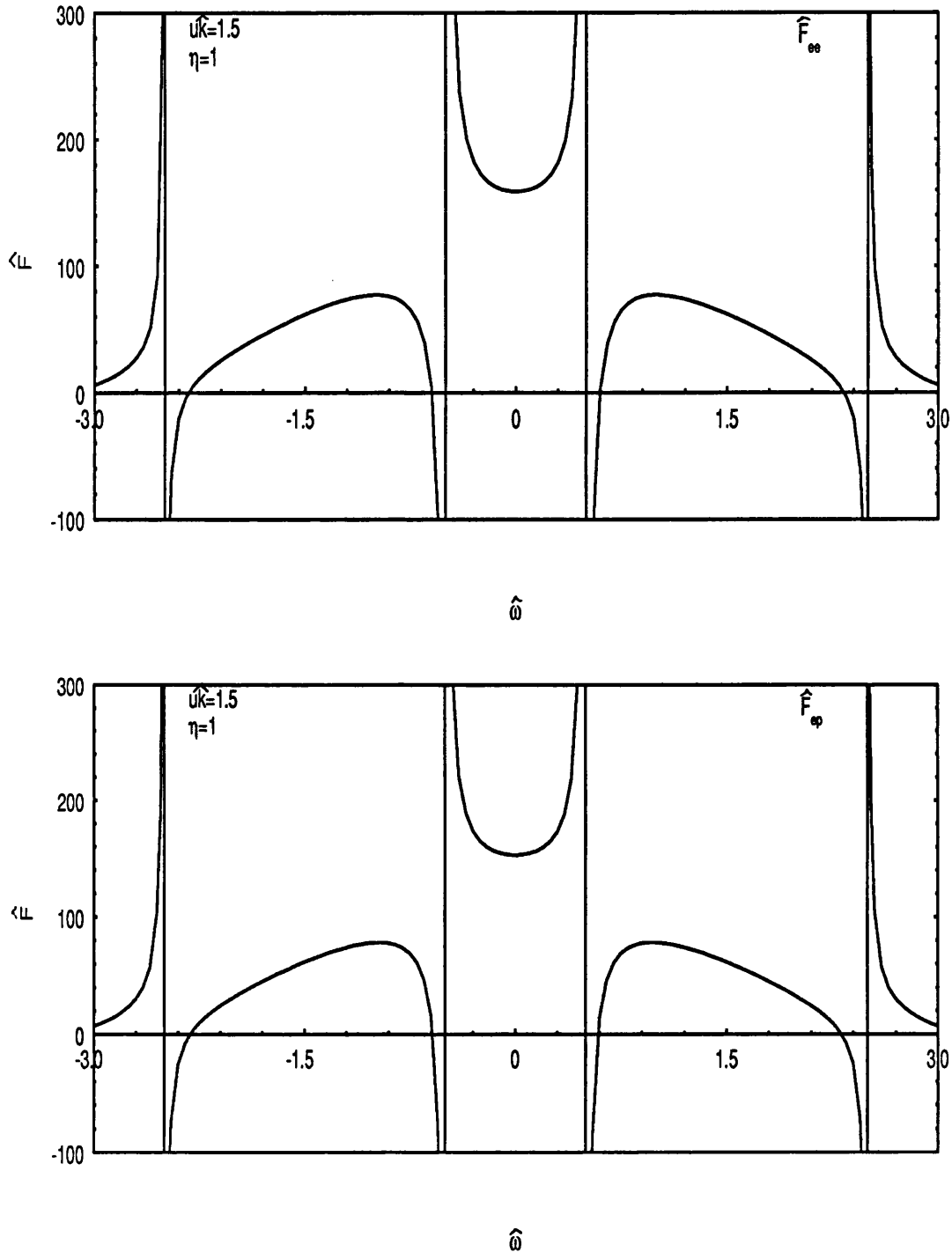

Figure 3.17: The function $\hat{F}(\hat{\omega})$ plotted against $\hat{\omega}$ for $u\hat{k} = 1.5$ and $\eta = 1$.

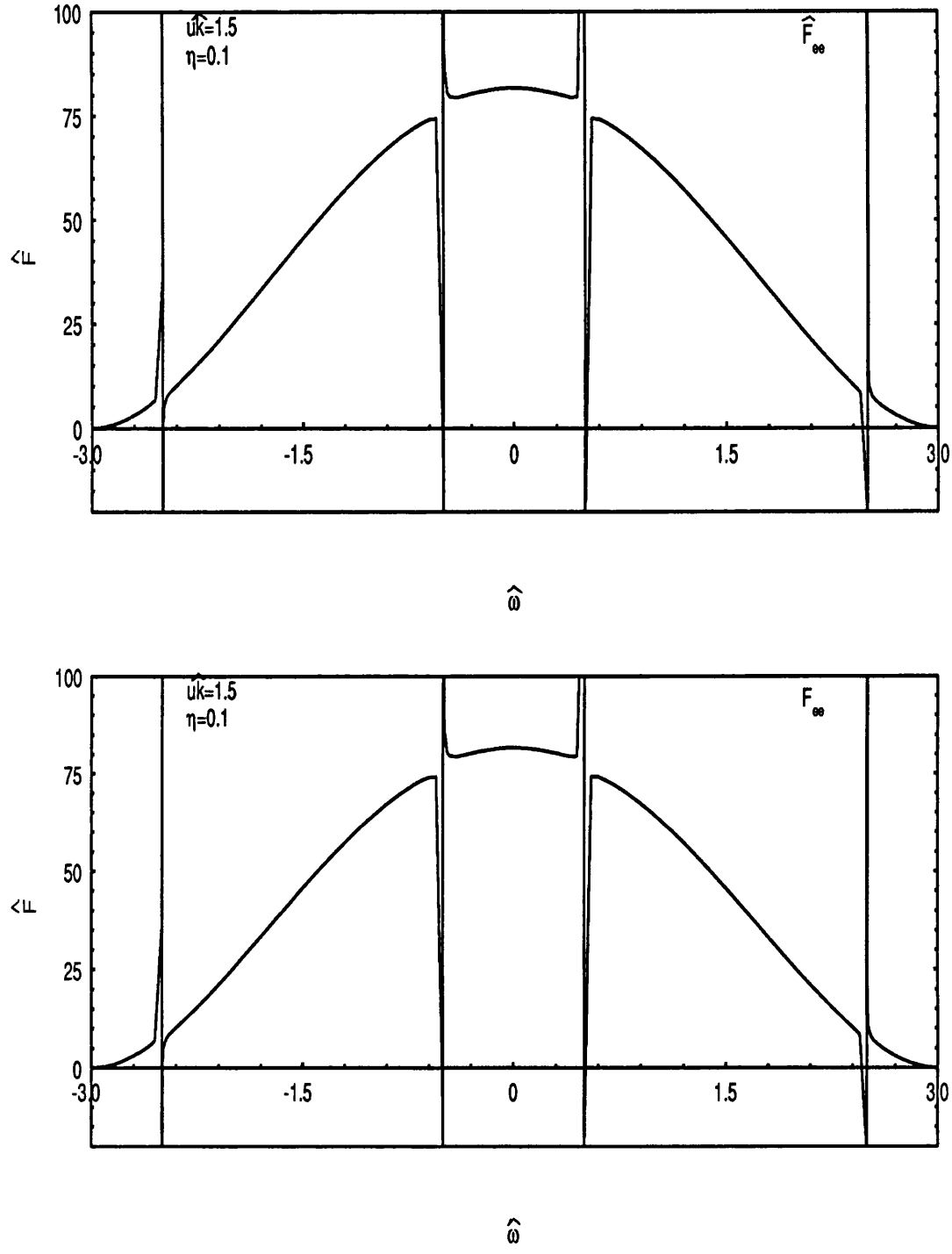

Figure 3.18: The function $\hat{F}(\hat{\omega})$ plotted against $\hat{\omega}$ for $u\hat{k} = 1.5$ and $\eta = 0.1$.

Chapter 4

Wave Propagation in Relativistic Thermal Plasmas

> I have yet to see a problem, however complicated, which, when you looked at it the right way, did not become yet more complicated
> *Poul Anderson*

The relativistic nature of the cold streaming plasmas studied in the last chapter did not pose any significant difficulties to our analysis. Relativity did not seem to add any new physics to the problem, rather it seemed merely to introduce Lorentz γ-factors into the various plasma frequency expressions thus causing shifts in their values.

We would now like to turn our attention to plasmas of a finite temperature. We will specify a distribution function with the form of a relativistic Maxwellian and again evaluate the components of the dielectric tensor. The distribution function we choose here is sufficiently different from its non-relativistic counterpart to make the analysis much more difficult. Indeed we will show that the integrals present in the components of $\underline{\underline{\mathbf{R}}}$ can no longer be solved analytically and numerical estimates must be found instead. As well as being mathematically more complex, we find that our results have several physical differences from the results of non-relativistic and weakly relativistic theory.

4.1 The Distribution Function

The relativistic Maxwellian distribution function we are going to use is assumed to include no streaming motion in the equilibrium state and,as described by Buti [27], is given by

$$f_0(p) = \frac{a}{4\pi m^3 c^3 K_2(a)} e^{-a\gamma} \tag{4.1}$$

where γ is the Lorentz factor $\left(1 + \frac{p_\parallel^2}{m^2c^2} + \frac{p_\perp^2}{m^2c^2}\right)^{1/2}$, K_2 is a modified Bessel function and the parameter a is the ratio of a particle's rest energy to its thermal energy,

$$a = \frac{mc^2}{\kappa T}. \tag{4.2}$$

The parameter a is a measure of how relativistic the plasma is. A value of a equal to unity means that a particle's energy is equal to its rest energy. $a \ll 1$ is the ultra-relativistic limit and $a \gg 1$ corresponds to the non-relativistic limit. In the latter case the distribution function (4.1) should reduce to its more usual non-relativistic Maxwellian form. To check this, we should note that when a is large the Bessel function $K_2(a)$ can be approximated by

$$K_2(a) \sim \sqrt{\frac{\pi}{2a}}\, e^{-a}. \tag{4.3}$$

In the non-relativistic limit the momentum p will be small compared to mc and the expression for γ can be expanded out to give

$$\gamma \sim 1 + \frac{p^2}{2m^2c^2}, \tag{4.4}$$

where we have assumed that the remaining terms in the expansion are small enough to neglect. Substituting these expressions into the distribution function (4.1) gives

$$f_0(p) \simeq \left(\frac{a}{2\pi m^2 c^2}\right)^{3/2} \exp\left(\frac{-ap^2}{2m^2c^2}\right) \tag{4.5}$$

and writing a explicitly as $mc^2/\kappa T$ gives the result:

$$f_0(p) \simeq \left(\frac{1}{2\pi m \kappa T}\right)^{3/2} \exp\left(\frac{-p^2}{2m\kappa T}\right) \tag{4.6}$$

which is the well-known non-relativistic Maxwellian distribution function, as expected.

4.2 Wave Propagation Perpendicular to the Magnetic Field

Now that we have chosen a form for the distribution function, we can substitute the expression for f_0 into the general expressions for the components of the dielectric tensor $\underline{\underline{\mathbf{R}}}$ given by equations (2.78)-(2.85). In an attempt to make the problem more tractable we assume that the waves propagate normal to the uniform magnetic field $\mathbf{B}_0$. In addition we again assume that the Laplace transform variable s is equal to $-i\,\omega$. The expressions for $\underline{\underline{\mathbf{R}}}$ can then be used to derive dispersion relations relating the frequency ω to the wave vector $k_\perp$. Taking all these conditions into account, we can write the components of $\underline{\underline{\mathbf{R}}}$ as:

$$R_{xx} = -\omega^2 + 2\,\pi\,\omega \sum_\nu \frac{\omega_{p\,\nu}^2\,\Omega_{0\,\nu}^2\,a_\nu\,\alpha_\nu}{k_\perp^2\,c^2} \times \sum_{n=-\infty}^{\infty} \int_{-\infty}^{\infty} dp_{\|} \int_0^{\infty} dp_\perp\,p_\perp\,\frac{n^2\,J_n^2(z_\nu)\,e^{-a_\nu\,\gamma_\nu}}{\gamma_\nu^2\,(\omega - n\,\Omega_\nu)} \quad (4.7)$$

$$R_{xy} = -R_{yx} = 2\,i\,\pi\,\omega \sum_\nu \frac{\omega_{p\,\nu}^2\,\Omega_{0\,\nu}^2\,a_\nu\,\alpha_\nu}{k_\perp\,m_\nu\,c^2} \times \sum_{n=-\infty}^{\infty} \int_{-\infty}^{\infty} dp_{\|} \int_0^{\infty} dp_\perp\,p_\perp^2\,\frac{n\,J_n(z_\nu)\,J_n'(z_\nu)\,e^{-a_\nu\,\gamma_\nu}}{\gamma_\nu^2\,(\omega - n\,\Omega_\nu)} \quad (4.8)$$

$$R_{xz} = R_{zx} = 2\,\pi\,\omega \sum_\nu \frac{\omega_{p\,\nu}^2\,\Omega_{0\,\nu}\,a_\nu\,\alpha_\nu}{k_\perp\,m_\nu\,c^2} \times \sum_{n=-\infty}^{\infty} \int_{-\infty}^{\infty} dp_{\|}\,p_{\|} \int_0^{\infty} dp_\perp\,p_\perp\,\frac{n\,J_n^2(z_\nu)\,e^{-a_\nu\,\gamma_\nu}}{\gamma_\nu^2\,(\omega - n\,\Omega_\nu)} \quad (4.9)$$

$$R_{yy} = -\omega^2 + c^2\,k_\perp^2 + 2\,\pi\,\omega \sum_\nu \frac{\omega_{p\,\nu}^2\,a_\nu\,\alpha_\nu}{m^2\,c^2} \times \sum_{n=-\infty}^{\infty} \int_{-\infty}^{\infty} dp_{\|} \int_0^{\infty} dp_\perp\,p_\perp^3\,\frac{[J_n'(z_\nu)]^2\,e^{-a_\nu\,\gamma_\nu}}{\gamma_\nu^2\,(\omega - n\,\Omega_\nu)} \quad (4.10)$$

$$R_{yz} = -R_{zy} = -2\,i\,\pi\,\omega \sum_\nu \frac{\omega_{p\,\nu}^2\,a_\nu\,\alpha_\nu}{m^2\,c^2} \times$$

$$\sum_{n=-\infty}^{\infty} \int_{-\infty}^{\infty} dp_{\parallel}\, p_{\parallel} \int_{0}^{\infty} dp_{\perp}\, p_{\perp}^{2}\, \frac{J_n(z_\nu)\, J_n'(z_\nu)\, e^{-a_\nu \gamma_\nu}}{\gamma_\nu^2 (\omega - n\,\Omega_\nu)} \quad (4.11)$$

$$R_{zz} = -\omega^2 + c^2 k_\perp^2 + 2\pi\omega \sum_{\nu} \frac{\omega_{p\nu}^2\, a_\nu\, \alpha_\nu}{k_\perp^2\, c^2} \times \sum_{n=-\infty}^{\infty} \int_{-\infty}^{\infty} dp_{\parallel} p_{\parallel}^{2} \int_{0}^{\infty} dp_{\perp}\, p_{\perp}\, \frac{J_n^2(z_\nu)\, e^{-a_\nu \gamma_\nu}}{\gamma_\nu^2 (\omega - n\,\Omega_\nu)} \quad (4.12)$$

where the argument of the Bessel functions is $z_\nu = k_\perp\, p_\perp / m_\nu\, \Omega_{0\nu}$, the non-relativistic plasma frequency is $\omega_{p\nu} = (n_{0\nu}\, q_\nu^2 / \epsilon_0\, m_\nu)^{1/2}$ and the relativistic cyclotron frequency is $\Omega_\nu = \Omega_{0\nu}/\gamma_\nu = q_\nu\, B_0 / m_\nu$.

4.3 Electron-Positron Plasmas

We will now write these components for the specific case of an electron-positron plasma. We assume that the two species have the same temperature: $T_e = T_p \equiv T$. The parameter a and the normalisation term α will then be the same for both species. The other quantities which are species-dependent are:

$$\begin{aligned} \omega_{pe} &= \omega_{pp} \equiv \omega_p \\ -\Omega_e &= \Omega_p \equiv \Omega \\ -z_e &= z_p \equiv z. \end{aligned}$$

The significance of this last expression is that the arguments of the Bessel functions have different signs for the two species: we have, for the xx-component, a $J_n^2(z)$ term for the positrons and a $J_n^2(-z)$ term for the electrons. The integrand contains a sum over species, so for an electron-positron plasma there will be two terms present. Some care needs to be taken when combining these terms to ensure that these Bessel function terms are properly treated. The same is also true for the remaining components of $\underline{\underline{\mathbf{R}}}$. After some manipulation the components reduce to the form:

$$R_{xx} = -\omega^2 + 4\pi\omega^2 \frac{\omega_p^2\, \Omega_0^2\, a\, \alpha}{k_\perp^2\, c^2} \times \sum_{n=-\infty}^{\infty} \int_{-\infty}^{\infty} dp_{\parallel} \int_{0}^{\infty} dp_{\perp}\, p_{\perp}\, \frac{n^2\, J_n^2(z)\, e^{-a\gamma}}{\gamma^2 \omega^2 - n^2\, \Omega_0^2} \quad (4.13)$$

$$R_{xy} = -R_{yx} = 4\,i\,\pi\,\omega^2\,\frac{\omega_p^2\,\Omega_0\,a\,\alpha}{k_\perp\,m\,c^2}\times \sum_{n=-\infty}^{\infty}\int_{-\infty}^{\infty} dp_{||}\int_0^{\infty} dp_\perp\,p_\perp^2\,\frac{n\,J_n(z)\,J_n'(z)\,e^{-a\,\gamma}}{\gamma^2\,\omega^2-n^2\,\Omega_0^2} \tag{4.14}$$

$$R_{xz} = R_{zx} = 4\,\pi\,\omega\,\frac{\omega_p^2\,\Omega_0^2\,a\,\alpha}{k_\perp\,m\,c^2}\times \sum_{n=-\infty}^{\infty}\int_{-\infty}^{\infty} dp_{||}p_{||}\int_0^{\infty} dp_\perp\,p_\perp\,\frac{n^2\,J_n^2(z)\,e^{-a\,\gamma}}{\gamma\,(\gamma^2\,\omega^2-n^2\,\Omega_0^2)} \tag{4.15}$$

$$R_{yy} = -\omega^2+c^2\,k_\perp^2+4\,\pi\,\omega^2\,\frac{\omega_p^2\,a\,\alpha}{m^2\,c^2}\times \sum_{n=-\infty}^{\infty}\int_{-\infty}^{\infty} dp_{||}\int_0^{\infty} dp_\perp\,p_\perp^3\,\frac{[J_n'(z)]^2\,e^{-a\,\gamma}}{\gamma^2\,\omega^2-n^2\,\Omega_0^2} \tag{4.16}$$

$$R_{yz} = -R_{yz} = -4\,i\,\pi\,\omega\,\frac{\omega_p^2\,\Omega_0\,a\,\alpha}{m^2\,c^2}\times \sum_{n=-\infty}^{\infty}\int_{-\infty}^{\infty} dp_{||}p_{||}\int_0^{\infty} dp_\perp\,p_\perp^2\,\frac{n\,J_n(z)\,J_n'(z)\,e^{-a\,\gamma}}{\gamma\,(\gamma^2\,\omega^2-n^2\,\Omega_0^2)} \tag{4.17}$$

$$R_{zz} = -\omega^2+c^2\,k_\perp^2+4\,\pi\,\omega^2\,\frac{\omega_p^2\,a\,\alpha}{m^2\,c^2}\times \sum_{n=-\infty}^{\infty}\int_{-\infty}^{\infty} dp_{||}\,p_{||}^2\int_0^{\infty} dp_\perp\,p_\perp\,\frac{J_n^2(z)\,e^{-a\,\gamma}}{\gamma^2\,\omega^2-n^2\,\Omega_0^2}. \tag{4.18}$$

If we look at the integrals in the R_{xz} and R_{yz} components above, we see that there is a single factor of $p_{||}$ present in each. The only other $p_{||}$-dependence in the integrands comes from the γ factors which means that, since γ depends only on $p_{||}^2$, the two integrands in question are odd functions of $p_{||}$ and consequently both are zero when integrated over the range $p_{||}\in(-\infty,+\infty)$. We thus have the result

$$R_{xz} = R_{zx} = 0$$
$$R_{yz} = -R_{zy} = 0$$

Look now at the sum over n. At the moment it exists as a doubly infinite sum (ie n summed from $-\infty$ to $+\infty$) in each component of the dielectric tensor. If possible, we would like to reduce it to a singly infinite sum over n, that is a sum from $n=0$ to $n=+\infty$. For each component in turn, we will investigate the integrand for positive

and negative values of n and compare the results. In doing so we will make use of the following two Bessel function identities:

$$J_{-n}(z) = (-1)^n J_n(z), \tag{4.19}$$

$$J'_n(z) = \frac{1}{2}\left[J_{n-1}(z) - J_{n+1}(z)\right]. \tag{4.20}$$

R_{xx} component: the part of the integrand that depends on n is

$$\frac{n^2 J_n^2(z)}{\gamma^2\omega^2 - n^2\Omega_0^2}. \tag{4.21}$$

Consider a negative value of n, that is $n = -m$ where $m > 0$. The integrand for this value of n is

$$\frac{(-m)^2 J_{-m}^2(z)}{\gamma^2\omega^2 - (-m)^2\Omega_0^2} = \frac{m^2\left[(-1)^m J_m(z)\right]^2}{\gamma^2\omega^2 - m^2\Omega_0^2} = \frac{m^2 J_m^2(z)}{\gamma^2\omega^2 - m^2\Omega_0^2}. \tag{4.22}$$

Thus the term for $n = -m$ is exactly the same as the corresponding term for $n = m$. We can also see that, due to the presence of the n^2 term in the numerator, the integrand is equal to zero for $n = 0$. This enables us to write the sum as

$$\sum_{n=-\infty}^{\infty} \frac{n^2 J_n^2(z)}{\gamma^2\omega^2 - n^2\Omega_0^2} = 2\sum_{n=1}^{\infty} \frac{n^2 J_n^2(z)}{\gamma^2\omega^2 - n^2\Omega_0^2} \tag{4.23}$$

R_{xy} component: the n-dependent terms here are

$$\frac{n J_n(z) J'_n(z)}{\gamma^2\omega^2 - n^2\Omega_0^2}. \tag{4.24}$$

Again consider a value of $n = -m$, where $m > 0$. Combining the Bessel function identities (4.19) and (4.20) allows us to write $J'_{-m}(z) = (-1)^m J'_m(z)$. So, for $n = -m$, the integrand is

$$\begin{aligned} \frac{-m J_{-m}(z) J'_{-m}(z)}{\gamma^2\omega^2 - m^2\Omega_0^2} &= -\frac{m(-1)^m J_m(z)(-1)^m J'_m(z)}{\gamma^2\omega^2 - m^2\Omega_0^2} \\ &= -\frac{m J_m(z) J'_m(z)}{\gamma^2\omega^2 - m^2\Omega_0^2}. \end{aligned} \tag{4.25}$$

Here the terms for $n = m$ and $n = -m$ have opposite signs and will cancel each other out when included in the sum, which then reduces to

$$\sum_{n=-\infty}^{\infty} \frac{n J_n(z) J'_n(z)}{\gamma^2\omega^2 - n^2\Omega_0^2} = \left[\frac{n J_n(z) J'_n(z)}{\gamma^2\omega^2 - n^2\Omega_0^2}\right]_{n=0}. \tag{4.26}$$

Again, however, the integrand is zero for $n = 0$ and the sum reduces to

$$\sum_{n=-\infty}^{\infty} \frac{n J_n(z) J_n'(z)}{\gamma^2 \omega^2 - n^2 \Omega_0^2} = 0. \tag{4.27}$$

R_{yy} component: the n-dependent terms in the integrand are

$$\frac{[J_n'(z)]^2}{\gamma^2 \omega^2 - n^2 \Omega_0^2}. \tag{4.28}$$

When $n = -m$, with $m > 0$, the corresponding integrand is

$$\frac{[J_{-m}'(z)]^2}{\gamma^2 \omega^2 - (-m)^2 \Omega_0^2} = \frac{[(-1)^m J_m'(z)]^2}{\gamma^2 \omega^2 - m^2 \Omega_0^2} = \frac{[J_m'(z)]^2}{\gamma^2 \omega^2 - m^2 \Omega_0^2}. \tag{4.29}$$

Since there is no factor of n in the numerator of the integrand, it does not vanish for $n = 0$ and so the sum over n is written as

$$\sum_{n=-\infty}^{\infty} \frac{[J_n'(z)]^2}{\gamma^2 \omega^2 - n^2 \Omega_0^2} = \left[\frac{[J_n'(z)]^2}{\gamma^2 \omega^2 - n^2 \Omega_0^2}\right]_{n=0} + 2 \sum_{n=1}^{\infty} \frac{[J_n'(z)]^2}{\gamma^2 \omega^2 - n^2 \Omega_0^2}. \tag{4.30}$$

R_{zz} component: the n-dependent terms here are

$$\frac{J_n^2(z)}{\gamma^2 \omega^2 - n^2 \Omega_0^2}. \tag{4.31}$$

For $n = -m$, where $m > 0$, the integrand is

$$\frac{J_{-m}^2(z)}{\gamma^2 \omega^2 - (-m)^2 \Omega_0^2} = \frac{[(-1)^m J_m(z)]^2}{\gamma^2 \omega^2 - m^2 \Omega_0^2} = \frac{J_m^2(z)}{\gamma^2 \omega^2 - m^2 \Omega_0^2}. \tag{4.32}$$

Again, since there is no factor of n present in the numerator, the expression for $n = 0$ is non-zero and the sum reduces to

$$\sum_{n=-\infty}^{\infty} \frac{J_n^2(z)}{\gamma^2 \omega^2 - n^2 \Omega_0^2} = \left[\frac{J_n^2(z)}{\gamma^2 \omega^2 - n^2 \Omega_0^2}\right]_{n=0} + 2 \sum_{n=1}^{\infty} \frac{J_n^2(z)}{\gamma^2 \omega^2 - n^2 \Omega_0^2}. \tag{4.33}$$

Our dielectric tensor has now reduced to a diagonal form:

$$\underline{\underline{\mathrm{R}}} = \begin{bmatrix} R_{xx} & 0 & 0 \\ 0 & R_{yy} & 0 \\ 0 & 0 & R_{zz} \end{bmatrix}. \tag{4.34}$$

The mass symmetries present in an electron-positron plasma thus simplify the analysis considerably by allowing us to study each component of the dielectric tensor separately.

Before investigating the remaining components of $\underline{\underline{\mathbf{R}}}$ in more detail, we will firstly normalise the variables; the perpendicular momentum $p_\perp$, for example, will be replaced by its non-dimensional counterpart $\hat{p}_\perp$.

Scale the momentum components to mc: $p_\perp = mc\,\hat{p}_\perp$, $p_{||} = mc\,\hat{p}_{||}$ so that the Lorentz factor can be written as $\gamma = \left(1 + \hat{p}_\perp^2 + \hat{p}_{||}^2\right)^{1/2}$. All frequency terms are scaled to the non-relativistic cyclotron frequency:

$$\hat{\omega} = \frac{\omega}{\Omega_0}, \qquad \eta = \frac{\omega_p}{\Omega_0}, \qquad \hat{k}_\perp = \frac{c\,k_\perp}{\Omega_0}. \tag{4.35}$$

We can then write the argument of the Bessel functions as $z = k_\perp\, p_\perp / m\,\Omega_0 = \hat{k}_\perp\,\hat{p}_\perp$. In terms of these dimensionless variables, the components of the dielectric tensor are:

$$\begin{aligned} R_{xx} \;=\; \Omega_0^2 \Bigg[& -\hat{\omega}^2 + \frac{2\,a^2\,\eta^2}{\hat{k}_\perp^2\,K_2(a)} \times \\ & \sum_{n=1}^{\infty} \int_0^\infty d\hat{p}_\perp\,\hat{p}_\perp\,n^2\,J_n^2(z) \int_{-\infty}^{\infty} d\hat{p}_{||} \frac{e^{-a\gamma}}{\gamma^2 - \frac{n^2}{\hat{\omega}^2}} \Bigg] \end{aligned} \tag{4.36}$$

$$\begin{aligned} R_{yy} \;=\; \Omega_0^2 \Bigg[& -\hat{\omega}^2 + \hat{k}_\perp^2 + \frac{a^2\,\eta^2}{K_2(a)} \Bigg\{ \int_0^\infty d\hat{p}_\perp\,\hat{p}_\perp^3\,\left[J_0'(z)\right]^2 \int_{-\infty}^{\infty} d\hat{p}_{||} \frac{e^{-a\gamma}}{\gamma^2} \\ & +2 \sum_{n=1}^{\infty} \int_0^\infty d\hat{p}_\perp\,\hat{p}_\perp^3\,\left[J_n'(z)\right]^2 \int_{-\infty}^{\infty} d\hat{p}_{||} \frac{e^{-a\gamma}}{\gamma^2 - \frac{n^2}{\hat{\omega}^2}} \Bigg\} \Bigg] \end{aligned} \tag{4.37}$$

$$\begin{aligned} R_{zz} \;=\; \Omega_0^2 \Bigg[& -\hat{\omega}^2 + \hat{k}_\perp^2 + \frac{a^2\,\eta^2}{K_2(a)} \Bigg\{ \int_0^\infty d\hat{p}_\perp\,\hat{p}_\perp\,J_0^2(z) \int_{-\infty}^{\infty} d\hat{p}_{||}\,\hat{p}_{||}^2 \frac{e^{-a\gamma}}{\gamma^2} \\ & +2 \sum_{n=1}^{\infty} \int_0^\infty d\hat{p}_\perp\,\hat{p}_\perp\,J_n^2(z) \int_{-\infty}^{\infty} d\hat{p}_{||}\,\hat{p}_{||}^2 \frac{e^{-a\gamma}}{\gamma^2 - \frac{n^2}{\hat{\omega}^2}} \Bigg\} \Bigg] . \end{aligned} \tag{4.38}$$

Manipulating the $\hat{p}_{||}$-integral in R_{zz} to rewrite it in the same form as the other two components gives:

$$R_{zz} \;=\; \Omega_0^2 \Bigg[-\hat{\omega}^2 + \hat{k}_\perp^2 + \frac{a^2\,\eta^2}{K_2(a)} \Bigg\{ 2 \sum_{n=1}^{\infty} \Bigg(\int_0^\infty d\hat{p}_\perp\,\hat{p}_\perp\,J_n^2(z) \int_{-\infty}^{\infty} d\hat{p}_{||}\,e^{-a\gamma}$$

$$
\begin{aligned}
&- \int_0^\infty d\hat{p}_\perp \, \hat{p}_\perp \, J_n^2(z) \int_{-\infty}^\infty d\hat{p}_{||} \left(1 + \hat{p}_\perp^2 - \frac{n^2}{\hat{\omega}^2} \right) \frac{e^{-a\gamma}}{\gamma^2 - \frac{n^2}{\hat{\omega}^2}} \Bigg) \\
&+ \int_0^\infty d\hat{p}_\perp \, \hat{p}_\perp \, J_0^2(z) \int_{-\infty}^\infty d\hat{p}_{||} \, e^{-a\gamma} \\
&- \int_0^\infty d\hat{p}_\perp \, \hat{p}_\perp \, J_0^2(z) \int_{-\infty}^\infty d\hat{p}_{||} \left(1 + \hat{p}_\perp^2 \right) \frac{e^{-a\gamma}}{\gamma^2} \Bigg\} \Bigg] .
\end{aligned}
$$

The integrals in the above expressions cannot be solved analytically and their form does not correspond to any of the standard integral formulae in books like Gradshteyn & Ryzhik [28]. The only path left open to us is that of numerical integration. In the remainder of this chapter we will set out the numerical techniques we have employed to evaluate these integrals. Firstly though we will write the integrals in a form that will make them easier to incorporate into a numerical code.

4.4 Singular Points

If the integrands in the components of the dielectric tensor given by equations (3.16)-(3.18) were all well-behaved continuous functions of the momentum components then we could simply use a standard numerical integration technique to obtain a value for each integral. However, it is clear that this approach is inadequate due to the presence of singular points in the integrands and some thought is required before any standard integration techniques can be used.

Each component contains an integral which has $(\gamma^2 - n^2/\hat{\omega}^2)^{-1}$ as part of its integrand. The value of γ, and thus of γ^2, must lie in the range $[1, \infty)$. So, if $n \geq \hat{\omega}$, then there exists the possibility that at some point in our integration $\gamma^2 = n^2/\hat{\omega}^2$ and the integrand will become infinite. We thus need to carry out some careful analysis, involving contour integration techniques, to enable us to write the integrals in such a way that we do not need to include the singular points in the Simpson approximation. A proper treatment of singularities in non-relativistic dispersion relations was first proposed by Landau, who carried out the analysis as an initial value problem. He assumed that there was an initial perturbation of the distribution function and then used a Laplace transform in the time variable, similar to that used in section 2.6.2, to follow the evolution of the distribution function following this initial disturbance.

We will follow his example and define a Landau contour which will enable us to solve our integral. A brief review of Landau's ideas is given at the end of Appendix B. Note, in particular, that for damping to occur the frequency ω must have a negative imaginary part.

The integral of interest is

$$\int_{-\infty}^{\infty} d\hat{p}_{\|} \frac{e^{-a\gamma}}{\gamma^2 - \frac{n^2}{\hat{\omega}^2}} \tag{4.39}$$

and this occurs in all three of the dielectric components. As already stated above, the existence of singularities depends on the relative magnitudes of n and $\hat{\omega}$. There are two distinct cases:

(i) $\frac{n}{\hat{\omega}} \geq 1$: $1 - \frac{n^2}{\hat{\omega}^2} \leq 0$ and it is possible that the denominator $\hat{p}_{\|}^2 + \hat{p}_{\perp}^2 + 1 - \frac{n^2}{\hat{\omega}^2}$ may take the value zero.

(ii) $\frac{n}{\hat{\omega}} < 1$: $1 - \frac{n^2}{\hat{\omega}^2} > 0$ and the denominator $\hat{p}_{\|}^2 + \hat{p}_{\perp}^2 + 1 - \frac{n^2}{\hat{\omega}^2}$ must always be strictly greater than zero. So there are no singularities present and the integrand is well-behaved.

We will now proceed as follows: if we are in the region where the singularities occur we will carry out the necessary contour integration to treat the integral properly and incorporate this into the Simpson rule and if we are in a region where the integrand is well-behaved we will simply carry out the Simpson rule as described in section 4.5.

Write the components of the dielectric tensor in the form

$$R_{xx} = -\Omega_0^2 \left[\hat{\omega}^2 - \frac{2\,a^2\,\eta^2}{\hat{k}_{\perp}^2\,K_2(a)} \sum_{n=1}^{\infty} I_{xx} \right] \tag{4.40}$$

$$R_{yy} = -\Omega_0^2 \left[\hat{\omega}^2 - \hat{k}_{\perp}^2 - \frac{a^2\,\eta^2}{K_2(a)} \left\{ I_{yy}(n=0) + 2 \sum_{n=1}^{\infty} I_{yy} \right\} \right] \tag{4.41}$$

$$R_{zz} = -\Omega_0^2 \left[\hat{\omega}^2 - \hat{k}_{\perp}^2 - \frac{a^2\,\eta^2}{K_2(a)} \left\{ 2\,I_{zz1}(n=0) + 4 \sum_{n=1}^{\infty} I_{zz1} \right.\right.$$
$$\left.\left. - I_{zz2}(n=0) - 2 \sum_{n=1}^{\infty} I_{zz2} \right\} \right] \tag{4.42}$$

where the form of the integral terms can be found by comparison with the equations (3.16)-(3.18).

For each case below, we will find the integrals I_{xx}, I_{yy}, I_{zz1} and I_{zz2} in a form suitable for evaluation by a compound Simpson rule.

4.4.1 Case (i) : $\frac{n}{\hat{\omega}} \geq 1$

Define the point b_{crit} to be: $b_{crit} = (\frac{n^2}{\hat{\omega}^2} - 1)^{1/2}$. The denominator is then $\hat{p}_{||}^2 + \hat{p}_{\perp}^2 + 1 - \frac{n^2}{\hat{\omega}^2} = \hat{p}_{||}^2 + \hat{p}_{\perp}^2 - b_{crit}^2$. For the integral (4.39), $\hat{p}_{\perp}$ is regarded as just another parameter so the values of $\hat{p}_{\perp}$ and b_{crit} are set. If we then set $\hat{p}_{||}^2 + \hat{p}_{\perp}^2 - b_{crit}^2 = 0$, this means that $\hat{p}_{||}^2 = b_{crit}^2 - \hat{p}_{\perp}^2$. Since $\hat{p}_{||}$ and $\hat{p}_{\perp}$ are real quantities, the denominator can only be zero if $b_{crit}^2 - \hat{p}_{\perp}^2 \geq 0$, that is $\hat{p}_{\perp} \leq b_{crit}$.

Thus, if $\hat{p}_{\perp} \leq b_{crit}$, there are singularities present in the integrand but if $\hat{p}_{\perp} > b_{crit}$, the integrand is well-behaved and there are no singular points.

$\hat{p}_{\perp} \leq b_{crit}$

To take care of the singular points present in the integrand we must follow the contour integration analysis outlined in Appendix B. Firstly, however, we will rescale the variables to express the problem in a more lucid form.

For the moment we shall concentrate our attention on the xx-component of $\underline{\underline{\mathbf{R}}}$, which contains the integral

$$I_{xx} = \int_0^{b_{crit}} d\hat{p}_{\perp}\, \hat{p}_{\perp}\, n^2\, J_n^2(z) \int_{-\infty}^{\infty} d\hat{p}_{||}\, \frac{e^{-a\gamma}}{\hat{p}_{||}^2 + \hat{p}_{\perp}^2 + 1 - \frac{n^2}{\hat{\omega}^2}}. \tag{4.43}$$

Scale all variables by the parameter a:

$$\hat{p}_{||} = \frac{u_{||}}{a}, \quad \hat{p}_{\perp} = \frac{u_{\perp}}{a}, \quad \gamma = \frac{\Gamma}{a}, \quad \frac{n}{\hat{\omega}} = \frac{B}{a}. \tag{4.44}$$

Note that, in terms of these new variables, b_{crit} can be written as

$$b_{crit} = \frac{(B^2 - a^2)^{1/2}}{a} \equiv \frac{C}{a}. \tag{4.45}$$

Thus the point C in the $u_{\perp}$-integration is equivalent to the point b_{crit} in the $\hat{p}_{\perp}$-integration. This means that the range of the $u_{\perp}$-integration is split at the point

C and here we are only looking at the range $u_\perp \in [0, C]$. Note also that $\Gamma = \left(u_{||}^2 + u_\perp^2 + a^2\right)^{1/2}$ in terms of these new variables, so

$$I_{xx} = \frac{1}{a} \int_0^C du_\perp \, u_\perp \, n^2 \, J_n^2(z) \int_{-\infty}^{\infty} du_{||} \, \frac{e^{-\Gamma}}{\Gamma^2 - B^2}, \tag{4.46}$$

where $z = \hat{k}_\perp \, u_\perp / a$. We notice now that there is no explicit mention of the parameter a in the integral (although, of course, several variables depend implicitly on a).

Define a new variable $A \equiv (B^2 - a^2 - u_\perp^2)^{1/2} = (C^2 - u_\perp^2)^{1/2}$ and rewrite the $u_\perp$ expressions in terms of A. Thus

$$I_{xx} = \frac{1}{a} \int_0^C dA \, A \, n^2 \, J_n^2(z) \int_{-\infty}^{\infty} du_{||} \, \frac{e^{-\Gamma}}{u_{||}^2 - A^2}, \tag{4.47}$$

where $\Gamma = \left(u_{||}^2 - A^2 + B^2\right)^{1/2}$ and $z = \hat{k}_\perp / a \, (C^2 - A^2)^{1/2}$.

Concentrate for the moment on the $u_{||}$-integral, which we will now write as

$$\int_{\Gamma_C} du_{||} \, \frac{e^{-\Gamma}}{u_{||}^2 - A^2} \tag{4.48}$$

where Γ_C represents a Landau contour similar to that shown in part (b) of Fig (B.1). In this representation $u_{||}$ should be regarded as a complex variable. Using the method of partial fractions we can write the integral as

$$\int_{\Gamma_C} du_{||} \, \frac{e^{-\Gamma}}{u_{||}^2 - A^2} = \frac{1}{2A} \left\{ \int_{\Gamma_C} du_{||} \, \frac{e^{-\Gamma}}{u_{||} - A} - \int_{\Gamma_C} du_{||} \, \frac{e^{-\Gamma}}{u_{||} + A} \right\}. \tag{4.49}$$

Here, each integrand has only one pole in the upper half-plane which lies on the real axis. For the first integrand the pole is at $u_{||} = A$ and for the second at $u_{||} = -A$. These poles are both simple so that, if we can prove that the quantity $\{R \times \text{maximum value of } |\text{integrand}| \text{ on } C_R\} \to 0$ as $R \to \infty$, then following the analysis in Appendix B we can express the integral as

$$\begin{aligned} \int_{\Gamma_C} du_{||} \, \frac{e^{-\Gamma}}{u_{||}^2 - A^2} \;=\; & \frac{1}{2A} \left\{ P \int_{\Gamma_C} du_{||} \, \frac{e^{-\Gamma}}{u_{||} - A} - i\pi \, Res\left(e^{-\Gamma}, u_{||} = A\right) \right. \\ & \left. - \; P \int_{\Gamma_C} du_{||} \, \frac{e^{-\Gamma}}{u_{||} + A} + i\pi \, Res\left(e^{-\Gamma}, u_{||} = -A\right) \right\}. \end{aligned} \tag{4.50}$$

Firstly, we must ensure that the maximum value of the magnitude of the integrand on the semi-circle C_R multiplied by the radius R tends to zero as $R \to \infty$.

For the first integral, we have

$$\left|\frac{e^{-\left(R^2-A^2+B^2\right)^{1/2}}}{R-A}\right| \times R \approx e^{-\left(R^2-A^2+B^2\right)^{1/2}} \text{ if } R \gg A$$
$$\rightarrow 0 \text{ as } R \rightarrow \infty.$$

The second integral also reduces to the exponential term alone in the limit of $R \gg A$ and thus also tends to zero as $R \rightarrow \infty$.

Look now at the two imaginary terms in equation (4.50):

$$Res\left(e^{-\Gamma}, u_{||} = A\right) = e^{-\frac{n^2}{\omega^2}} \tag{4.51}$$

$$Res\left(e^{-\Gamma}, u_{||} = -A\right) = e^{-\frac{n^2}{\omega^2}}. \tag{4.52}$$

When these two terms are inserted into equation (4.50) we see that they cancel each other out, leaving no imaginary terms in the dispersion relation. Following the analysis in Appendix B, there can therefore be no damping of the waves.

Note also, if we substitute $v = -u_{||}$ into the second principal part integral in equation (4.50) we have

$$P\int_{-\infty}^{\infty} du_{||}\,\frac{e^{-\Gamma}}{u_{||}+A} = -P\int_{-\infty}^{\infty} dv\,\frac{e^{-\Gamma}}{v-A}, \tag{4.53}$$

where $\Gamma = \left(v^2 - A^2 + B^2\right)^{1/2}$.

Since the integration variable v can be treated as a dummy variable, we can simply set $v = u_{||}$ to give

$$P\int_{-\infty}^{\infty} du_{||}\,\frac{e^{-\Gamma}}{u_{||}+A} = -P\int_{-\infty}^{\infty} du_{||}\,\frac{e^{-\Gamma}}{u_{||}-A}. \tag{4.54}$$

Substituting all these results into equation (4.50) reduces the integral to

$$\int_{\Gamma_C} du_{||}\,\frac{e^{-\Gamma}}{u_{||}^2 - A^2} = \frac{1}{A}\,P\int_{-\infty}^{\infty} du_{||}\,\frac{e^{-\Gamma}}{u_{||}-A}. \tag{4.55}$$

Returning to equation (4.47), we can now write the integral I_{xx} as

$$I_{xx} = \frac{1}{a}\int_0^C dA\,P\int_{-\infty}^{\infty} du_{||}\,\frac{n^2\,J_n^2(z)\,e^{-\Gamma}}{u_{||}-A}. \tag{4.56}$$

As all three components of $\underline{\underline{\mathbf{R}}}$ have been written in such a way that the troublesome $u_{||}$-integrals are all the same, then the contour analysis carried out above for

I_{xx} will also hold for the integrals in the other two components. These can thus be written as

$$I_{yy} = \frac{1}{a^3}\int_0^C dA\left(C^2-A^2\right)P\int_{-\infty}^{\infty} du_{||}\,\frac{\left[J_n'(z)\right]^2 e^{-\Gamma}}{u_{||}-A} \tag{4.57}$$

$$I_{zz1} = \int_0^C du_\perp\, u_\perp \left(a^2+u_\perp^2\right)^{1/2} J_n^2(z)\, K_1\left[\left(a^2+u_\perp^2\right)^{1/2}\right] \tag{4.58}$$

$$I_{zz2} = \frac{1}{a^3}\int_0^C dA\, A^2\, P\int_{-\infty}^{\infty} du_{||}\,\frac{J_n^2(z)\, e^{-\Gamma}}{u_{||}-A} \tag{4.59}$$

Note that the I_{zz1} integral is well-behaved as there are no singularities present. In fact, we are able to carry out the $u_{||}$-integration and reduce the expression to a single integral in $u_\perp$. It is included here, and in the following cases, only for completeness.

One important point to note about the $u_{||}$-integral in these expressions is the denominator, namely $u_{||}-A$. The singularity in each $u_{||}$-integration occurs at the point $u_{||}=A$ but, as we are also integrating over the variable A, this position can vary between 0 and C and will change each time we evaluate the $u_{||}$-integral. Initial runs with this form of the integrand suggested that having the singularities occuring at different positions throughout the range of integration was having an adverse effect on the performance of the FORTRAN code we had written. Another change of variable was called upon to try and overcome this problem by trying to express the denominator above in a slightly simpler way.

We thus introduce the variable $x = u_{||}/A$. In terms of this variable, the integral becomes

$$I_{xx} = \frac{1}{a}\int_0^C dA\, P\int_{-\infty}^{\infty} dx\,\frac{n^2\, J_n^2(z)\, e^{-\Gamma}}{x-1}, \tag{4.60}$$

where $\Gamma = \left[B^2+A^2\left(x^2-1\right)\right]^{1/2}$. The position of the singularities in the x-integral does not depend on the value of the second variable A; in fact the singularities always occur at the same point, $x=1$. As we now know exactly where the singular points are (and that this position doesn't change) this should have the desired result of simplifying the problem.

Rescaling the $u_{||}$ variable in the other expressions follows in a similar fashion and this enables us to write all the integrals in the range $u_\perp \in [0, C]$ (which is equivalent

to $\hat{p}_\perp \in [0, b_{crit}]$) as follows:

$$I_{xx} = \frac{1}{a}\int_0^C dA\, P \int_{-\infty}^{\infty} dx\, \frac{n^2\, J_n^2(z)\, e^{-\Gamma}}{x-1} \tag{4.61}$$

$$I_{yy} = \frac{1}{a^3}\int_0^C dA\, \left(C^2 - A^2\right) P \int_{-\infty}^{\infty} dx\, \frac{\left[J_n'(z)\right]^2\, e^{-\Gamma}}{x-1} \tag{4.62}$$

$$I_{zz1} = \int_0^C du_\perp\, u_\perp \left(a^2 + u_\perp^2\right)^{1/2} J_n^2(z)\, K_1\left[\left(a^2 + u_\perp^2\right)^{1/2}\right] \tag{4.63}$$

$$I_{zz2} = \frac{1}{a^3}\int_0^C dA\, A^2\, P \int_{-\infty}^{\infty} dx\, \frac{J_n^2(z)\, e^{-\Gamma}}{x-1} \tag{4.64}$$

$\hat{p}_\perp > b_{crit}$

In this region the denominator $\hat{p}_\parallel^2 + \hat{p}_\perp^2 - b_{crit}^2$ is always strictly greater than zero and there can be no singularities present in the integrand. The integration can therefore be carried out without the need for contour analysis. Recall that for this range the integral I_{xx} is

$$I_{xx} = \int_{b_{crit}}^{\infty} d\hat{p}_\perp \hat{p}_\perp\, n^2\, J_n^2(z) \int_{-\infty}^{\infty} d\hat{p}_\parallel \frac{e^{-a\gamma}}{\hat{p}_\parallel^2 + \hat{p}_\perp^2 + 1 - \frac{n^2}{\hat{\omega}^2}} \tag{4.65}$$

Scale the variables by the parameter a, following the definitions given by (4.44). The integral is then

$$I_{xx} = \frac{1}{a}\int_C^{\infty} du_\perp u_\perp\, n^2\, J_n^2(z) \int_{-\infty}^{\infty} du_\parallel \frac{e^{-\Gamma}}{\Gamma^2 - B^2}, \tag{4.66}$$

where $C = a\, b_{crit}$, $\Gamma = \left(u_\parallel^2 + u_\perp^2 + a^2\right)^{1/2}$ and $z = \hat{k}_\perp\, u_\perp / a$.

Define a new variable $\Delta \equiv (u_\perp^2 + a^2 - B^2)^{1/2} = (u_\perp^2 - C^2)^{1/2}$. The expression for I_{xx} then becomes

$$I_{xx} = \frac{1}{a}\int_0^{\infty} d\Delta\, \Delta\, n^2\, J_n^2(z) \int_{-\infty}^{\infty} du_\parallel \frac{e^{-\Gamma}}{u_\parallel^2 + \Delta^2}, \tag{4.67}$$

The denominator here is $u_\parallel^2 + \Delta^2$. If we again scale one variable to the other, we can define $x \equiv u_\parallel / \Delta$. So, writing the integral in terms of Δ and x, we have

$$I_{xx} = \frac{1}{a}\int_0^{\infty} d\Delta \int_{-\infty}^{\infty} dx\, \frac{n^2\, J_n^2(z)\, e^{-\Gamma}}{x^2 + 1}, \tag{4.68}$$

where $\Gamma = [B^2 + \Delta^2\ (x^2+1)]^{1/2}$ and $z = \hat{k}_\perp / a\ (\Delta^2 + C^2)^{1/2}$.

Similarly, the other components can be written in terms of Δ and $u_{||}$ as

$$I_{yy} = \frac{1}{a^3}\int_0^\infty d\Delta\,\Delta\left(\Delta^2+C^2\right)^{1/2}\int_{-\infty}^{\infty} du_{||}\,\frac{[J_n'(z)]^2\,e^{-\Gamma}}{u_{||}^2+\Delta^2} \tag{4.69}$$

$$I_{zz1} = \int_C^\infty du_\perp\,u_\perp\left(a^2+u_\perp^2\right)^{1/2} J_n^2(z)\,K_1\left[\left(a^2+u_\perp^2\right)^{1/2}\right] \tag{4.70}$$

$$I_{zz2} = \frac{1}{a^3}\int_0^\infty d\Delta\,\Delta^3\int_{-\infty}^{\infty} du_{||}\,\frac{J_n^2(z)\,e^{-\Gamma}}{u_{||}^2+\Delta^2} \tag{4.71}$$

$$\tag{4.72}$$

and in terms of Δ and the scaled variable x as:

$$I_{yy} = \frac{1}{a^3}\int_0^\infty d\Delta\left(\Delta^2+C^2\right)^{1/2}\int_{-\infty}^{\infty} dx\,\frac{[J_n'(z)]^2\,e^{-\Gamma}}{x^2+1} \tag{4.73}$$

$$I_{zz1} = \int_C^\infty du_\perp\,u_\perp\left(a^2+u_\perp^2\right)^{1/2} J_n^2(z)\,K_1\left[\left(a^2+u_\perp^2\right)^{1/2}\right] \tag{4.74}$$

$$I_{zz2} = \frac{1}{a^3}\int_0^\infty d\Delta\,\Delta^2\int_{-\infty}^{\infty} dx\,\frac{J_n^2(z)\,e^{-\Gamma}}{x^2+1} \tag{4.75}$$

$$\tag{4.76}$$

Behaviour at $\hat{p}_\perp = b_{crit}$

The point b_{crit} is defined to be the last point in the $\hat{p}_\perp$-integration for which the integrand contains singular points. The analysis carried out above has resulted in two completely distinct forms for the integrand; the integral in the range $\hat{p}_\perp \in [0, b_{crit}]$ is written in terms of the variable A and in the range $\hat{p}_\perp \in (b_{crit}, \infty)$ as an integral over Δ. The variables A and Δ are dimensionless variables and the point $\hat{p}_\perp = b_{crit}$ corresponds to the point $u_\perp = C$, where $u_\perp$ is the dimensionless perpendicular momentum variable. We would now like to investigate the behaviour of these two integrals as both A and Δ tend towards the point $u_\perp = C$.

xx-component

Recall, from equations (4.61) and (4.68), that the xx-integral can be split into the

following two integrals

$$I_A = \frac{1}{a}\int_0^C dA\, n^2\, J_n^2(z)\; P\int_{-\infty}^{\infty} dx\, \frac{e^{-\Gamma}}{x-1}\;,\; A^2 = C^2 - u_\perp^2 \tag{4.77}$$

$$I_\Delta = \frac{1}{a}\int_0^\infty d\Delta\, n^2\, J_n^2 \int_{-\infty}^{\infty} dx\, \frac{e^{-\Gamma}}{x^2+1}\;,\; \Delta^2 = u_\perp^2 - C^2 \tag{4.78}$$

Here, we have used the final form of the integrals involving the variables A, Δ and x as this is the most convenient form for the analysis we are about to carry out.

Now as $u_\perp \to C$, $A \to 0$ and $\Gamma = [B^2 + A^2\,(x^2+1)]^{1/2} \to B$.

Therefore, as $A \to 0$

$$P\int_{-\infty}^{\infty} dx\, \frac{e^{-\Gamma}}{x-1} \to e^{-B}\, P\int_{-\infty}^{\infty} \frac{dx}{x-1}. \tag{4.79}$$

In the limit $A \to 0$, $x = u_{||}/A$ will become quite large. Thus over the infinite integral above we will ignore the constant term in the denominator so that the integral reduces to

$$P\int_{-\infty}^{\infty} \frac{dx}{x}. \tag{4.80}$$

The integrand thus reduces to an odd function of x and, since we are integrating the function from $-\infty$ to ∞, the value of the integral must be zero.

Look now at the Δ-integration. As $u_\perp \to C$, the variable $\Delta \to 0$. In this limit, $\Gamma = [B^2 + \Delta^2\,(x^2+1)]^{1/2} \to B$ as before and the x-integral becomes

$$\int_{-\infty}^{\infty} dx\, \frac{e^{-\Gamma}}{x^2+1} \to e^{-B}\, 2\int_0^\infty \frac{dx}{x^2+1} = e^{-B}\,\pi. \tag{4.81}$$

The integrand of the Δ-integral is then

$$n^2\, J_n^2(z)\, e^{-B}\,\pi \to \pi\, e^{-B}\, n^2\, J_n^2(z_0) \tag{4.82}$$

in the limit $\Delta \to 0$, where $z_0 = \hat{k}_\perp\, C/a$.

We thus have the following two results:

$$I_A \to 0 \text{ as } A \to 0 \tag{4.83}$$

$$I_\Delta \to \pi\, e^{-B}\, n^2\, J_n^2\left(\frac{\hat{k}_\perp\, C}{a}\right) \text{ as } \Delta \to 0. \tag{4.84}$$

We can therefore conclude that the double integral is discontinuous at the point $u_\perp = C$ (which corresponds to $\hat{p}_\perp = b_{crit}$).

yy-component

The I_{yy} integral can be split into ((4.62) and (4.73))

$$I_{yy} = \frac{1}{a^3}\int_0^C dA\left(C^2-A^2\right)\left[J_n'(z)\right]^2 P\int_{-\infty}^{\infty} dx\,\frac{e^{-\Gamma}}{x-1} \tag{4.85}$$

$$I_{yy} = \frac{1}{a^3}\int_0^{\infty} d\Delta\left(\Delta^2+C^2\right)^{1/2}\left[J_n'(z)\right]^2\int_{-\infty}^{\infty} dx\,\frac{e^{-\Gamma}}{x^2+1}. \tag{4.86}$$

The x-integrals in both of these expressions are the same as their counterparts in the xx-component. We can therefore write the limiting forms for I_A and I_Δ without any further work:

$$I_A \rightarrow 0 \text{ as } A\rightarrow 0 \tag{4.87}$$

$$I_\Delta \rightarrow \pi e^{-B} C\left[J_n'\left(\frac{\hat{k}_\perp C}{a}\right)\right]^2 \text{ as } \Delta\rightarrow 0. \tag{4.88}$$

As for the xx-component, we can again conclude that the double integral is discontinuous at the point $u_\perp = C$ (corresponding to $\hat{p}_\perp = b_{crit}$).

zz-component

The I_{zz} integral has been written as the sum of the two integrals I_{zz1} and I_{zz2}. The first of these has been reduced to a single integral over $u_\perp$ and has the same form throughout the entire range of the integration. As such, there is no need to consider this integral here. Instead we will concentrate on the latter integral which has the same form as the I_{xx} and I_{yy} integrals and can be split into the integrals ((4.64) and (4.75)):

$$I_A = \frac{1}{a^3}\int_0^C dA\,A^2 J_n^2(z)\,P\int_{-\infty}^{\infty} dx\,\frac{e^{-\Gamma}}{x-1} \tag{4.89}$$

$$I_\Delta = \frac{1}{a^3}\int_0^{\infty} d\Delta\,\Delta^2 J_n^2(z)\int_{-\infty}^{\infty} dx\,\frac{e^{-\Gamma}}{x^2+1} \tag{4.90}$$

The x-integrals in both of these expressions are again the same as those in the xx-component. We can therefore write the limiting forms for I_A and I_Δ as:

$$I_A \rightarrow 0 \text{ as } A\rightarrow 0 \tag{4.91}$$

$$I_\Delta = \pi e^{-B}\Delta^2 J_n^2\left(\frac{\hat{k}_\perp C}{a}\right) \tag{4.92}$$

$$\rightarrow 0 \text{ as } \Delta\rightarrow 0. \tag{4.93}$$

Therefore I_A and I_Δ both tend to zero as their respective integration variables tend to the point $u_\perp = C$. We can thus conclude that the double integral in the zz-component is the only one of the three to be continuous at this point. The discontinuities in the xx- and yy- integrals will be taken into consideration later as we come to describe some of the main details of the integration code.

4.4.2 Case (ii) : $\frac{n}{\hat{\omega}} < 1$

When $n < \hat{\omega}$, we can no longer define b_{crit} to be $\left(\frac{n^2}{\hat{\omega}^2} - 1\right)^{1/2}$ as this would now be an imaginary quantity. Other than this, however, the integral here is treated in a very similar way to that for $\hat{p}_\perp \in (b_{crit}, \infty)$ in the previous case.

As there are no singularities present there is no need to split the integration into two parts and we can integrate $\hat{p}_\perp$ over the entire range $[0, \infty)$ in a single integral. So for I_{xx} we have

$$I_{xx} = \int_0^\infty d\hat{p}_\perp \, \hat{p}_\perp \, n^2 \, J_n^2(z) \int_{-\infty}^\infty d\hat{p}_\parallel \frac{e^{-a\gamma}}{\hat{p}_\parallel^2 + \hat{p}_\perp^2 + 1 - \frac{n^2}{\hat{\omega}^2}}. \tag{4.94}$$

Scale the variables by the parameter a as defined in (4.44), so that

$$I_{xx} = \frac{1}{a} \int_0^\infty du_\perp \, u_\perp \int_{-\infty}^\infty du_\parallel \frac{n^2 \, J_n^2(z) \, e^{-\Gamma}}{\Gamma^2 - B^2}, \tag{4.95}$$

where $\Gamma = \left(u_\parallel^2 + u_\perp^2 + a^2\right)^{1/2}$ and $z = \hat{k}_\perp \, u_\perp / a$.

Here we will now define the variable $\Phi \equiv \left(u_\perp^2 + a^2 - B^2\right)^{1/2}$, which enables us to write the integral as

$$I_{xx} = \frac{1}{a} \int_{\Phi_0}^\infty d\Phi \, \Phi \int_{-\infty}^\infty du_\parallel \frac{n^2 \, J_n^2(z) \, e^{-\Gamma}}{u_\parallel^2 + \Phi^2}. \tag{4.96}$$

Introducing the variable $x = u_\parallel / \Phi$ allows us to write the integral as

$$I_{xx} = \frac{1}{a} \int_{\Phi_0}^\infty d\Phi \int_{-\infty}^\infty dx \frac{n^2 \, J_n^2(z) \, e^{-\Gamma}}{x^2 + 1}, \tag{4.97}$$

where $\Phi_0 = \left(a^2 - B^2\right)^{1/2}$, $\Gamma = \left[B^2 + \Phi^2 \, (x^2 + 1)\right]^{1/2}$ and the Bessel function argument is $z = \hat{k}_\perp \, \left(\Phi^2 - a^2 + B^2\right)^{1/2} / a$.

Similarly, the $yy-$ and $zz-$integrals can be written in terms of Φ and $u_\parallel$ as follows:

$$I_{yy} = \frac{1}{a^3} \int_{\Phi_0}^\infty d\Phi \, \Phi \left(\Phi^2 - a^2 + B^2\right) \int_{-\infty}^\infty du_\parallel \frac{\left[J_n'(z)\right]^2 \, e^{-\Gamma}}{u_\parallel^2 + \Phi^2} \tag{4.98}$$

$$I_{zz1} = \int_0^\infty du_\perp \, u_\perp \left(a^2 + u_\perp^2\right)^{1/2} J_n^2(z) \, K_1\left[\left(a^2 + u_\perp^2\right)^{1/2}\right] \tag{4.99}$$

$$I_{zz2} = \frac{1}{a^3} \int_{\Phi_0}^\infty d\Phi \, \Phi^3 \int_{-\infty}^\infty du_{||} \, \frac{J_n^2(z) \, e^{-\Gamma}}{u_{||}^2 + \Phi^2}. \tag{4.100}$$

If we then introduce the scaled variable $x = u_{||}/\Phi$, they become

$$I_{yy} = \frac{1}{a^3} \int_{\Phi_0}^\infty d\Phi \left(\Phi^2 - a^2 + B^2\right) \int_{-\infty}^\infty dx \, \frac{[J_n'(z)]^2 \, e^{-\Gamma}}{x^2 + 1} \tag{4.101}$$

$$I_{zz1} = \int_0^\infty du_\perp \, u_\perp \left(a^2 + u_\perp^2\right)^{1/2} J_n^2(z) \, K_1\left[\left(a^2 + u_\perp^2\right)^{1/2}\right] \tag{4.102}$$

$$I_{zz2} = \frac{1}{a^3} \int_{\Phi_0}^\infty d\Phi \, \Phi^2 \int_{-\infty}^\infty dx \, \frac{J_n^2(z) \, e^{-\Gamma}}{x^2 + 1}. \tag{4.103}$$

4.5 Numerical Evaluation of the Integrals

In the last section we expressed the integrals I_{xx}, I_{yy} and I_{zz} in terms of integrals which were well-behaved and did not contain any singularities in their defined range of integration. We can now use a standard integration technique to evaluate these integrals.

Each integral term consists of a double integral in the dimensionless momentum components $u_\perp$ and x (recall that x represents a scaled form of the parallel momentum component $u_{||}$). We will use a one-dimensional compound Simpson rule to evaluate each of the $u_\perp$ and x integrals separately. This approach was thought to be more flexible than a $2-D$ Simpson rule which would have been difficult to implement in light of the singularities present in the integrand.

The compound Simpson rule, details of which can be found in Appendix C, represents the integral of the function $f(x)$ over the integral $x \in [a, b]$ as

$$\int_a^b f(x) \approx \frac{h}{3}\left[f_0 + 4 \sum_{m \ odd} f_m + 2 \sum_{m \ even} f_m + f_{2n}\right] \tag{4.104}$$

This rule defines $2n+1$ equally-spaced points along the interval $[a, b]$, $a = y_0 < y_1 < \ldots < y_{2n-1} < y_{2n} = b$. The function f is evaluated at each of these points (where $f_m = f(y_m)$) and the results scaled by a suitable weighting factor before being summed together. The weighting factor for each point arises from approximating the function between three consecutive points by a parabola. The quantity h is the separation of the points, defined to be $h = (b-a)/2n$.

In our case each integral is of the form

$$\int_0^\infty du_\perp F(u_\perp), \quad \text{where } F(u_\perp) = \int_{-\infty}^{\infty} dx\, f(u_\perp, x). \tag{4.105}$$

We cannot, however, use a Simpson rule over an infinite range so we must try to cut off the ranges at finite end-points. For the moment, we will specify $u_\perp \in [a_1, b_1]$ and $x \in [c_1, d_1]$. The double integral above can then be written as

$$\int_{a_1}^{b_1} du_\perp F(u_\perp), \quad \text{where} F(u_\perp) = \int_{c_1}^{d_1} dx\, f(u_\perp, x), \tag{4.106}$$

so that the Simpson rule applied to the $u_\perp$-integration gives

$$\int_{a_1}^{b_1} du_\perp F(u_\perp) \approx \frac{h}{3}\left[F_0 + 4\sum_{m\ odd} F_m + 2\sum_{m\ even} F_m + F_{2p}\right], \tag{4.107}$$

where the interval has been split into $2p$ sub-intervals and the spacing of the points is $h = (b_1 - a_1)/2p$.

But each function F is an integral over x, which can also be evaluated using Simpson's rule, ie

$$F_m = F(y_m) \approx \frac{l}{3}\left[f_{m\,0} + 4\sum_{n\ odd} f_{m\,n} + 2\sum_{n\ even} f_{m\,n} + f_{m\,2q}\right], \tag{4.108}$$

where $l = (d_1 - c_1)/2q$ and $f_{m\,n} = f\ (y_m, z_n)$ where $y_m = a_1 + m\,h$ and $z_n = c_1 + n\,l$.

So for each point $y_m \in [a_1, b_1]$ in the $u_\perp$-integration we must work out the x-integral for this point using a $2q$-point Simpson rule and treat the result as a function of $u_\perp$. We can then apply a $2p$-point Simpson rule to the $u_\perp$-integral, summing the weighted values of the x-integrals to give an estimate for the full double integral.

4.5.1 Splitting The Range of Integration

Recall that some of the integrals we will evaluate using the Simpson rule represent only part of the full integral. For the case $n \geq \hat{\omega}$, we split the $u_\perp$-integration range into two at the point C. Some care has to be taken over the position of this point as the compound Simpson rule can only be applied to an odd number of points. As C need not coincide with one of the points where the function is evaluated, we will denote b_m to be the Simpson point immediately before C, where b_m is defined to be equal to $a_1 + m_{crit} * h$. We thus have two cases:

m_{crit} odd: When m_{crit} is odd there is an even number of points before C and a compound Simpson rule alone does not *fit in*. After C, there is an odd number of points and there are no problems in this range. This situation is represented schematically in part (a) of Fig 4.9. To overcome this problem we will use a Simpson rule to evaluate the integral between the points a_1 and $a_1 + (m_{crit} - 1) * h$ and then use a Trapezoidal rule to evaluate the integral over the last sub-interval before C.

The Trapezoidal rule is the simplest numerical integration technique and approximates the integral between two points a and b to the area under the straight line drawn through these points. Hence we have

$$\int_a^b f(x)\,dx \approx \frac{1}{2}(b-a)\,[f(a)+f(b)], \tag{4.109}$$

or, in this case,

$$\int_{b_m-h}^{b_m} F(u_\perp)\,du_\perp \approx \frac{h}{2}\,[F(b_m-h)+F(b_m)]. \tag{4.110}$$

For more details on the Trapezoidal rule consult Riley [29].

m_{crit} even: When m_{crit} is even there is an odd number of points before C but an even number in the second part of the range, shown in part (b) of Fig 4.9. So here we need an extra Trapezoidal rule after the point C rather than before it.

We note here that the integral is not evaluated at all between the points $a_1 + m_{crit} * h$ and $a_1 + (m_{crit} + 1) * h$, which will introduce an error into the final estimate for the integral. To minimise this error we will ensure that the step-size h is small so that the contribution from each sub-interval is a small fraction of the total.

We would also like to take into account the fact that the integrals I_{xx} and I_{yy} are discontinuous at the point C, as we proved in Section 4.4.1. We would like to make use of the limiting values of the integrals as $u_\perp \to C$. To ensure that the discontinuity is properly incorporated into the code, we will set the integral to be equal to its limiting value if the integration point happens to lie very close to the point C (ie within a distance $h/2$).

For the case $n \geq \hat{\omega}$ and in the range $u_\perp \leq C$ there is a singularity in the x-integral at the point $x = 1$. The problem has been formulated so that the singularities coincide with one of the points where the Simpson rule evaluates the integrand. The

contour analysis carried out in section 4.4.1 enables us to omit this point from the numerical integration but this means that we also have to split up the x-integral and use two separate Simpson rules. We cannot simply use the same procedure as defined above for the $u_\perp$-integration as here we have to omit a point completely from the Simpson rule.

We define the integration point immediately before $x = 1$ to be $c + q1 * l$. We again require two different solutions depending on whether $q1$ is odd or even.

$q1$ odd: When $q1$ is odd there is an even number of points in each integration range and we have to include two Trapezoidal rules, one on either side of the point $x = 1$, as shown in part (a) of Fig 4.2.

$q1$ even: When $q1$ is even there is an odd number of points in each range and the two compound Simpson rules are all that are needed. This is illustrated in part (b) of Fig 4.2.

When there is a singular point at $x = 1$, we do not evaluate the integral between the points $1 - l$ and $1 + l$. However, if we again refer back to the analysis in section 4.4.1, we see that as long as the size of the interval, $2\,l$, is small then the contributions from either side of the singular point should cancel each other out.

The value of C depends on the parameter a and the values of $\hat{\omega}$ and n. The integrals involving C are contained within a sum over n and we take $\hat{\omega}$ over a range of values, so C may take many different values over all the integrals present in the dielectric components. Before we carry out the various integration rules described above, we must first ensure that they can be suitably carried out with regard to the position of C within the range of integration. If it is near one of the end-points of the range there may not be enough points in the corresponding sub-interval to apply the appropriate rule. There are several special cases that we must take into consideration:

$m_{crit} = 0$ or 1	:	do not need the first Simpson rule
$2p - m_{crit} = 1$ or 2	:	do not need the second Simpson rule
$2p \leq m_{crit}$	:	need only the first Simpson rule

4.5.2 Evaluation of the Bessel Functions

The Bessel functions $J_n(z)$ and $K_n(z)$ are, in general, not included in any libraries of special functions for arbitrary values of n and have to be evaluated within the program. The NAG library contains routines to evaluate J_0, J_1, K_0 and K_1 (routines s17aef, s17aff, s18acf and s18adf respectively), so their values can easily be found. We can then use these values in recurrence relations to evaluate the values of J_n and K_n, for any integer value of n. The algorithms used to evaluate J_n and K_n were taken from the book of numerical recipes by Press et al [30]. The relevant recurrence relations used are

$$J_{n+1}(z) = \frac{2n}{z} J_n(z) - J_{n-1}(z) \tag{4.111}$$

$$K_{n+1}(z) = \frac{2n}{z} K_n(z) + K_{n-1}(z). \tag{4.112}$$

The upward recurrence relation for J_n is only stable for $n < x$. To overcome the problem of instability for $n > x$, the algorithm is started from some arbitrarily large value of $n = m$ where J_m and J_{m+1} are set equal to one and zero respectively. The recurrence relation is then applied downwards until J_0 and J_1 are reached and the values of the resultant Bessel functions are then normalised using the sum

$$1 = J_0(z) + 2J_2(z) + 2J_4(z) + \ldots . \tag{4.113}$$

The value of m has to be chosen large enough to ensure that when the required value of n is reached the answer is sufficiently accurate.

The situation for K_n is simpler. Although the upward recurrence is again unstable, K_n itself is growing and the instability does not affect the result. Starting from K_0 and K_1, whose values we know from the NAG routines, we can then just use the recurrence relation until the required value of K_n is obtained.

The integral I_{yy} contains the derivative of J_n rather than the Bessel function itself. This derivative is evaluated using the following identity:

$$J_n'(z) = \frac{1}{2}\left[J_{n-1}(z) - J_{n+1}(z)\right], \tag{4.114}$$

which involves evaluating J_{n-1} and J_{n+1} and combining them as shown to give J_n'.

Recurrence relations like the ones above require a lot of work to evaluate one Bessel function and, since we need to evaluate two Bessel functions to get the derivative, J_n' requires even more effort. It would thus be sensible to evaluate the Bessel functions as few times as possible. We notice that the J_n Bessel functions that appear inside the integrals depend on only one of the integration variables ($u_\perp$). To keep the computing time to a minimum we only evaluate J_n once for each value of $u_\perp$ and assign this value to a variable. It is this variable which is then passed to all the x-integrations for that particular value of $u_\perp$. Similarly, J_n' is only evaluated for I_{yy} as it is not present in the other two components.

We would also like to note here that the only other library routine used in the code was the NAG routine x01aaf, which assigned the appropriate value to π.

4.6 The Integration Code

A listing of the integration code is included in Appendix D. The code is written in FORTRAN and was developed using the Salford FORTRAN compiler for PCs. When it came to carrying out full-scale runs of the code, however, it quickly became apparent that the PC was too slow to run the code in a reasonable time. The solution to this problem was to transfer the code to the local SPARC 10/40 workstation. There the running time was reduced to a few hours, provided there were no other large jobs running.

Our first task was to decide what range to choose for our integrals. We clearly cannot apply a Simpson rule to an infinite range but at the same time we cannot cut off the integral too soon or we will introduce unacceptable errors into the calculation. The presence of the $e^{-\Gamma}$ factor in the integrands means that their values fall away quickly as the integration variables increase and this helps us to justify our decision to take a small integration range.

In the code, we have taken the range of $u_\perp$ to be $[0, 4]$ and that of x to be $[-4, 4]$. The number of points in the x-integral is taken to be 40, giving a step-size of $l = 0.2$. The step-size of the $u_\perp$-integration is taken to be equal to l, resulting in a 20-point compound Simpson rule for this integral. To check that the ranges of these intervals

are large enough to give us accurate results, we increased their size to $-6 \leq x \leq 6$ and $0 \leq u_\perp \leq 6$ respectively, while keeping the step-sizes constant. The results obtained for these increased ranges are not always identical to our initial results but the differences are small enough to indicate that there is little to be gained from using intervals larger than our original range $u_\perp \in [0,4]$ and $x \in [-4,4]$. Another consideration has to be the size of the steps we use in the integration routines. We doubled the number of points used in each interval so that the step-sizes h and l were both reduced to a value of 0.1. This again had very little effect on the solutions to the dispersion relations; the results obtained were almost the same as the results for the larger step-size. We therefore concluded that a step-size of 0.2 was accurate enough for the needs of our calculations.

We now have to assign values to the parameters a and η. Recall that a is a measure of how relativistic the plasma particles are. We will look at a range of values, centred on the value $a = 1$. The full range of values studied is

$$0.1 \qquad 0.2 \qquad 0.5 \qquad 1 \qquad 2 \qquad 5 \qquad 10, \tag{4.115}$$

which stretches from the highly relativistic to the weakly relativistic regime. η is equal to the ratio of the plasma frequency to the non-relativistic cyclotron frequency and, for the purposes of our analysis, will be assumed to be equal to $\sqrt{5}$ throughout.

The infinite sum over n in each component of $\underline{\underline{\mathbf{R}}}$ has to be cut off at some finite value. We thus sum n from 0 to $nmax$, where $nmax = 4$. To check the accuracy of this truncated sum, we increased $nmax$ to a value of 8 and re-evaluated the results. There was little difference in the two sets of results and we felt justified in keeping $nmax = 4$ as the upper limit of the sum over n.

The main body of the program is a double loop in the variables λ ($\equiv \hat{k}_\perp^2/a$) and $\hat{\omega}$. The chosen component of $\underline{\underline{\mathbf{R}}}$ is then evaluated over a certain range of $(\lambda, \hat{\omega})$-space using the methods described throughout this chapter. For each two consecutive values of R_{ii}, where $i = 1, 2$ or 3, we divide the latter value by the former and determine the sign of the quotient. If the sign is negative then the value of R_{ii} must have changed sign somewhere between these two values of $\hat{\omega}$, which means in turn that there must be a solution of $R_{ii} = 0$ in this region.

The most accurate way to proceed from this point would be to use these known values of $\hat{\omega}$ in a root finding scheme, Newton's Method for example. This would enable us to get a better estimate for the solution of $R_{ii} = 0$. We have decided, however, to take a less accurate (and therefore less time-consuming) approach. If we find that R_{ii} has changed sign between the points $\hat{\omega}_1$ and $\hat{\omega}_2$ say, then we specify $\hat{\omega}_2$ to be the required solution. As the real solution could lie anywhere between the two points, the maximum possible error in this answer is the separation of the points. We realise that this over-simplified method is not ideal but if we evaluate R_{ii} over a relatively dense grid of points then the separation of the points will be small and our approximate solutions should give us a good idea what the overall shapes of the dispersion curves look like.

When the code finds a solution to the dispersion relation $R_{ii} = 0$, the corresponding values of λ and $\hat{\omega}$ are written to a file. At the end of the run, we are thus left with a series of points which we can plot on a graph of $\hat{\omega}$ against λ to represent the dispersion curve in that region of $(\lambda, \hat{\omega})$-space. For a given set of parameters, we find the roots of the three dielectric components separately but plot the resultant curves on the same graph.

4.7 Non-relativistic Thermal Plasmas

Before presenting our results we will try to put them into context by firstly reviewing the case of perpendicular waves in a non-relativistic Maxwellian plasma. Standard textbooks such as Krall & Trivelpiece [22] and Cairns [31] give an analysis of perpendicular wave propagation in a thermal, non-relativistic plasma. For the case of an electron-ion plasma, the dielectric tensor for perpendicular propagation has the form

$$\underline{\underline{\mathbf{R}}} = \begin{bmatrix} R_{xx} & R_{xy} & 0 \\ -R_{xy} & R_{yy} & 0 \\ 0 & 0 & R_{zz} \end{bmatrix}. \tag{4.116}$$

Only high frequency wave modes are considered so that the motion of the ions may be neglected. For non-trivial solutions to the equation $\underline{\underline{\mathbf{R}}} \cdot \mathbf{E} = 0$ for the electric

field $\mathbf{E}$ we have

$$R_{xx}\,R_{yy} + R_{xy}^2 = 0 \tag{4.117}$$

or

$$R_{zz} = 0. \tag{4.118}$$

For the first of these relations, the electric field is perpendicular to the magnetic field $\mathbf{B}_0$. The relation, as it stands, is rather complex and the eigenmodes cannot be found easily. However, if we assume that $k^2\,c^2 \gg \omega_p^2$ then the R_{xy} component is much smaller than the $k^2\,c^2/\omega_p^2$ term in the R_{yy} component and can be neglected. In this limit of low phase velocity, there are then two approximate solutions given by $R_{xx} = 0$ and $R_{yy} = 0$. We will now briefly summarise the characteristics of each of these three modes.

4.7.1 The Bernstein Modes

The dispersion relation $R_{xx} = 0$, as given in Krall & Trivelpiece [22], can be written as

$$k^2 = \sum_{n=1}^{\infty} \sum_{\alpha} \frac{2\,n^2\,\omega_{p\,\alpha}^2\,\omega_{c\,\alpha}^2}{\omega^2 - n^2\,\omega_{c\,\alpha}^2}\,\frac{m_\alpha}{\kappa\,T_\alpha}\,I_n\left(\frac{k^2}{\omega_{c\,\alpha}^2}\,\frac{\kappa\,T_\alpha}{m_\alpha}\right)\exp\left(-\frac{k^2}{\omega_{c\,\alpha}^2}\,\frac{\kappa\,T_\alpha}{m_\alpha}\right), \tag{4.119}$$

where $\omega_{p\,\alpha}$ is the plasma frequency, $\omega_{c\,\alpha}$ is the cyclotron frequency, I_n is a modified Bessel function and the subscript α represents the plasma species.

The solutions to this equation are longitudinal electron waves, which were treated correctly for the first time by Bernstein [32] (thus their name). Unlike previous (erroneous) attempts to treat this problem, he proved that for the specific case of a collisionless plasma, and in the limit $c \to \infty$, this class of waves exists at frequencies close to the harmonics of the electron cyclotron frequency. For small wave numbers, one solution of (4.119) exists close to the upper hybrid frequency $\omega_{u\,h} = \sqrt{\omega_{p\,e}^2 + \omega_{c\,e}^2}$. Above this frequency, a gap exists between each of the Bernstein modes where no solutions are found. See Crawford [33] for a graphical collection of Bernstein modes for several different values of the parameter $\omega_{p\,e}/\omega_{c\,e}$.

If we assume that the plasma consists of electrons and positrons at the same equilibrium temperature, then the expression on the right hand side of (4.119) is the

same for each species and the dispersion relation reduces to

$$k^2 = \sum_{n=1}^{\infty} \frac{4\,n^2\,\omega_p^2\,\omega_c^2}{\omega^2 - n^2\,\omega_c^2}\,\frac{m}{\kappa T}\,I_n\left(\frac{k^2}{\omega_c^2}\,\frac{\kappa T}{m}\right)\exp\left(-\frac{k^2}{\omega_c^2}\,\frac{\kappa T}{m}\right). \tag{4.120}$$

A computer code has been written to find the solutions to this dispersion relation using the same principle as the code developed to solve the relativistic dispersion relations described earlier in the chapter. Here the problem is greatly simplified by the removal of all the integrals from the expression. The only real difficulty is the evaluation of the Bessel functions I_n. Again, the appropriate numerical recipe from Press et al [30] was used. Our first task, though, is to define the dimensionless variables

$$\hat{\omega} = \frac{\omega}{\omega_c}, \qquad \eta = \frac{\omega_p}{\omega_c}, \qquad \lambda = \frac{\kappa T\,k^2}{m\,\omega_c^2}. \tag{4.121}$$

In terms of these variables, the relation (4.120) becomes

$$1 - \sum_{n=1}^{\infty} \frac{4\,n^2\,\eta^2}{\hat{\omega}^2 - n^2}\,\frac{1}{\lambda}\,I_n(\lambda)\,e^{-\lambda} = 0. \tag{4.122}$$

The code evaluates the left hand side of the equation over an array of $\hat{\omega}$ and λ values, picking out the points where it changes sign. These points are saved to a file and the resulting curves plotted in Fig 4.1. As in the relativistic case, these curves are evaluated for $\eta = \sqrt{5}$ and only the first four terms are included in the sum over n. The curves look remarkably similar to those shown in Crawford [33]. An artefact of the method used, however, was the inclusion of horizontal lines along the cyclotron harmonics. The points $\hat{\omega} = n$ were neglected from the routine to avoid the singularities there but there must be a change of sign as we go through these points which is being picked up by the program. Note that for an electron-positron plasma the upper hybrid frequency is defined to be

$$\omega_{uh}^2 = 2\,\omega_p^2 + \omega_c^2, \tag{4.123}$$

where $2\,\omega_p^2$ is the plasma frequency of the whole plasma, and, in terms of dimensionless quantities is,

$$\hat{\omega}_{uh} = \sqrt{2\,\eta^2 + 1} = \sqrt{11}. \tag{4.124}$$

If we look at Fig 4.1 again, we see that one of the curves is very close to that value for $\lambda = 0$ and the curves both above and below $\hat{\omega}_{uh}$ behave as expected.

4.7.2 The Extraordinary Mode

The solution to the dispersion relation $R_{yy} = 0$ is known as the extraordinary mode. For this mode the electric field is nearly normal to $\mathbf{k}$ and it is almost a pure electromagnetic wave. The component, obtained from [22] (correcting the typographical error), is

$$R_{yy} = 1 - \frac{k^2 c^2}{\omega^2} - \frac{2\pi}{\omega} \sum_{n=-\infty}^{\infty} \sum_{\alpha} \omega_{p\alpha}^2 \left(\frac{m_\alpha}{2\pi\kappa T_\alpha}\right)^{3/2} \frac{m_\alpha}{\kappa T_\alpha} \times \int_{-\infty}^{\infty} dv_{\parallel} \int_0^{\infty} dv_\perp \frac{v_\perp^3 (J_n')^2}{\omega - n\omega_{c\alpha}} \exp\left(-\frac{m_\alpha v^2}{2\kappa T_\alpha}\right), \quad (4.125)$$

and for the case of an electron-positron plasma (with $T_e = T_p \equiv T$)

$$R_{yy} = 1 - \frac{k^2 c^2}{\omega^2} - 4\pi\omega_p^2 \left(\frac{m}{2\pi\kappa T}\right)^{3/2} \frac{m}{\kappa T} \times \sum_{n=-\infty}^{\infty} \frac{1}{\omega^2 - n^2\omega_c^2} \int_{-\infty}^{\infty} dv_{\parallel} \int_0^{\infty} dv_\perp v_\perp^3 (J_n')^2 \exp\left(-\frac{m v^2}{2\kappa T}\right). \quad (4.126)$$

4.7.3 The Ordinary Mode

The solution to the dispersion relation $R_{zz} = 0$ is a pure electromagnetic wave with $\mathbf{E} \parallel \mathbf{B}_0$, and is known as the ordinary mode because the electrons following the electric field E_z do not see the magnetic field $\mathbf{B}_0$. The component (again correcting the errors in [22]) is

$$R_{zz} = 1 - \frac{k^2 c^2}{\omega^2} - \frac{2\pi}{\omega} \sum_{n=-\infty}^{\infty} \sum_{\alpha} \omega_{p\alpha}^2 \left(\frac{m_\alpha}{2\pi\kappa T_\alpha}\right)^{3/2} \frac{m_\alpha}{\kappa T_\alpha} \times \int_{-\infty}^{\infty} dv_{\parallel} v_{\parallel}^2 \int_0^{\infty} dv_\perp \frac{v_\perp J_n^2}{\omega - n\omega_{c\alpha}} \exp\left(-\frac{m_\alpha v^2}{2\kappa T_\alpha}\right). \quad (4.127)$$

For an electron-positron plasma with both species at temperature T, this component becomes

$$R_{zz} = 1 - \frac{k^2 c^2}{\omega^2} - 4\pi\omega_p^2 \left(\frac{m}{2\pi\kappa T}\right)^{3/2} \frac{m}{\kappa T} \times \sum_{n=-\infty}^{\infty} \frac{1}{\omega^2 - n^2\omega_c^2} \int_{-\infty}^{\infty} dv_{\parallel} v_{\parallel}^2 \int_0^{\infty} dv_\perp v_\perp J_n^2 \exp\left(-\frac{m v^2}{2\kappa T}\right). \quad (4.128)$$

4.8 Results for a Relativistic Thermal Plasma

Returning to the case of a relativistic Maxwellian plasma, we would now like to present the solutions for the relativistic dispersion relations we found using our computer code. The method used to find these solutions has already been explained in some detail. The three curves obtained for each value of the parameter a are presented on a single graph and, in total, seven values of a were considered. The results are presented in Figs 4.2-4.8.

Fig 4.2 shows the dispersion curves for $a = 10$, which is tending towards the weakly-relativistic limit. The solution for $R_{xx} = 0$ does seem to bear some similarity to the non-relativistic Bernstein modes for larger λ values (which correspond to large $\hat{k}_\perp$) in that the curves seem to be drawn out along the harmonics of the cyclotron frequency. It is also clear that as the value of a is progressively decreased, the solution of $R_{xx} = 0$ becomes less significant: the behaviour around the cyclotron harmonics disappears and the whole curve seems to shrink away to zero.

The behaviour of the other two dispersion curves is less dramatic and the curves maintain a similar shape for all values of a under consideration. If we transform the horizontal variable from λ to $\hat{k}_\perp$, then we find that both these curves tend towards straight lines with a gradient of unity, ie $\hat{\omega} = \hat{k}_\perp$, for large $\hat{k}_\perp$ values. In terms of the dimensional variables, this corresponds to $\omega \simeq c\,k_\perp$, which is the dispersion relation for electromagnetic waves in vacuo. The ordinary and extraordinary waves in non-relativistic plasma theory are both electromagnetic (to a good approximation) and they too will be governed by this dispersion relation in the limit of small wavelength.

If we look closely at all the graphs, we see that the solutions for $R_{xx} = 0$ and $R_{yy} = 0$ have the same value for $\lambda = 0$. We should be able to check this result analytically. Look firstly at the xx-component.

$$R_{xx} = -\Omega_0^2 \left[\hat{\omega}^2 - \frac{2\,a^2\,\eta^2}{\hat{k}_\perp^2\,K_2(a)} \sum_{n=1}^{\infty} \int_0^\infty d\hat{p}_\perp\,\hat{p}_\perp \int_{-\infty}^{\infty} d\hat{p}_\parallel \frac{n^2\,J_n^2(z)\,e^{-a\gamma}}{\gamma^2 - n^2/\hat{\omega}^2} \right]. \quad (4.129)$$

Here, we cannot simply set λ (and thus $\hat{k}_\perp$) equal to zero as there is a $\hat{k}_\perp^2$ term in the denominator. Instead we let $\lambda \to 0$. In the limit of small $z(= \hat{k}_\perp\,\hat{p}_\perp)$, we have

$$J_n(z) \sim \frac{(z/2)^n}{\Gamma(n+1)}. \quad (4.130)$$

Substituting this into the component removes the $\hat{k}_\perp$ factor from the denominator and allows us to set $\lambda = 0$. When we do this, the only non-zero contribution from the sum over n is the term for $n = 1$. Thus, the xx-component is given by

$$R_{xx} = -\Omega_0^2 \left[\hat{\omega}^2 - \frac{a^2 \eta^2}{2 K_2(a)} \int_0^\infty d\hat{p}_\perp \hat{p}_\perp^3 \int_{-\infty}^\infty d\hat{p}_\parallel \frac{e^{-a\gamma}}{\gamma^2 - 1/\hat{\omega}^2} \right]. \tag{4.131}$$

The yy-component is

$$\begin{aligned} R_{yy} \;=\; -\Omega_0^2 \Bigg[\hat{\omega}^2 - \hat{k}_\perp^2 - \frac{a^2 \eta^2}{K_2(a)} \Bigg\{ & \int_0^\infty d\hat{p}_\perp \hat{p}_\perp^3 \int_{-\infty}^\infty d\hat{p}_\parallel \frac{[J_0'(z)]^2 \, e^{-a\gamma}}{\gamma^2} \\ & + 2 \sum_{n=1}^\infty \int_0^\infty d\hat{p}_\perp \hat{p}_\perp^3 \int_{-\infty}^\infty d\hat{p}_\parallel \frac{[J_n'(z)]^2 \, e^{-a\gamma}}{\gamma^2 - n^2/\hat{\omega}^2} \Bigg\} \Bigg]. \end{aligned} \tag{4.132}$$

As there are no factors of $\hat{k}_\perp$ in the denominator we can safely set $\lambda = 0$. Again, the $n = 1$ term is the only non-zero term in the sum and the component reduces to the form

$$R_{yy} = -\Omega_0^2 \left[\hat{\omega}^2 - \frac{a^2 \eta^2}{2 K_2(a)} \int_0^\infty d\hat{p}_\perp \hat{p}_\perp^3 \int_{-\infty}^\infty d\hat{p}_\parallel \frac{e^{-a\gamma}}{\gamma^2 - 1/\hat{\omega}^2} \right]. \tag{4.133}$$

Therefore, we see that R_{xx} indeed equals R_{yy} for $\lambda = 0$ and so would expect their solutions to coincide at this value of λ, as we have already shown in our graphs.

4.9 Comparison with the Non-relativistic Case

We would expect that the solutions we presented in the last section to be the relativistic counterparts of the non-relativistic dispersion curves given in Section 4.7. If this is true, then we would expect our dispersion relations to reduce to the expressions in (4.120), (4.126) and (4.128) in the non-relativistic limit.

We will look at the form of the dielectric components which are still written in terms of fully dimensional variables, that is:

$$\begin{aligned} R_{xx} \;=\; -\omega^2 + 4\pi\omega^2 \frac{\omega_p^2 \Omega_0^2 \, a \, \alpha}{k_\perp^2 c^2} \times & \\ \sum_{n=-\infty}^\infty \int_{-\infty}^\infty dp_\parallel \int_0^\infty dp_\perp \, p_\perp \frac{n^2 J_n^2(z) \, e^{-a\gamma}}{\gamma^2 \omega^2 - n^2 \Omega_0^2} & \end{aligned} \tag{4.134}$$

$$R_{yy} = -\omega^2 + c^2 k_\perp^2 + 4\pi\omega^2 \frac{\omega_p^2 a \alpha}{m^2 c^2} \times \sum_{n=-\infty}^{\infty} \int_{-\infty}^{\infty} dp_\parallel \int_0^\infty dp_\perp p_\perp^3 \frac{[J_n'(z)]^2 e^{-a\gamma}}{\gamma^2\omega^2 - n^2\Omega_0^2} \quad (4.135)$$

$$R_{zz} = -\omega^2 + c^2 k_\perp^2 + 4\pi\omega^2 \frac{\omega_p^2 a \alpha}{m^2 c^2} \times \sum_{n=-\infty}^{\infty} \int_{-\infty}^{\infty} dp_\parallel p_\parallel^2 \int_0^\infty dp_\perp p_\perp \frac{J_n^2(z) e^{-a\gamma}}{\gamma^2\omega^2 - n^2\Omega_0^2}, \quad (4.136)$$

where

$$\alpha = \frac{a}{4\pi m^3 c^3 K_2(a)} \quad (4.137)$$

is the normalisation constant for the relativistic Maxwellian distribution. We have already shown in Section 4.1 that

$$f_0(p) = \alpha e^{-a\gamma} \rightarrow \left(\frac{1}{2\pi m\kappa T}\right)^{3/2} \exp\left(\frac{-p^2}{2 m\kappa T}\right) \quad (4.138)$$

in the non-relativistic limit. If we substitute this into each component of $\underline{\underline{\mathbf{R}}}$ in turn and let $\gamma \rightarrow 1$, then we get:

xx-component

$$R_{xx} \rightarrow -\omega^2 + 4\pi\omega^2 \frac{\omega_p^2\Omega_0^2}{k_\perp^2} \frac{m}{\kappa T} \frac{1}{(2\pi m\kappa T)^{3/2}} \sum_{n=-\infty}^{\infty} \frac{2n^2}{\omega^2 - n^2\Omega_0^2} \times \int_{-\infty}^{\infty} dp_\parallel \exp\frac{-p_\parallel^2}{2 m\kappa T} \int_0^\infty dp_\perp p_\perp J_n^2(z) \exp\left(\frac{-p_\parallel^2}{2 m\kappa T}\right) \quad (4.139)$$

$$= -\omega^2 + 4\omega^2 \frac{\omega_p^2\Omega_0^2}{k_\perp^2} \frac{m}{\kappa T} \sum_{n=1}^{\infty} \frac{n^2}{\omega^2 - n^2\Omega_0^2} \times \exp\left(-\frac{k_\perp^2}{\Omega_0^2} m\kappa T\right) I_n\left(\frac{k_\perp^2}{\Omega_0^2} m\kappa T\right), \quad (4.140)$$

using the integral relations

$$\int_0^\infty e^{-q^2x^2} dx = \frac{\sqrt{\pi}}{2q} \quad (q > 0) \quad (4.141)$$

$$\int_0^\infty e^{-qx^2} J_n^2(\beta x)\, x\, dx = \frac{1}{2q} e^{-\beta^2/2q} I_n\left(\frac{\beta^2}{2q}\right) \quad (q > 0). \quad (4.142)$$

This expression for R_{xx} is very similar to the equation (4.120). Apart from the different notation, the only real difference is that occurrences of the term $m\kappa T$

here are replaced by $\kappa T/m$ there. This is due to the difference in the normalisation terms for the two different distribution functions. The Maxwellian distribution used to derive (4.120) is defined in terms of the velocity of the particles, ie

$$f_0(v) = \left(\frac{m}{2\pi\kappa T}\right)^{3/2} \exp\left(-\frac{m v^2}{2\kappa T}\right), \tag{4.143}$$

as opposed to the definition we obtained in (4.138) above.

yy-component

$$R_{yy} \rightarrow -\omega^2 + c^2 k_\perp^2 + 4\pi\omega^2\omega_p^2 \frac{1}{(2\pi m\kappa T)^{3/2}} \frac{1}{m\kappa T} \times \sum_{n=-\infty}^{\infty} \frac{1}{\omega^2 - n^2\Omega_0^2} \int_{-\infty}^{\infty} dp_\parallel \int_0^{\infty} dp_\perp\, p_\perp^3\, [J_n(z)]^2 \exp\left(\frac{-p^2}{2m\kappa T}\right) \tag{4.144}$$

which, again making allowances for the change in position of the mass terms, is the same as the expression (4.126).

zz-component

$$R_{zz} \rightarrow -\omega^2 + c^2 k_\perp^2 + 4\pi\omega^2\omega_p^2 \frac{1}{(2\pi m\kappa T)^{3/2}} \frac{1}{m\kappa T} \times \sum_{n=-\infty}^{\infty} \frac{1}{\omega^2 - n^2\Omega_0^2} \int_{-\infty}^{\infty} dp_\parallel\, p_\parallel^2 \int_0^{\infty} dp_\perp\, p_\perp\, J_n^2(z) \exp\left(\frac{-p^2}{2m\kappa T}\right) \tag{4.145}$$

which is the same as the component given in (4.128) apart from the difference in the mass terms.

We have thus satisfied ourselves that the solutions we obtained in Figs 4.2-4.8 are the relativistic counterparts of the Bernstein modes (R_{xx} component), the extraordinary mode (R_{yy} component) and the ordinary mode (R_{zz} component).

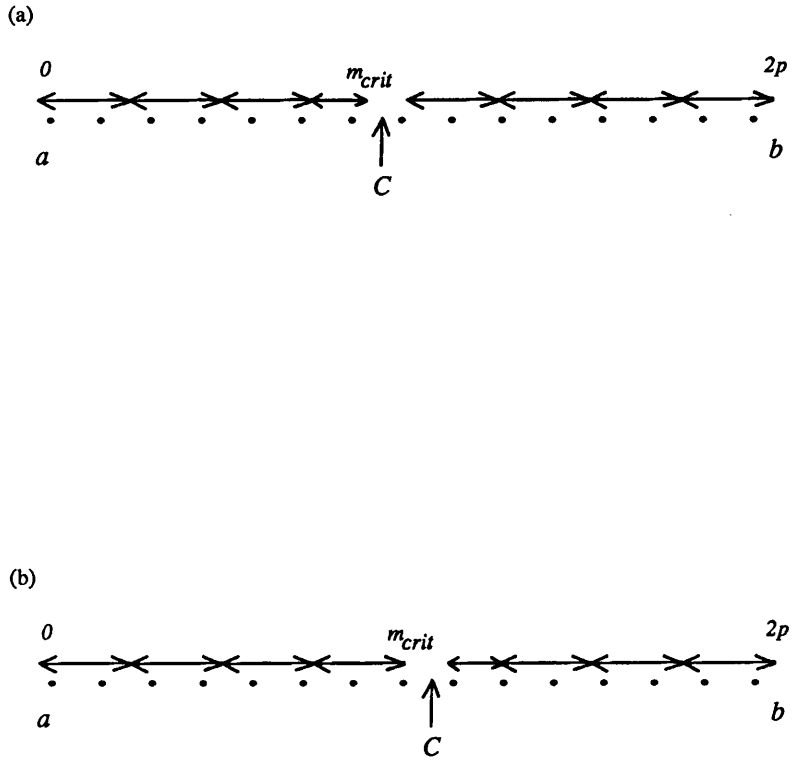

Figure 4.1: The range of the $u_\perp$-integral split into its various sub-intervals for (a) m_{crit} odd and (b) m_{crit} even.

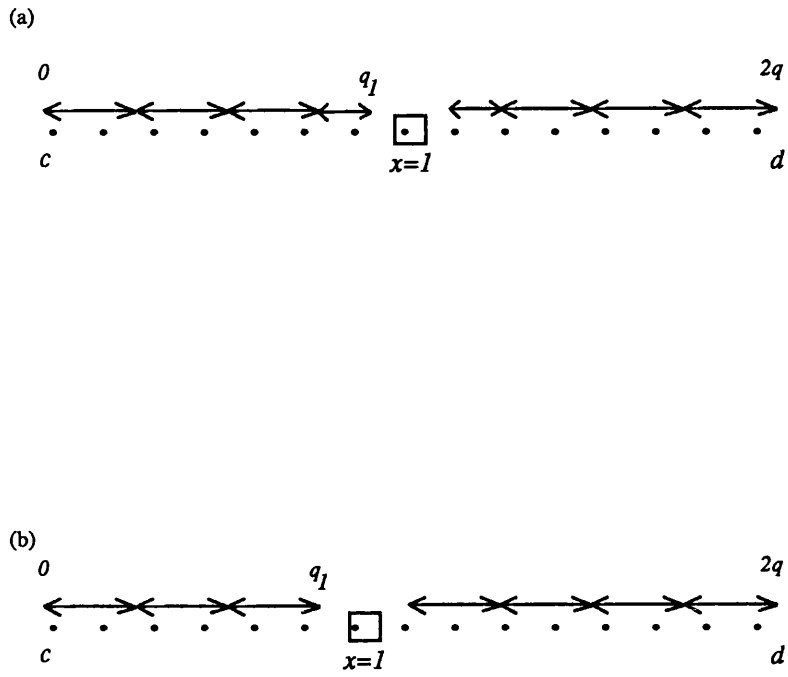

Figure 4.2: The range of the x-integral split into its various sub-intervals for (a) q_1 odd and (b) q_1 even.

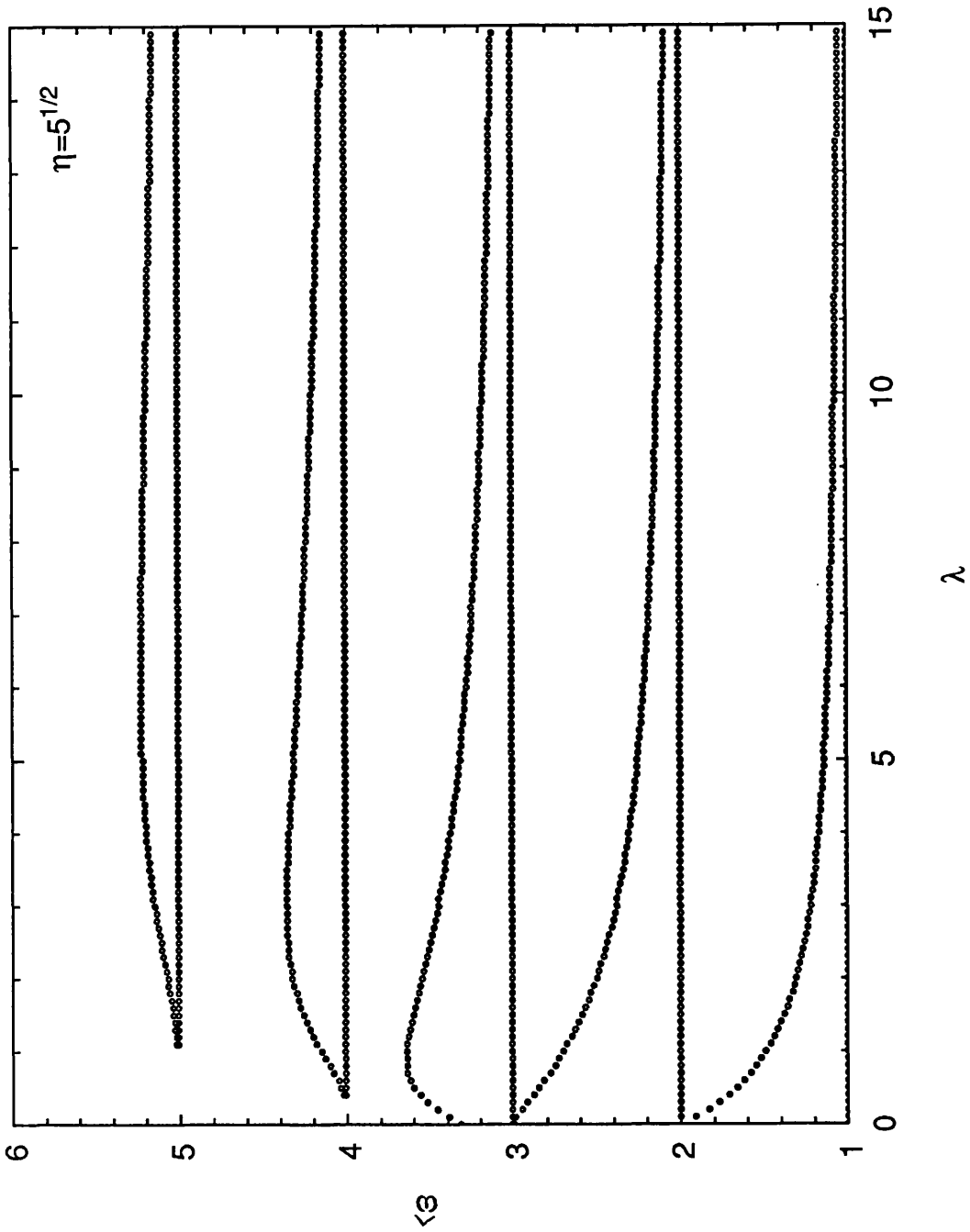

Figure 4.3: The Bernstein modes for a non-relativistic electron-positron plasma with $\eta = 5^{1/2}$.

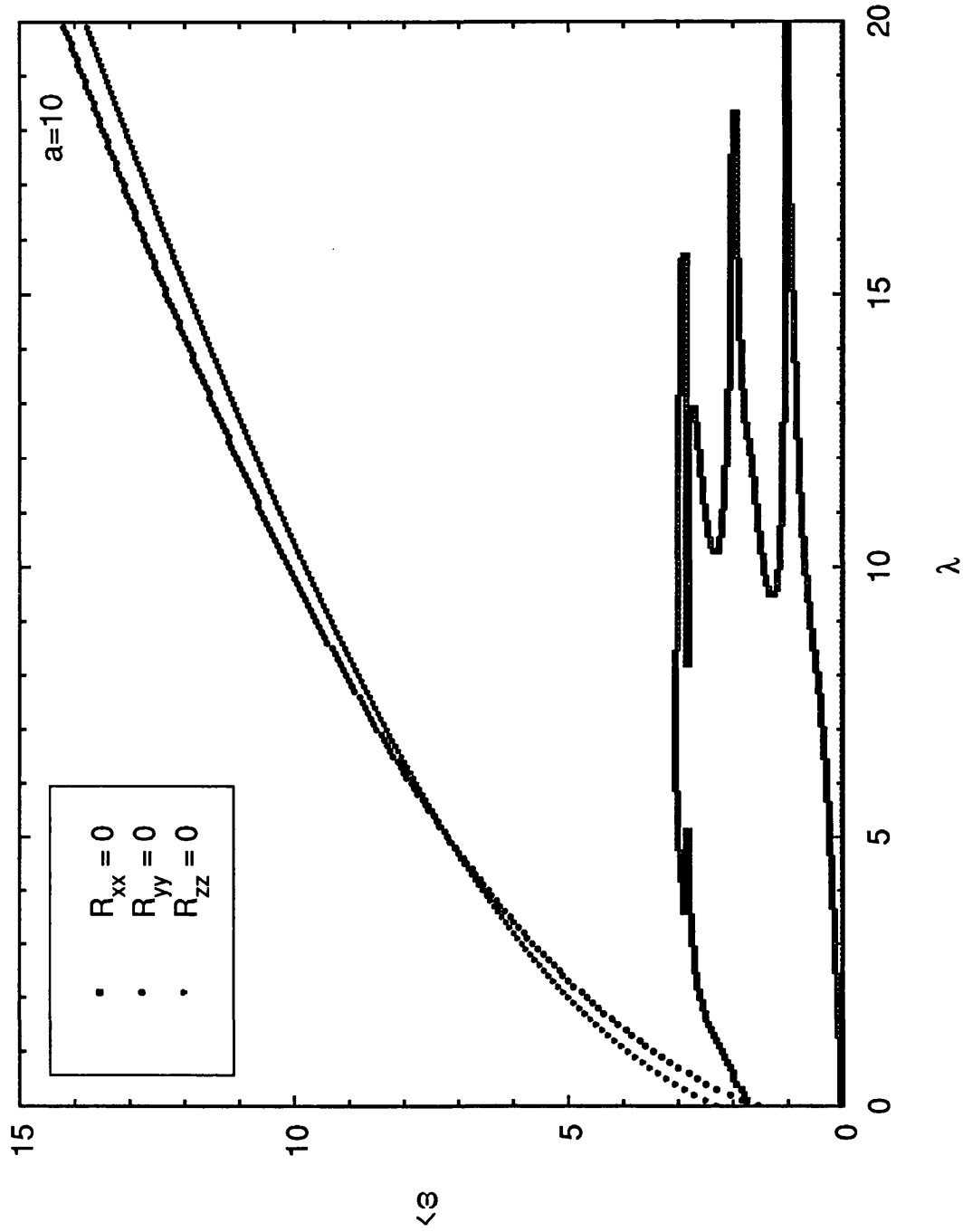

Figure 4.4: The relativistic dispersion curves for $a = 10$.

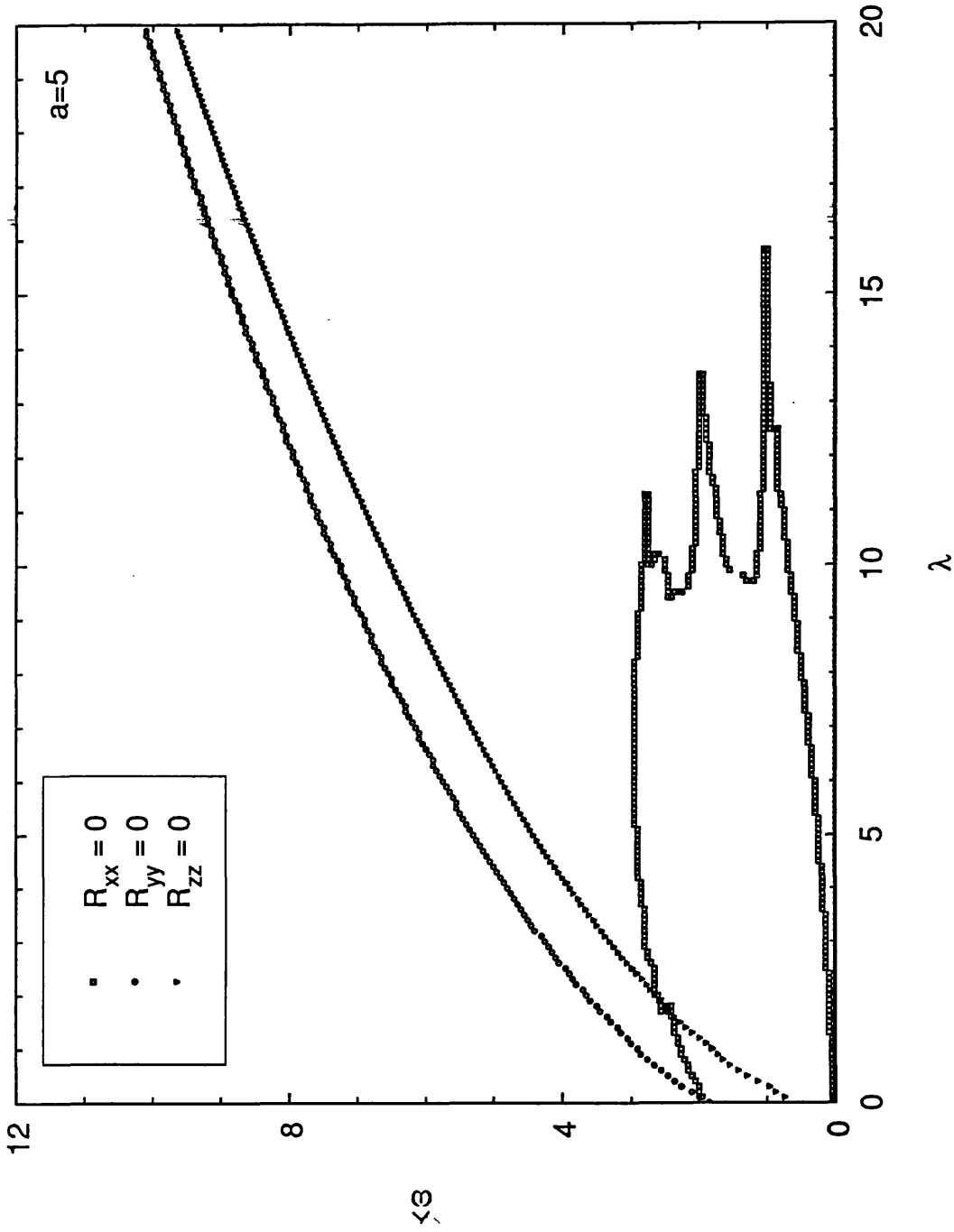

Figure 4.5: The relativistic dispersion curves for $a = 5$.

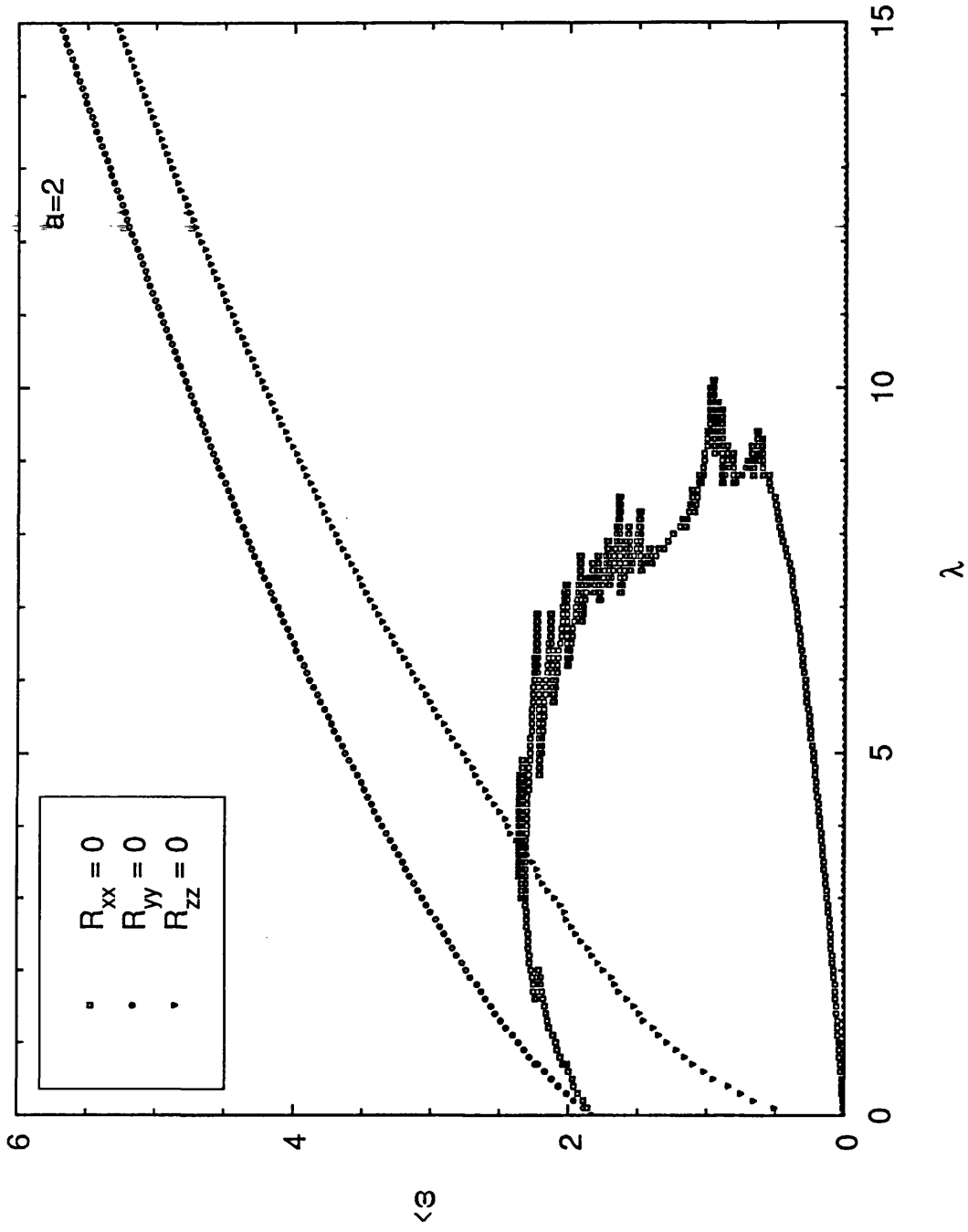

Figure 4.6: The relativistic dispersion curves for $a = 2$.

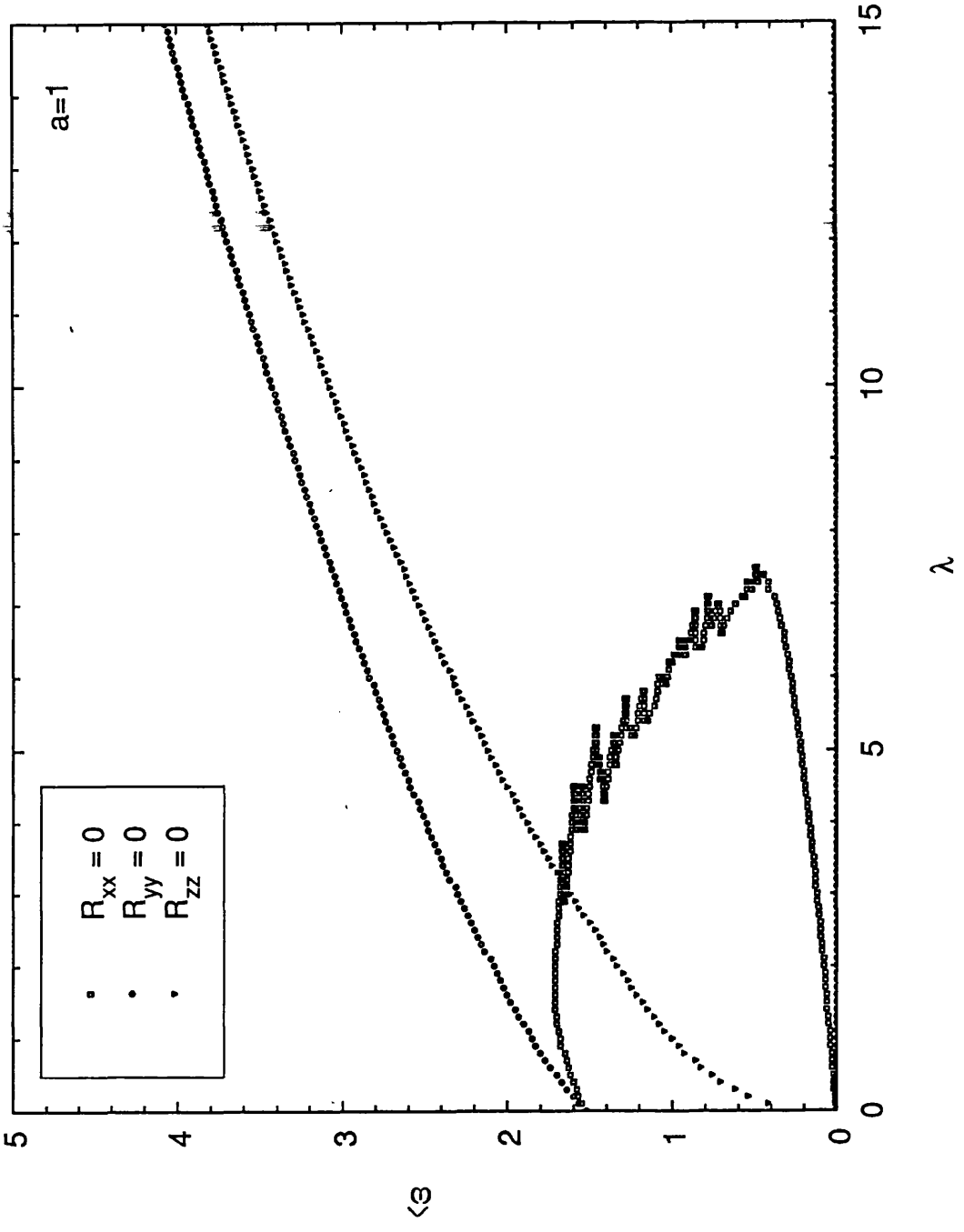

Figure 4.7: The relativistic dispersion curves for $a = 1$.

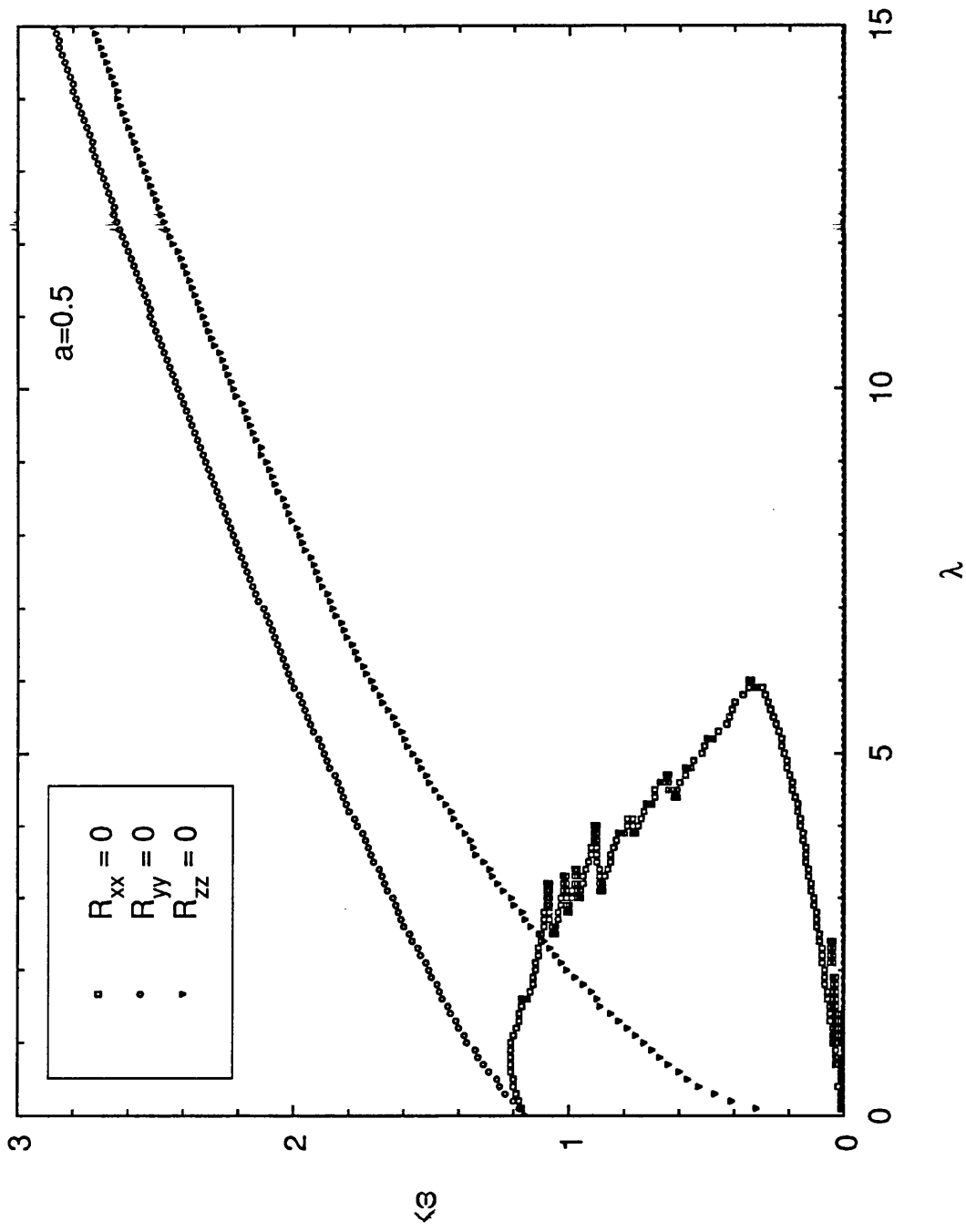

Figure 4.8: The relativistic dispersion curves for $a = 0.5$.

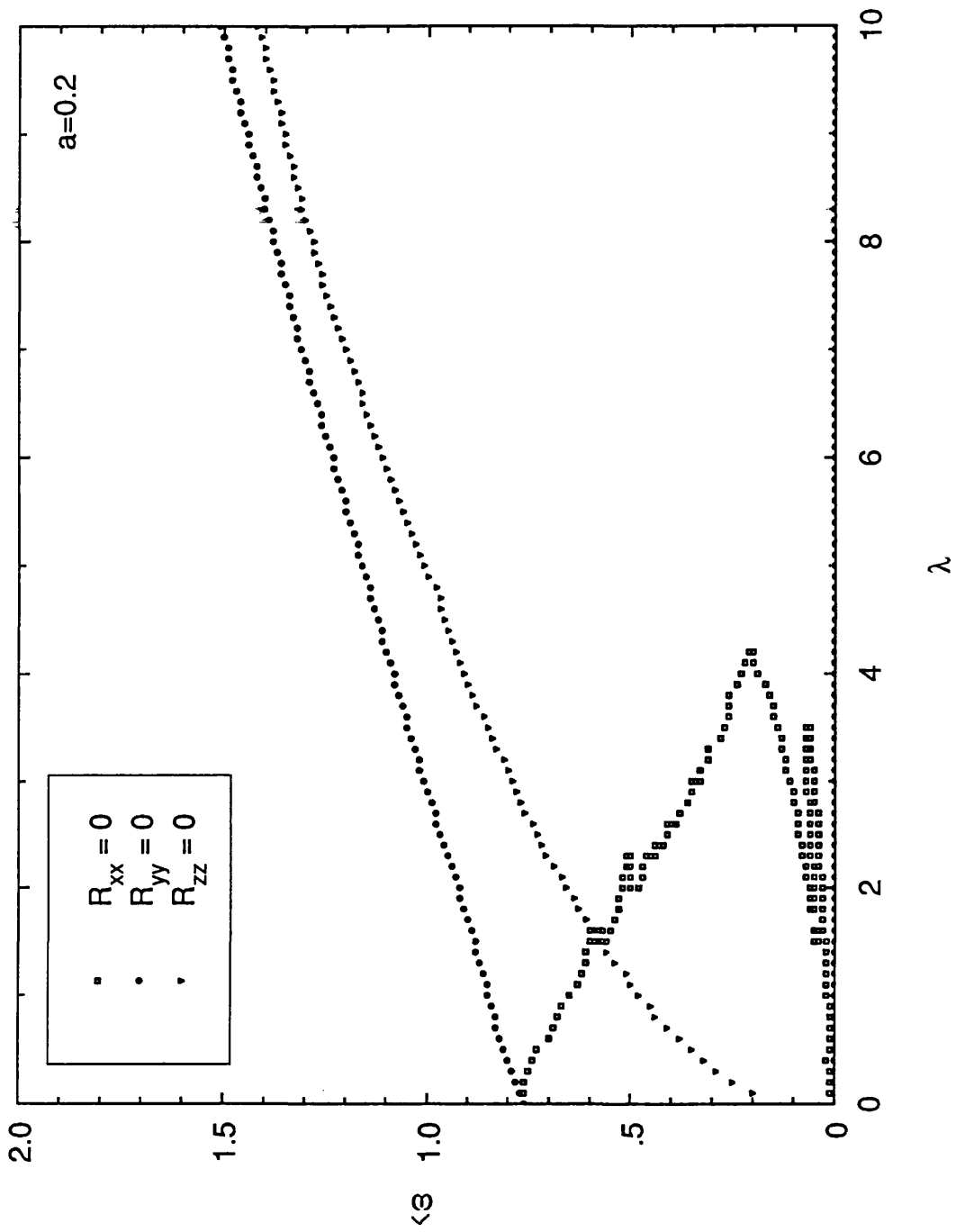

Figure 4.9: The relativistic dispersion curves for $a = 0.2$.

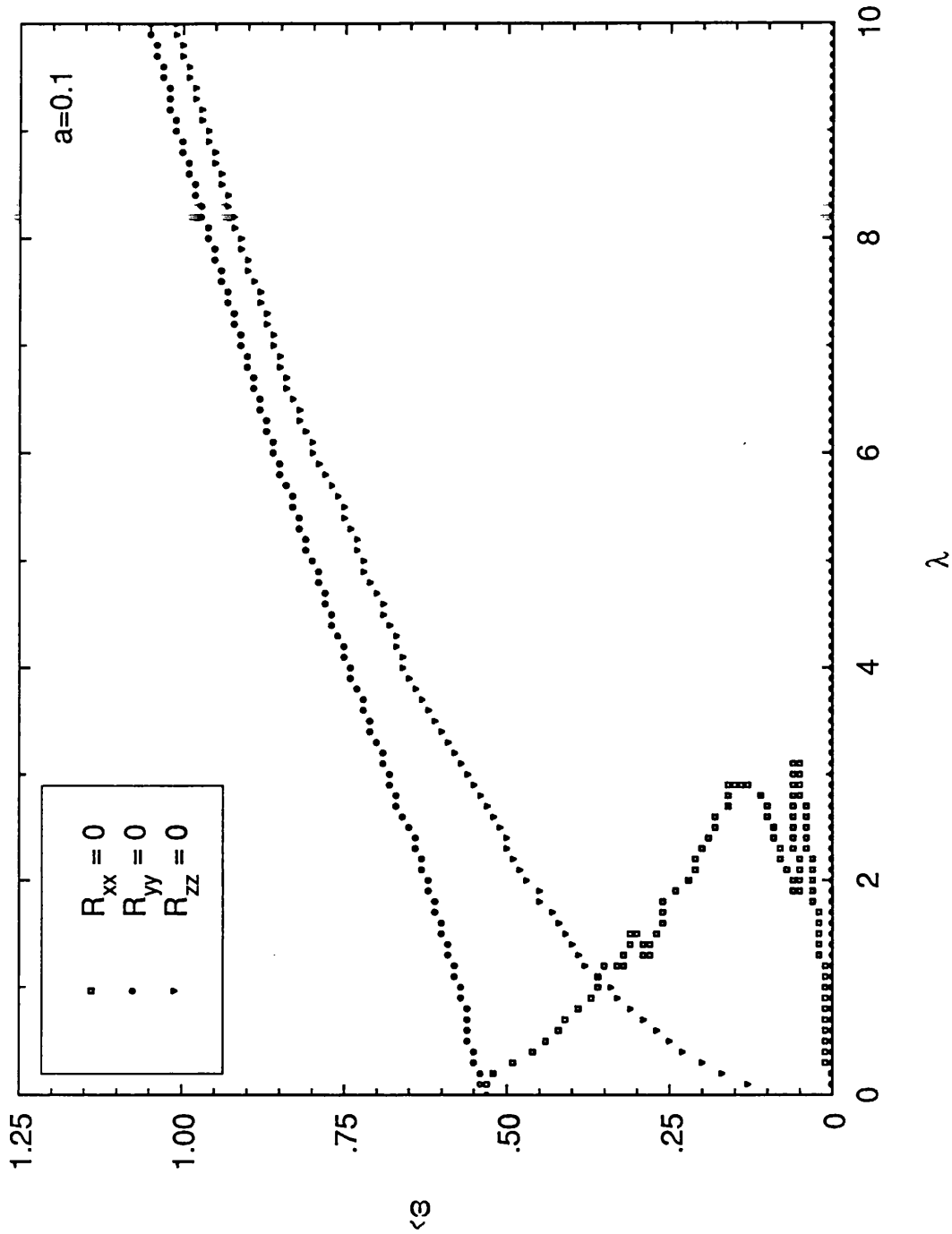

Figure 4.10: The relativistic dispersion curves for $a = 0.1$.

Chapter 5

Conclusions and Future Work

> Facts are chiels that winna ding, an' downa be disputed
> *Rabbie Burns*

In this thesis we set out to investigate wave propagation in relativistic electron-positron plasmas. Using a collisionless kinetic theory, we have studied two different plasma systems. In chapter three we looked at the case of cold streaming plasmas, in particular the specific cases of counterstreaming electron-electron and electron-positron beams. For wave propagation parallel to the equilibrium magnetic field, we found the dispersion relations for both the longitudinal and transverse wave modes. The longitudinal mode is subject to the two-stream instability and this instability is very similar in a relativistic plasma to its counterpart in a non-relativistic plasma. The only effect of relativity is to change the range of frequencies over which the wave mode is unstable. Our results show that in a relativistic plasma, replacing one of the electron streams by a positron stream does not change the physics of the system in any way as we get exactly the same dispersion relation in each case. The two-stream instability, therefore, occurs in the electron-positron plasma for the same frequency range as in the electron-ion plasma.

Turning our attention to the transverse mode, we found that the dispersion relations for the electron-ion and electron-positron plasmas differed only slightly from each other. We did find a marked difference in their behaviour though. The two-stream electron plasma is stable for all the frequencies studied. The streaming

electron-positron plasma, on the other hand, is unstable for $u\,\hat{k} < 1$ for certain values of the parameter η, which represents the ratio of the plasma frequency to the cyclotron frequency. For a given $u\,\hat{k}$ value, the instability occurs for a certain range of η values and as $u\,\hat{k} \rightarrow 1$, the range of the instability increases to include all η values. There is a change in behaviour of the system at $u\,\hat{k} = 1$, however. For $u\hat{k}$ equal to or greater than this value, the plasma is stable for all values of η. So we have shown that, under certain conditions, the electron-positron plasma seems to be fundamentally less stable than its equivalent electron-ion counterpart.

In chapter four, we went on to investigate wave propagation in relativistic, thermal electron-positron plasmas. We assumed that both species had a relativistic Maxwellian distribution in equilibrium and that the equilibrium temperatures of the electrons and positrons were the same. For wave propagation perpendicular to the equilibrium magnetic field, the dielectric tensor $\underline{\underline{\mathbf{R}}}$ reduces to form three separate wave modes which we have shown reduce to the more usual Bernstein modes (R_{xx} component), the extraordinary mode (R_{yy}) and the ordinary mode (R_{zz}) in the non-relativistic limit. We discovered that for $\kappa T > m\,c^2$, there is no sign of the infinite series of Bernstein modes along the cyclotron harmonics found in the non-relativistic plasma. However, if we let our plasma tend towards the weakly relativistic limit, eg $\kappa T = 0.1\,m\,c^2$, then the solution to the dispersion relation $R_{xx} = 0$ does start to show some features at the harmonics of the cyclotron frequency which we believe to be the start of the formation of the more usual non-relativistic solutions. Looking to the solutions of the other two dispersion relations, we find that their form does not change significantly for the different energy regimes we studied. We did note, however, that if the curves were plotted on an $\hat{\omega}$-$\hat{k}_\perp$ graph rather than an $\hat{\omega}$-λ graph (where $\lambda = a\,\hat{k}_\perp^2$), then the gradients of both the R_{yy} and R_{zz} solutions tend to unity as $\hat{k}_\perp$ becomes large. This corresponds to a wave $\omega \approx c\,k$, which means that both these solutions become electromagnetic waves in the limit of small wavelengths.

Our investigations into relativistic Maxwellian plasmas were concerned with values of a in the range $0.1 \leq a \leq 10$. Even at the low-energy end of this range, $a = 10$ still represents a problem where the relativistic effects are very important to the physics of the situation. At the moment our work is being extended into the

weakly-relativistic regime. Here, a standard relativistic treatment of the plasma is used but once the dielectric tensor (or dispersion relations) have been found, a large value of a ($a \gg 1$) is assumed. The resulting expressions then describe the plasma in the weakly-relativistic limit.

Our work can be extended in several other ways. In our analysis we have excluded reactions that can create or destroy particles. Under certain conditions these types of reactions must have a significant effect on the equilibrium state of the electron-positron plasma. As outlined in chapter one, there has been a considerable amount of work carried out on the subject of equilibria in electron-positron plasmas in astrophysical situations. In general, though, this body of work does not actually study the *plasma properties* of these plasmas; to describe the plasmas fully these two bodies of work have to be reconciled.

Another related omission in our work is the neglect of radiation in the plasma. Electron-positron pairs are produced from gamma rays of energy $0.511 MeV$ or higher. The presence of large numbers of these energetic gamma rays will affect the physical behaviour of the plasma and their presence could surely be as important as either of the particle species. Radiation must therefore be included in the description of the plasma to give a more accurate model for the plasma as a whole.

In some areas our work was simplified considerably to make the analysis more accessible. We have restricted our attention to a linear analysis throughout. This method works well for small amplitude perturbations and waves but on some occasions, if unstable modes are under investigation for example, the waves are growing in amplitude and a linear analysis would no longer be adequate. The complex field of nonlinear kinetic theory would then have to be used in its place. In the course of this thesis, we have also only looked at uniform magnetic fields in the equilibrium state. For many important applications, pulsars and tokamaks for example, this assumption is clearly not valid and a more complex form has to be chosen for $\mathbf{B}_0$. Assigning *any* spatial or temporal dependence to $\mathbf{B}_0$, though, would significantly increase the difficulty of the analysis and the form of the magnetic field would have to be chosen very carefully to ensure that any sort of headway could be made on the problem.

There has been surprisingly little work done in the field of electron-positron plasmas, or equal-mass plasmas in general. In previous studies (described in chapter one), wave propagation in cold equal-mass plasmas and transport theory in non-relativistic electron-positron plasmas have been investigated. Here we have extended this work to study wave propagation in relativistic electron-positron plasmas. Introducing relativistic effects into the plasma model can make the analysis far more complicated, even for a standard linear treatment of the problem. If this work is to be extended to include collisional or nonlinear effects, or even a non-uniform equilibrium magnetic field, then the analysis will become even more intractable and computers will be increasingly relied upon to provide numerical solutions to the problems. The work carried out on equal-mass plasmas so far suggests that the unique characteristics of this type of plasma make it an interesting and intriguing subject of study and it provides us with a valuable viewpoint on plasma behaviour which is distinct from that gained from studying electron-ion plasmas.

Appendix A

Bessel Function Identities

The particular form of the integrands in the expression for $\underline{\underline{\sigma}} \cdot \mathbf{E}$ (2.77) can most easily be solved by utilising well-known Bessel function identities. To help explain the procedure we used, we will now set out the relevant identities using the notation of Montgomery & Tidman [24].

We make use of the following two identities:

$$e^{i z \sin\phi} = \sum_n e^{i n,\phi} J_n(z) \tag{A.1}$$

$$e^{-i z \sin(\phi-\alpha)} = \sum_n e^{-i n,(\phi-\alpha)} J_n(z). \tag{A.2}$$

Taking the derivative of these two expressions with respect to the variable z, we get

$$i \sin\phi\, e^{i z \sin\phi} = \sum_n e^{i n,\phi} J_n'(z) \tag{A.3}$$

$$-i \sin(\phi-\alpha)\, e^{-i z \sin(\phi-\alpha)} = \sum_n e^{-i n,(\phi-\alpha)} J_n'(z). \tag{A.4}$$

Now consider the following integral, which is present in one of the components of(2.77):

$$\int_0^{2\pi} d\phi\, e^{-i z[\sin(\phi-\alpha)-\sin\phi]} \sin\phi \sin(\phi-\alpha) \tag{A.5}$$

$$= \int_0^{2\pi} d\phi \sin(\phi-\alpha)\, e^{-i z \sin(\phi-\alpha)} \sin\phi\, e^{i z \sin\phi} \tag{A.6}$$

$$= 2\pi \sum_n e^{i n \alpha} \left[J_n'(z)\right]^2, \tag{A.7}$$

making use of the above identities.

If we also take the derivative of (A.1) with respect to ϕ to give

$$i\,z\,\cos\phi\,e^{i\,z\,\sin\phi} = i\,n\,e^{i\,n\,\phi}\,J_n\,(z), \tag{A.8}$$

we can then represent all the integrals present in the components of $\underline{\underline{\sigma}}\cdot\mathbf{E}$ as a sum of Bessel functions using a similar procedure to that used on the example above. The full list of these expressions is

$$\int_0^{2\,\pi} d\phi\,e^{-i\,z\,[\sin(\phi-\alpha)-\sin\phi]}\,\sin\phi\,\sin(\phi-\alpha) = 2\,\pi\sum_n e^{i\,n\,\alpha}\,\left[J_n'\,(z)\right]^2 \tag{A.9}$$

$$\int_0^{2\,\pi} d\phi\,e^{-i\,z\,[\sin(\phi-\alpha)-\sin\phi]}\,\sin\phi\,\cos(\phi-\alpha) = 2\,\pi\sum_n -\frac{i\,n}{z}\,e^{i\,n\,\alpha}\,J_n\,(z)\,J_n'\,(z) \tag{A.10}$$

$$\int_0^{2\,\pi} d\phi\,e^{-i\,z\,[\sin(\phi-\alpha)-\sin\phi]}\,\cos\phi\,\sin(\phi-\alpha) = 2\,\pi\sum_n \frac{i\,n}{z}\,e^{i\,n\,\alpha}\,J_n\,(z)\,J_n'\,(z) \tag{A.11}$$

$$\int_0^{2\,\pi} d\phi\,e^{-i\,z\,[\sin(\phi-\alpha)-\sin\phi]}\,\cos\phi\,\cos(\phi-\alpha) = 2\,\pi\sum_n \frac{n^2}{z^2}\,e^{i\,n\,\alpha}\,J_n^2\,(z) \tag{A.12}$$

$$\int_0^{2\,\pi} d\phi\,e^{-i\,z\,[\sin(\phi-\alpha)-\sin\phi]} = 2\,\pi\sum_n e^{i\,n\,\alpha}\,J_n^2\,(z) \tag{A.13}$$

$$\int_0^{2\,\pi} d\phi\,e^{-i\,z\,[\sin(\phi-\alpha)-\sin\phi]}\,\sin\phi = 2\,\pi\sum_n -i\,e^{i\,n\,\alpha}\,J_n\,(z)\,J_n'\,(z) \tag{A.14}$$

$$\int_0^{2\,\pi} d\phi\,e^{-i\,z\,[\sin(\phi-\alpha)-\sin\phi]}\,\cos\phi = 2\,\pi\sum_n \frac{n}{z}\,e^{i\,n\,\alpha}\,J_n^2\,(z) \tag{A.15}$$

$$\int_0^{2\,\pi} d\phi\,e^{-i\,z\,[\sin(\phi-\alpha)-\sin\phi]}\,\sin(\phi-\alpha) = 2\,\pi\sum_n ie^{i\,n\,\alpha}\,J_n\,(z)\,J_n'\,(z) \tag{A.16}$$

$$\int_0^{2\,\pi} d\phi\,e^{-i\,z\,[\sin(\phi-\alpha)-\sin\phi]}\,\cos(\phi-\alpha) = 2\,\pi\sum_n \frac{n}{z}\,e^{i\,n\,\alpha}\,J_n^2\,(z) \tag{A.17}$$

Appendix B

Contour Integration

The residue theorem states that if $f(z)$ (where z is complex) is analytic on and inside a closed contour C, as shown in part (a) of Fig B.1, except for a finite number of isolated singularities at $z = a_1, a_2, \ldots, a_n$, which are all located inside C, then

$$\oint_C f(z)\,dz = 2\pi i \sum_{k=1}^{n} Res\,(f(a_k)). \tag{B.1}$$

We can make use of this theorem to evaluate some types of infinite integrals. The background to the analysis which follows was obtained from Riley [29] and Butkov [34]. If we can specify the three following conditions:

(i) $f(z)$ is analytic in the upper half-plane, $\Im(z) \geq 0$ except for a finite number of singularities, none of which lie on the real axis

(ii) on the semicircle C_R, of radius R, $\{R\times$ maximum value of $|f(z)|$ on $C_R\}$ tends to 0 as $R \to \infty$

(iii) $\int_{-\infty}^{0} f(x)\,dx$ and $\int_{0}^{\infty} f(x)\,dx$ both exist

then

$$\int_{-\infty}^{\infty} f(x)\,dx = 2\pi i \sum \text{residues at the poles with } \Im(z) \geq 0. \tag{B.2}$$

This analysis can be extended to include functions which have a *simple pole* on the real axis, as shown in part (b) of Fig B.1. We avoid this pole by indenting the contour in the form of a semi-circle of radius r into the upper half-plane which has the effect of removing the pole from the interior of the contour. If the pole is at the

point $z = a$ then the full contour integration can then be written as

$$\oint_C f(z)\,dz = \int_{-R}^{a-r} f(x)\,dx + \int_{C_r} f(z)\,dz + \int_{a+r}^{R} f(x)\,dx + \int_{C_R} f(z)\,dz. \quad \text{(B.3)}$$

As $r \to 0$ the two integrals along the real axis can be combined to give a definition for the *principal value* of the integral:

$$P\int_{-R}^{R} f(x)\,dx \equiv \lim_{r\to 0}\left\{\int_{-R}^{a-r} f(x)\,dx + \int_{a+r}^{R} f(x)\,dx\right\}. \quad \text{(B.4)}$$

If we assume condition (ii) above is still valid, then the calculation is similar to the one above but with the additional contribution from the semi-circle C_r, which is equal to $-i\,\pi\,Res(f(a))$ (The negative sign arises since C_r is transversed in a clockwise, or negative, sense).

So, in the limit $r \to 0$ and $R \to \infty$, the integral can thus be written as

$$\oint_C f(z)\,dz = P\int_{-\infty}^{\infty} f(x)\,dx - i\,\pi \sum \text{residues at the simple poles lying on the real axis} \quad \text{(B.5)}$$

or, if we make use of the Residue Theorem (B.1), as

$$P\int_{-\infty}^{\infty} f(x)\,dx = 2\,\pi\,i \sum \text{residues at poles in upper half} - \text{plane} + \pi\,i \sum \text{residues of the simple poles lying on the real axis.} \quad \text{(B.6)}$$

B.1 Landau's Contour

In section 2.6.2, we introduced the Laplace transform

$$\mathbf{E}(\mathbf{k}, s) = \int_0^{\infty} dt\, e^{-s\,t}\, \mathbf{E}_k(\mathbf{k}, t). \quad \text{(B.7)}$$

The inverse transform is defined to be

$$\mathbf{E}_k(\mathbf{k}, t) = \frac{1}{2\,\pi\,i}\int_C ds\, e^{s\,t}\, \mathbf{E}(\mathbf{k}, s), \quad \text{(B.8)}$$

where C represents the straight line $s = \sigma - i\,\infty$ to $s = \sigma + i\,\infty$ and σ is chosen so that C lies to the right of all the singularities of $\mathbf{E}(\mathbf{k}, s)$. We have used the electric

field in the definitions above because Landau's original analysis was carried out on the electric field for the case of electrostatic oscillations of an unmagnetised electron plasma.

The details of Landau's treatment are rather involved and we will include just a brief outline here. Fuller descriptions of the analysis are given in most good plasma texts such as Stix [35] or Laing [36].

Using a Fourier-Laplace transform of the Vlasov equation in combination with Poisson's equation, $\nabla^2 \mathbf{E} = \nabla \rho/\epsilon_0$ where ρ is the total charge density, an expression is obtained for $\mathbf{E}(\mathbf{k}, s)$. An inverse Fourier-Laplace transform can then be applied to this result to give an expression for $\mathbf{E}(\mathbf{x}, t)$. Here we shall concentrate only on the inverse Laplace transform.

As already stated above, the inverse Laplace transform is carried out along a contour C. Landau, however, proposed to carry out the transform along a second contour, C_2, which is displaced to the left but which goes round all the poles that it meets (all the poles occur in the left hand half-plane) as shown in Fig B.2. (The contour made up of C_2 and the infinite semi-circle encircling the left hand half-plane is often referred to as the Bromwich contour.) These two line integrals will be equivalent as long as there are no singularities of $\mathbf{E}(\mathbf{k}, s)$ in the region between them. The analytic continuation of $\mathbf{E}(\mathbf{k}, s)$ has to be found in the region of the contour C_2. This task is made easier if $\mathbf{E}(\mathbf{k}, s)$ can be shown to be the ratio of two entire functions. If C_2 is chosen to have a large negative real part then, as t gets large, the $e^{\sigma t}$ term in the inverse transform B.8 can be made arbitrarily small, which means that the only contribution to the integral must come from the singularities and this is equal to the sum of their residues. If the poles have real parts denoted by s_m, then each of these contributions will contain a term $e^{s_m t}$ where s_m is negative. So as t gets large, only the pole which is furthest to the right, that is the pole with the smallest negative real part, will be significant.

If the numerator of $\mathbf{E}(\mathbf{k}, s)$ can be shown to be an entire function, then the poles can only come from the denominator. Setting this denominator equal to zero gives

the Landau dispersion relation and we find that s has the following complex form:

$$s = -\omega_r - i\omega_i. \tag{B.9}$$

The imaginary part contributes a term of the form $e^{-i\omega_i}$ which is an oscillatory term. The real part, however, leads to a damping term $e^{-\omega_r}$. This damping is now widely known as Landau damping.

In our analysis in chapter 4, we defined the Laplace transform variable to be of the form

$$s = -i\omega, \tag{B.10}$$

which means that the exponential term in the inverse Laplace transform has the form $e^{-i\omega}$. If we now define $\omega = \omega_r + i\omega_i$, then we have

$$e^{-i\omega} = e^{-i\omega_r}\, e^{\omega_i}. \tag{B.11}$$

In this case, we can see that it is the occurence of an imaginary part in ω which leads to instability ($\omega_i > 0$) or damping ($\omega_i < 0$).

(a)

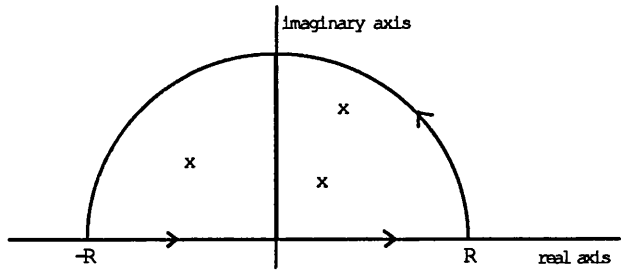

(b)

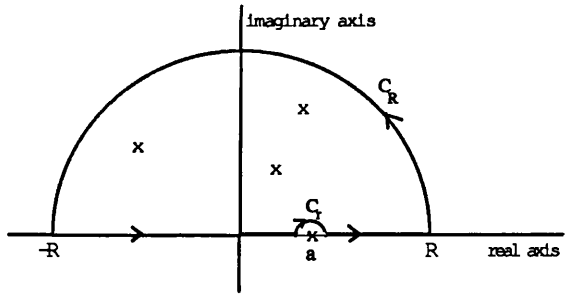

Figure B.1: (a) represents a closed contour C over which the function f is integrated and (b) represents a similar curve which has a simple pole lying on the real axis.

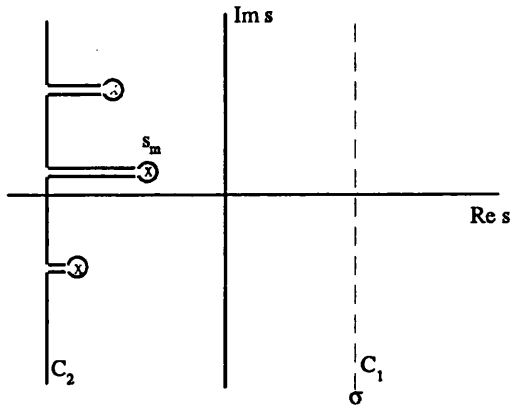

Figure B.2: The contours C_1 and C_2, where C_2 represents the Landau contour.

Appendix C

Simpson's Rule

Numerical integration techniques, as described in Davis & Rabinowitz [37], usually try to evaluate an integral expression by estimating the area under the curve of the integrand. Consider the following integral:

$$I = \int_a^b f(x)\,dx. \tag{C.1}$$

Simpson's rule works by drawing a parabola which goes through the end-points of the interval and approximating the value of the integral to the area under this parabola, that is

$$\int_a^b f(x)\,dx \approx \frac{b-a}{6}\left[f(a) + 4\,f(\frac{a+b}{2}) + f(b)\right]. \tag{C.2}$$

This rule will be exact for polynomials of degree three or less but only an approximation for higher-order polynomials.

For most functions, approximating them by a single parabola over the entire interval $[a, b]$ would be woefully inadequate. It is therefore more common to extend the Simpson rule into its compound form. This involves dividing the interval into smaller sections and applying Simpson's rule to pairs of these sections separately. Let us divide the interval $a \leq x \leq b$ into $2\,n$ equal sub-intervals. Then each sub-interval would have a length $h = (b-a)/2\,n$. Define the end-points of these sub-intervals to be

$$a = x_0 < x_1 < \ldots < x_{2n-1} < x_{2n} = b \tag{C.3}$$

so that these points are equally spaced, with a separation h.

If we consider the point x_i (where i is odd), then we assume we can represent the function $f(x)$ by

$$f(x_i + y) = f_i + a\,y + b\,y^2, \tag{C.4}$$

where we have set $f_i = f(x_i)$. We can then obtain the following two expressions:

$$f_{i+1} = f(x_i + h) = f_i + a\,h + b\,h^2 \tag{C.5}$$

$$f_{i-1} = f(x_i - h) = f_i - a\,h + b\,h^2. \tag{C.6}$$

Thus,

$$b\,h^2 = \frac{1}{2}\,(f_{i+1} + f_{i-1} - 2\,f_i)\,. \tag{C.7}$$

The area under the curve between x_{i-1} and x_{i+1} is then estimated to be

$$I_i = \int_{-h}^{h} \left(f_i + a\,y + b\,y^2\right)\,dy = 2\,h\,f_i + \frac{2\,b}{3}\,h^3. \tag{C.8}$$

Substituting for $b\,h^2$ from (C.7) above then gives

$$I_i = \frac{1}{3}\,h\,(4\,f_i + f_{i+1} + f_{i-1})\,. \tag{C.9}$$

If we then repeat this procedure for every point x_i in the interval, we can then represent the integral as follows:

$$\int_{x_0}^{x_{2\,n}} f(x)\,dx = \frac{h}{3}\left[f_0 + 4\sum_{modd} f_m + 2\sum_{meven} f_m + f_{2\,n}\right] + E_n, \tag{C.10}$$

where E_n is an indication of the error involved in the estimate of the integral and is given by

$$E_n = -\frac{n\,h^5}{90}\,f^4(\xi)\,, \quad a < \xi < b. \tag{C.11}$$

For most (well-behaved) functions, the compound Simpson rule expressed as

$$\int_{x_0}^{x_{2\,n}} f(x) \approx \frac{h}{3}\left[f_0 + 4\sum_{modd} f_m + 2\sum_{meven} f_m + f_{2\,n}\right] \tag{C.12}$$

is a more than adequate approximation to the integral.

Appendix D

Integration Code

This appendix contains a listing of the FORTRAN code that was developed to find the solutions to the dispersion relations for a relativistic Maxwellian plasma.

```
C     USE SIMPSON'S RULE TO EVALUATE INTEGRALS
c     ****************************************
C     ..Local Scalars..
      DOUBLE PRECISION eta, K2, Intalpha, Int,
     * omega, lambda, det0, det1, q, test, h, sumz
      INTEGER nout, nmax, count, zero
C     ..Define array to hold components of R..
      DOUBLE PRECISION R(4)
C     ..Scalars in Common..
      DOUBLE PRECISION a, kperp, psi, B, C, Intpll,
      Jn, dJn
      INTEGER i, n
C     ..Intrinsic Functions..
      INTRINSIC dsqrt
C     ..Function to define the tensor component..
      DOUBLE PRECISION Rij
      EXTERNAL Rij
C     ..Formula for Modified Bessel Function..
      DOUBLE PRECISION BESSK
      EXTERNAL BESSK
c     ..Common Blocks..
      common /values/ a
      common /values2/ kperp
      common /values3/ psi
      common /values4/ Intpll
      common /values5/ B, C
      common /values6/ i, n, Jn, dJn
C
c     ..Executable Statements..
c     ..nout = 6 writes to screen, nout = 7 writes to file..
      data nout /6/
c     open (nout, file='test4')
c     ..Define parameters..
      a = 0.5d0
      eta = dsqrt(5.0d0)
      nmax = 4
      write (nout,99996)
      write (nout,99997)
      write (nout,99998) a, eta, nmax
      h = 0.1d0
c     ..Use this to define first value of det0..
      zero = 0
c     ..Loop over lambda values..
      do 14 lambda = 0.0d0, 15.0d0, h
      kperp = dsqrt(a*lambda)
c     ..Keep track of the number of solutions..
      count = 0
      do 15 omega = 0.1d-02, 15.0d0, 0.01d0
c           ..Evaluate each component..
            do 30 i = 4, 4
                  Int = 0.0d0
c                 ..Sum over n..
                  do 20 n = 0, nmax
                        Intalpha = 0.0d0
                        psi = n/omega
                        B = a*n/omega
                        if (psi.gt.1.0d0) then
c                             ..Need to split up integral..
                              C = dsqrt(B**2 - a**2)
                        else
                              C = 0.0d0
                        endif
c                       ..Integrate..
                        call ALPHAINT(Intalpha)
                        if (n.eq.0) Intalpha = Intalpha/2.0d0
                        if (i.eq.4) then
                              Int = Int - Intalpha
c                             ..This sum over n is negative for Rzz..
                        else
                              Int = Int + Intalpha
                        endif
                        if (i.eq.4) then
                              sumz = 0.0d0
                              call Intz(n,sumz)
                              Int = Int + sumz
                        endif
c                       ..Int holds the value for the sum of the integrals..
   20                continue
                     K2 = BESSK(2,a)
                     R(i) = Rij(i,omega,eta,kperp,K2,Int)
   30          continue
               det1 = R(4)
c              write (6,99992) omega, det1
               if (zero.eq.0) then
                     det0 = det1
                     zero = zero + 1
               endif
               if (det0.ne.0.0d0) q = det1/det0
               test = sign(1.0d0,q)
               if (test.lt.0) then
                     count = count + 1
                     write(6,99992) lambda, omega
               endif
               det0 = det1
   15       continue
   14       continue
            stop
99992 format (d16.8, 1x, d16.8/)
99996 format ('/td xy'/)
99997 format (4x, 'a', 10x, 'eta', 10x, 'n')
99998 format (d8.2, 4x, d8.2, 6x, i3/)
      end
C
c     ..Subroutine to evaluate the integral..
      SUBROUTINE ALPHAINT(Intalpha)
c     ..Scalar arguments..
      DOUBLE PRECISION Intalpha
c     ..Local Scalars..
      DOUBLE PRECISION aa, bb, cc, d, h, l, z, zz, xx, Alpha, Cbar,
     & sumalpha, Delta, f1, f2, D1, D2, dd,
     & Phi, Phi1, Phi2, hPhi, hDelta, bm
      INTEGER m, j, w, j1, j2, j3, pj, p, q, mcrit, test,
     & btest, fail1, fail2
c     ..Scalars in common..
      DOUBLE PRECISION a, kperp, psi, Intpll, B, C, Jn, dJn
      INTEGER i, n
c     ..Function References..
```

```
      DOUBLE PRECISION Alphalim, Deltalim
      INTEGER WEIGHTS
      EXTERNAL Alphalim, Deltalim, WEIGHTS
c     ..Intrinsic Functions..
      INTRINSIC dsqrt, dexp, idint, mod
c     ..Formulae for Bessel Functions & their Derivatives..
      DOUBLE PRECISION BESSJ, derivj
      EXTERNAL BESSJ, derivj
c     ..Common Blocks..
      common /values/ a
      common /values2/ kperp
      common /values3/ psi
      common /values4/ Intpll
      common /values5/ B, C
      common /values6/ i, n, Jn, dJn
c     ..
c     ..Limits of the ppll - integration..
      cc = -0.4d01
      d = 0.4d01
c     ..Use a q - point rule for ppll - integral..
      q = 40
c     ..Define the spacing of the points..
c     ..Spacing for ppll - integration..
      l = (d-cc)/q
c     ..Spacing for pperp - integration..
      h = l
c     ..Limits of the pperp - integration..
      aa = 0.0d0
      bb = 0.4d01
c     ..Number of points for pperp - integration..
      p = idint((bb-aa-(h/5.0d0))/h)
      p = p + 1
c     ..Decide whether we need to split the integral..
      if (psi.lt.1.0d0) then
c           ..Can do the integral in one go..
            C = 0.0d0
            Cbar = dsqrt(a**2 - B**2)
            Phi1 = Cbar
            phi2 = dsqrt(bb**2 + a**2 - B**2)
            hPhi = (Phi2 - Phi1)/p
            sumalpha = 0.0d0
            do 21 j = 0, p
                  Phi = Phi1 + j*hPhi
                  w = WEIGHTS(j,p)
                  zz = Phi**2 - a**2 + B**2
                  if (j.eq.0) zz = 0.0d0
                  z = kperp*dsqrt(zz)/a
                  Jn = BESSJ(n,z)
                  dJn = 0.0d0
                  if (i.eq.3) then
                        dJn = DERIVJ(n,z)
                  endif
c                 ..Evaluate the ppll integral..
                  call PPLLINT3(j,Phi,cc,q,l)
                  sumalpha = sumalpha + w*Intpll
   21       continue
            sumalpha = sumalpha*hPhi/3.0d0
c           ..Add this contribution to integral evaluation..
            Intalpha = Intalpha + sumalpha
            go to 99
      endif
c     ..Evaluate critical value of pperp..
      xx = 0.0d0
      m = 0
   17 m = m + 1
      xx = aa + m*h
      if (C.gt.xx) go to 17
      if (C.lt.bb) then
c           ..have an mcrit-point rule for the Alpha-integration..
            mcrit = m - 1
            btest = 0
c           ..Define the point bm..
            bm = aa + mcrit*h
      else
c           mcrit = idint((b-aa)/h)+1
            mcrit = p
            btest = 1
      endif
c     ..Where do we place Trapezoidal rule ?..
      fail1 = 0
      fail2 = 0
      if (mod(mcrit,2).eq.1) then
c           ..Need Trapezoidal rule on lhs of C..
c           ..Last point of Simpson rule on lhs..
            j1 = mcrit - 1
c           ..First point of Trapezoidal rule (on lhs)..
            j2 = j1
c           ..First point of Simpson rule on rhs..
            j3 = mcrit + 1
            test = 0
            if ((p-mcrit).eq.1) fail2 = 1
      else
c           ..Need a Trapezoidal rule on rhs of C..
c           ..Last point of Simpson rule on lhs..
            j1 = mcrit
c           ..First point of Trapezoidal rule (on rhs)..
            j2 = mcrit + 1
c           ..First point of Simpson rule on rhs..
            j3 = j2 + 1
            test = 1
            if (p.eq.mcrit) fail1 = 1
            if ((p-mcrit).eq.2) fail2 = 1
      endif
c     ..Have a pj - point rule for Delta-integration..
      if ((fail1.ne.1).and.(fail2.ne.1)) then
            if (test.eq.0) then
                  pj = p - j3
            else if (test.eq.1) then
                  pj = p - j2
            endif
      endif
c     ..Define end-points of Delta-integral..
      if (C.lt.bb) then
            dd = (bm+h)**2 - C**2
            D1 = dsqrt(dd)
            dd = bb**2 - C**2
            D2 = dsqrt(dd)
            hDelta = (D2-D1)/pj
```

```
      endif
c     ..If mcrit at start of range, don't have 1st Simpson rule..
      If ((mcrit.eq.0).or.(mcrit.eq.1)) go to 98
c     ..Evaluate the Alpha-integral up to this critical value..
      sumalpha = 0.0d0
c     ..First Simpson rule from aa to aa + j1*h..
      do 5 j = 0, j1
            Alpha = C - j*h
            w = WEIGHTS(j,j1)
            zz = C**2 - Alpha**2
            if (abs(zz).lt.1d-08) zz = 0d0
            z = kperp*dsqrt(zz)/a
            Jn = BESSJ(n,z)
            dJn = 0.0d0
            if (i.eq.3) then
                  dJn = DERIVJ(n,z)
            endif
c           ..Evaluate the ppll integral..
            call PPLLINT(Alpha,cc,l,q)
            if (((j.eq.j1).and.(test.eq.1)).and.
     *      ((C-Alpha).lt.h/2.0d0)) then
                  Intpll = Alphalim(i)
            endif
            sumalpha = sumalpha + w*Intpll
    5 continue
      sumalpha = - sumalpha*h/3.0d0
c     ..Add this contribution to integral evaluation..
      Intalpha = Intalpha + sumalpha
      if (btest.eq.1) go to 99
      if (fail1.eq.1) go to 99
   98 if (test.eq.0) then
c           ..Trapezoidal part evaluated in Alpha - integral..
            sumalpha = 0.0d0
            Alpha = C - j2*h
            zz = C**2 - Alpha**2
            if (abs(zz).lt.1d-08) zz = 0d0
            z = kperp*dsqrt(zz)/a
            Jn = BESSJ(n,z)
            dJn = 0.0d0
            if (i.eq.3) then
                  dJn = DERIVJ(n,z)
            endif
            call PPLLINT(Alpha,cc,l,q)
            f1 = Intpll
            Alpha = C - (j2+1)*h
            zz = C**2 - Alpha**2
            z = kperp*dsqrt(zz)/a
            Jn = BESSJ(n,z)
            dJn = 0.0d0
            if (i.eq.3) then
                  dJn = DERIVJ(n,z)
            endif
            call PPLLINT(Alpha,cc,l,q)
            if ((C-Alpha).lt.h/2.0d0) then
                  Intpll = Alphalim(i)
            endif
            f2 = Intpll
            sumalpha = (f1 + f2)*h/2.0d0
            Intalpha = Intalpha + sumalpha
      else if (test.eq.1) then
            sumalpha = 0.0d0
c           ..Rule used to right of pole in delta integral..
            Delta = D1
            zz = Delta**2 + C**2
            z = kperp*dsqrt(zz)/a
            Jn = BESSJ(n,z)
            dJn = 0.0d0
            if (i.eq.3) then
                  dJn = DERIVJ(n,z)
            endif
            call PPLLINT2(Delta,cc,q,l)
            if ((Delta-C).lt.hDelta/2.0d0) then
                  Intpll = Deltalim(i,n)
            endif
            f1 = Intpll
            Delta = D1 + hDelta
            zz = Delta**2 + C**2
            z = kperp*dsqrt(zz)/a
            Jn = BESSJ(n,z)
            dJn = 0.0d0
            if (i.eq.3) then
                  dJn = DERIVJ(n,z)
            endif
            call PPLLINT2(Delta,cc,q,l)
            f2 = Intpll
            sumalpha = (f1 + f2)*hDelta/2.0d0
            Intalpha = Intalpha + sumalpha
      endif
      if (fail2.eq.1) go to 99
c     ..Evaluate second integral, which is in the variable Delta..
c     ..Is the Trapezoidal rule in this integral?..
      if (test.eq.0) then
c           ..Answer is no..
            D1 = D1
      else if (test.eq.1) then
c           ..Answer is yes..
            D1 = D1 + hDelta
      endif
      sumalpha = 0.0d0
      do 6 j = 0, pj
            if (j.eq.0) then
                  Delta = D1 + 1.0d-08
            else
                  Delta = D1 + j*hDelta
            endif
            w = WEIGHTS(j,pj)
            zz = Delta**2 + C**2
            z = kperp*dsqrt(zz)/a
            Jn = BESSJ(n,z)
            dJn = 0.0d0
            if (i.eq.3) then
                  dJn = DERIVJ(n,z)
            endif
c           ..Evaluate the ppll integral..
            call PPLLINT2(Delta,cc,q,l)
            if ((j.eq.0).and.(test.eq.0).and.((Delta-C)
     *      .lt.hDelta/2.0d0)) Intpll = Deltalim(i,n)
            sumalpha = sumalpha + w*Intpll
```

```
    6 continue
      sumalpha = sumalpha*hDelta/3.0d0
      Intalpha = Intalpha + sumalpha
c     ..Intalpha contains estimate for the double integral..
   99 end
C
c     ..Subroutine to evaluate the ppll - integral..
      SUBROUTINE PPLLINT(Alpha,cc,l,q)
c     ..Scalar Arguments..
      DOUBLE PRECISION Alpha, cc, l
      INTEGER q
c     ..Local Scalars..
      INTEGER q1, k1, k2, k3
c     ..Scalars in Common..
      DOUBLE PRECISION Intpll
c     ..Intrinsic Functions..
      INTRINSIC idint, mod
c     ..Common Blocks..
      common /values4/ Intpll
C
c     ..Number of steps before singularity..
      q1 = idint((1.0d0-cc-(l/5.0d0))/l)
      if (mod(q1,2).eq.1) then
c     ..Need a Trapezoidal rule on either side of pole..
c           ..Last point of Simpson rule on lhs..
            k1 = q1 - 1
c           ..First point of Trapezoidal rule on rhs..
            k2 = q1 + 2
c           ..First point of Simpson rule on rhs..
            k3 = k2 + 1
      else
c     ..Can accommodate a Simpson rule on either side of pole
c     without having to use the Trapezoidal rule..
            k1 = q1
            k3 = q1 + 2
      endif
c     ..Intpll keeps track of the ppll - integration..
      Intpll = 0.0d0
      call SIMPSON(Alpha,cc,k1,l)
      call SIMPSON(Alpha,cc+k3*l,q-k3,l)
      if (mod(q1,2).eq.1) then
            call TRAPZ(Alpha,cc,k1,l)
            call TRAPZ(Alpha,cc,k2,l)
      endif
      end
C
c     ..Subroutine to evaluate Simpson rule for 1st integrand..
      SUBROUTINE SIMPSON(Alpha,cc,q,l)
c     ..Scalar Arguments..
      DOUBLE PRECISION Alpha, cc, l
      INTEGER q
c     ..Local Scalars..
      DOUBLE PRECISION x, sumpll, F
      INTEGER k, v
c     ..Scalars in Common..
      DOUBLE PRECISION Intpll
c     ..Function References..
      INTEGER WEIGHTS
      EXTERNAL WEIGHTS
c     ..Common Blocks..
      common /values4/ Intpll
c     ..
c     ..Extended Simpson's rule from cc to cc+q*l..
      sumpll = 0.0d0
      do 10 k = 0, q
            x = cc + k*l
            v = WEIGHTS(k,q)
            call FST1(Alpha,x,F)
            sumpll = sumpll + v*F
   10 continue
      sumpll = sumpll*l/3.0d0
c     ..Add this contribution to integral evaluation..
      Intpll = Intpll + sumpll
      end
C
c     ..Subroutine to evaluate Trapezoidal rule..
      SUBROUTINE TRAPZ(Alpha,cc,k,l)
c     ..Scalar Arguments..
      DOUBLE PRECISION Alpha, cc, l
      INTEGER k
c     ..Local Scalars..
      DOUBLE PRECISION x, F, f1, f2
c     ..Scalars in Common..
      DOUBLE PRECISION Intpll
c     ..Common Blocks..
      common /values4/ Intpll
c     ..
c     ..Trapezoidal rule from cc+k*l to cc+(k+1)*l..
c     ..Evaluate Function at the end-points..
      x = cc + k*l
      call FST1(Alpha,x,F)
      f1 = F
      x = cc + (k+1)*l
      call FST1(Alpha,x,F)
      f2 = F
c     ..Include this in Approximation of the Integral..
      Intpll = Intpll + l*(f1+f2)/2.0d0
      end
C
c     ..Subroutine to evaluate Simpson rule for second integrand..
      SUBROUTINE PPLLINT2(Delta,cc,q,l)
c     ..Scalar Arguments..
      DOUBLE PRECISION Delta, cc, l
      INTEGER q
c     ..Local Scalars..
      DOUBLE PRECISION x, F
      INTEGER k, v
c     ..Scalars in Common..
      DOUBLE PRECISION Intpll
c     ..Function References..
      INTEGER WEIGHTS
      EXTERNAL WEIGHTS
c     ..Common Blocks..
      common /values4/ Intpll
c     ..
c     ..Extended Simpson's rule from cc to cc+q*l..
      Intpll = 0.0d0
      do 10 k = 0, q
```

```
            x = cc + k*l
            v = WEIGHTS(k,q)
            call FST2(Delta,x,F)
            Intpll = Intpll + v*F
   10 continue
c     ..Contribution to integral evaluation..
      Intpll = Intpll*l/3.0d0
      end
C
c     ..Subroutine to evaluate Simpson rule for 2nd integrand..
      SUBROUTINE PPLLINT3(j,Phi,cc,q,l)
c     ..Scalar Arguments..
      DOUBLE PRECISION Phi, cc, l
      INTEGER j, q
c     ..Local Scalars..
      DOUBLE PRECISION x, F
      INTEGER k, v
c     ..Scalars in Common..
      DOUBLE PRECISION Intpll
c     ..Function References..
      INTEGER WEIGHTS
      EXTERNAL WEIGHTS
c     ..Common Blocks.2.
      common /values4/ Intpll
c     ..
c     ..Extended Simpson's rule from cc to cc+q*l..
      Intpll = 0.0d0
      do 10 k = 0, q
            x = cc + k*l
            v = WEIGHTS(k,q)
            call FST3(j,Phi,x,F)
            Intpll = Intpll + v*F
   10 continue
c     ..Contribution to integral evaluation..
      Intpll = Intpll*l/3.0d0
      end
C
c     ..Function to define the limit as alpha tends to zero..
      DOUBLE PRECISION FUNCTION Alphalim(i)
c     ..Scalar Arguments..
      INTEGER i
c     ..
      Alphalim = 0.0d0
      return
      end
C
c     ..Function to define the limit as Delta tends to zero..
      DOUBLE PRECISION FUNCTION Deltalim(i,n)
c     ..Scalar Arguments..
      INTEGER i, n
c     ..Local Scalars..
      DOUBLE PRECISION z, Jn, dJn, Pi
c     ..Scalars in Common..
      DOUBLE PRECISION a, kperp, B, C
c     ..External Functions..
      DOUBLE PRECISION x01aaf
      EXTERNAL x01aaf
c     ..Intrinsic Functions..
      INTRINSIC dsqrt, dexp
c     ..Formulae for Bessel Functions & their Derivatives..
      DOUBLE PRECISION BESSJ, derivj
      EXTERNAL BESSJ, derivj
c     ..Common Blocks..
      common /values/ a
      common /values2/ kperp
      common /values5/ B, C
c     ..
      Pi = x01aaf(0.0d0)
      z = kperp*C/a
      Jn = BESSJ(n,z)
      dJn = derivj(n,z)
      if (i.eq.1) then
            Deltalim = Pi*dexp(-B)*Jn**2
      else if (i.eq.3) then
            Deltalim = Pi*dexp(-B)*C**2*dJn**2
      else if (i.eq.4) then
            Deltalim = 0.0d0
      endif
      return
      end
C
c     ..Function to evaluate the Simpson rule weighting factors..
      INTEGER FUNCTION WEIGHTS(j,p)
c     ..Scalar arguments..
      INTEGER j, p
c     ..Intrinsic functions..
      INTRINSIC mod
C
c     ..Definition of Function..
      if ((j.eq.0).or.(j.eq.p)) then
            weights = 1
      else if (mod(j,2).eq.1) then
            weights = 4
      else if (mod(j,2).eq.0) then
            weights = 2
      endif
      return
      end
C
c     ..Subroutine to evaluate integrand..
      SUBROUTINE FST1(Alpha,x,F)
c     ..Scalar arguments..
      DOUBLE PRECISION Alpha, x, F
c     ..Scalars in common..
      DOUBLE PRECISION a, psi, B, C, Jn, dJn
      INTEGER i, n
c     ..Local scalars..
      DOUBLE PRECISION gg, G
c     ..Intrinsic functions..
      INTRINSIC dexp, dsqrt
c     ..Common blocks..
      common /values/ a
      common /values3/ psi
      common /values5/ B, C
      common /values6/ i, n, Jn, dJn
C
c     ..Definition of function..
      gg = B**2 + Alpha**2*(x**2-1.0d0)
```

```
      G = dsqrt(gg)
      if (i.eq.1) then
            F = n**2*Jn**2*dexp(-G)/(x - 1.0d0)
      else if (i.eq.3) then
            F = dJn**2*(C**2 - Alpha**2)*dexp(-G)
                /(x - 1.0d0)
      else if (i.eq.4) then
            F = - Jn**2*Alpha**2*dexp(-G)/(x - 1.0d0)
      endif
      end
C
c     ..Subroutine to evaluate second integrand..
      SUBROUTINE FST2(Delta,x,F)
c     ..Scalar arguments..
      DOUBLE PRECISION Delta, x, F
c     ..Scalars in common..
      DOUBLE PRECISION a, psi, B, C, Jn, dJn
      INTEGER i, n
c     ..Local Scalars..
      DOUBLE PRECISION gg, G
c     ..Intrinsic functions..
      INTRINSIC dexp, dsqrt
c     ..Common blocks..
      common /values/ a
      common /values3/ psi
      common /values5/ B, C
      common /values6/ i, n, Jn, dJn
C
c     ..Definition of integrand..
      gg = B**2 + Delta**2*(x**2 + 1.0d0)
      G = dsqrt(gg)
      if (i.eq.1) then
            F = n**2*Jn**2*dexp(-G)/(x**2 + 1.0d0)
      else if (i.eq.3) then
            F = dJn**2*(C**2 + Delta**2)*dexp(-G)
                /(x**2 + 1.0d0)
      else if (i.eq.4) then
            F = Jn**2*Delta**2*dexp(-G)/(x**2 + 1.0d0)
      endif
      end
C
c     ..Subroutine to evaluate second integrand..
      SUBROUTINE FST3(j,Phi,x,F)
c     ..Scalar arguments..
      DOUBLE PRECISION Phi, x, F
      INTEGER j
c     ..Scalars in common..
      DOUBLE PRECISION a, psi, B, C, Jn, dJn
      INTEGER i, n
c     ..Local Scalars..
      DOUBLE PRECISION gg, G
c     ..Intrinsic functions..
      INTRINSIC dexp, dsqrt
c     ..Common blocks..
      common /values/ a
      common /values3/ psi
      common /values5/ B, C
      common /values6/ i, n, Jn, dJn
C
c     ..Definition of integrand..
      gg = B**2 + Phi**2*(x**2 + 1.0d0)
      G = dsqrt(gg)
      if (i.eq.1) then
            F = n**2*Jn**2*dexp(-G)/(x**2 + 1.0d0)
      else if (i.eq.3) then
            F = dJn**2*(Phi**2 - a**2 + B**2)*dexp(-G)
                /(x**2 + 1.0d0)
      else if (i.eq.4) then
            F = Jn**2*Phi**2*dexp(-G)/(x**2 + 1.0d0)
      endif
      end
C
c     ..Subroutine to evaluate the additional zz-integral..
      SUBROUTINE Intz(n,sumz)
c     ..Local arguments..
      DOUBLE PRECISION sumz
      INTEGER n
c     ..Local scalars..
      DOUBLE PRECISION F, u, z, y, l, Jn, K1
      INTEGER j, last, v
c     ..Scalars in common..
      DOUBLE PRECISION a, kperp
c     ..Intrinsic functions..
      INTRINSIC dsqrt
c     ..Formulae for the Bessel functions..
      DOUBLE PRECISION bessj, bessk
      EXTERNAL bessj, bessk
c     ..Define weight for Simpson rule points..
      INTEGER WEIGHTS
      EXTERNAL WEIGHTS
c     ..Common blocks..
      common /values/ a
      common /values2/ kperp
C
c     ..Carry out integration using a Simpson rule..
      l = 0.5
      last = 200
      do 33 j = 0, last
            u = 0.0d0 +j*l
c           ..Define the variables..
            z = kperp*u/a
            y = dsqrt(a**2+u**2)
            Jn = bessj(n,z)
            K1 = bessk(1,y)
c           ..Define integrand..
            F = u*Jn**2*y*K1
            v = WEIGHTS(j,last)
            sumz = sumz + v*F
   33 continue
c     ..Contribution to integral evaluation..
      sumz = sumz*l/3.0d0
      if (n.eq.0) sumz = sumz/2.0d0
      end
C
c     ..Function to define the tensor component..
      DOUBLE PRECISION FUNCTION Rij(i,omega,eta,kperp,K2,Int)
c     ..Local arguments..
      DOUBLE PRECISION omega, eta, kperp, K2, Int
```

```
      INTEGER i
c     ..Scalars in common..
      DOUBLE PRECISION a
c     ..Common blocks..
      common /values/ a
C
c     ..Define component..
      if (i.eq.1) then
            Rij = -omega**2 + 2.0d0*(a*eta**2)
                 /(kperp**2*K2)*Int
      else if (i.eq.3) then
            Rij = -omega**2 + kperp**2 + 2.0d0*eta**2
                 /(a*K2)*Int
      else if (i.eq.4) then
            Rij = -omega**2 + kperp**2 + 2.0d0*eta**2
                 /(a*K2)*Int
      endif
      return
      end
C
c     ..Function to find the bessels..
      DOUBLE PRECISION FUNCTION BESSJ(n,x)
c     ..Local arguments..
      DOUBLE PRECISION x
      INTEGER n
c     ..Local scalars..
      DOUBLE PRECISION y, j0, j1, ax, tox, sum,
     & jn, jnminus, jnplus
      INTEGER ifail, an
c     .. External functions ..
      INTRINSIC abs, dabs, idint
      DOUBLE PRECISION s17aef, s17aff
      EXTERNAL s17aef, s17aff
c     ..Local parameters..
      DOUBLE PRECISION bigno, bigni, ll, dfloat
      PARAMETER (iacc = 40, bigno = 1.0d10,
     & bigni = 1.0d-10, dfloat = 1.0d0)
      ax = dabs(x)
      ifail = 1
      y = s17aef(ax,ifail)
      j0 = y
      ifail = 1
      y = s17aff(ax,ifail)
      j1 = y
c     ..Take care of negative orders..
      an = abs(n)
      if (an.eq.0) then
            bessj = j0
      else if (an.eq.1) then
            bessj = j1
      else if (ax.lt.0.1d-08) then
            bessj = 0.0d0
      else if (ax.gt.dfloat*(an)) then
c           ..Upward recurrence okay for n ¡ x..
            tox = 2.0d0/ax
            jnminus = j0
            jn = j1
            do 20 j = 1, an-1
                  jnplus = j*tox*jn - jnminus
                  jnminus = jn
                  jn = jnplus
   20       continue
            bessj = jn
      else
c           ..Downward recurrence for n ¿ x..
            tox = 2.0d0/ax
            ll=dfloat*(iacc*an)
c           ..First point for recurrence relation..
            m = 2*((an+idint(dsqrt(ll)))/2)
c           ..Better accuracy for larger m..
            bessj = 0.0d0
            jsum = 0
            sum = 0.0d0
c           ..Initial guess for jn+1 and jn..
            jnplus = 0.0d0
            jn = 1.0d0
            do 30 j = m, 1, -1
                  jnminus = j*tox*jn - jnplus
                  jnplus = jn
                  jn = jnminus
                  if (dabs(jn).gt.bigno) then
c                       ..Renormalise to prevent overflow..
                        jn = jn*bigni
                        jnplus = jnplus*bigni
                        bessj = bessj*bigni
                        sum = sum*bigni
                  endif
c                 ..Accumulate the sum..
                  if (jsum.ne.0) sum = sum + jn
c                 ..Change 0 to 1 or vice-versa..
                  jsum = 1 - jsum
c                 ..Save the unnormalised answer..
                  if (j.eq.an) bessj = jnplus
   30       continue
c           ..Compute normalising sum of bessels..
            sum = 2.0d0*sum - jn
c           ..And use it to normalise answer..
            bessj = bessj/sum
      endif
      if ((x.lt.0.0).and.(mod(an,2).eq.1)) bessj = -bessj
      if (n.lt.0) bessj = (-1)**(an)*bessj
      return
      end
c
c     ..Function to evaluate the modified Bessel functions Kn..
      DOUBLE PRECISION FUNCTION BESSK(n,x)
c     ..Scalar arguments..
      DOUBLE PRECISION x
      INTEGER n
c     ..Local scalars..
      DOUBLE PRECISION y, K0, K1, KN, KNminus, KNplus, tox
      INTEGER ifail, j
c     ..External functions..
      DOUBLE PRECISION s18acf, s18adf
      EXTERNAL s18acf, s18adf
c     ..Executable statements..
      ifail = 1
      y = s18acf(x,ifail)
```

```
      K0 = y
      ifail = 1
      y = s18adf(x,ifail)
      K1 = y
      if (n.eq.0) then
            bessk = K0
      else if (n.eq.1) then
            bessk = K1
c     else if (x.lt.0.1d-08) then
c           bessk = 0.0d0
      else
c           ..Use upward recurrence relation..
            tox = 2.0d0/x
            KNminus = K0
            KN = K1
            do 11 j = 1, n-1
                  KNplus = KNminus + j * tox * KN
                  KNminus = KN
                  KN = KNplus
   11       continue
            bessk = KN
      endif
      return
      end
c
c     ..function to find derivative of bessels..
      double precision function derivj(n,x)
c     ..local arguments..
      double precision x
      integer n
c     ..local scalars..
      double precision djn, yy, zz
c     ..function references..
      double precision bessj
      external bessj
c     ..
c     ..executable statements..
      yy = bessj(n-1,x)
      zz = bessj(n+1,x)
      djn = (yy - zz)/2.0d0
      derivj = djn
      return
      end
```

Bibliography

[1] P.C. Johnson. *Plasma Physics An Introductory Course*, chapter 13 (ed R.O. Dendy). Cambridge University Press, 1993.

[2] G.A. Stewart and E.W. Laing. Wave propagation in equal-mass plasmas. *J. Plas. Phys.*, 47:295–319, 1992.

[3] S.Y. Abdul-Rassak and E.W. Laing. Transport coefficients for an equal-mass plasma in a uniform magnetic field. *J. Plas. Phys.*, 50:125–144, 1993.

[4] V.S. et al Imshennik. Mathematical simulation and experimental analysis of nonlinear interaction of positive and negative ion beams. *Computer Methods in Applied Mechanics and Engineering*, 9:1–23, 1976.

[5] C.M. et al Surko. *The Positron Trap - A Tool for Plasma Physics Positron Studies of Solids, Surfaces and Atoms: A Symposium to Celebrate Stephan Berko's 60th Birthday*, pages 221–233. World Scientific, 1986.

[6] C.J. MacCallum and M. Leventhal. *Positron-Electron Pairs in Astrophysics, AIP Conference Proceedings No 101*, pages 211–229 (ed. M.L. Burns, A.K. Harding and R. Ramaty). AIP, 1983.

[7] I.D. Novikov and V.P. Frolov. *Physics of Black Holes.* Kluwer Academic Publishers, 1989.

[8] G. et al Ghisellini. The role of electron-positron pairs in parsec-scale radio jets. *Mon. Not. R. astron. Soc.*, 258:776–786, 1992.

[9] U. Achatz and R. Schlickeiser. Electromagnetic stability of electron-positron beams. *Astronomy and Astrophysics*, 274:165–173, 1993.

[10] M.A. Ruderman and P.G. Sutherland. Theory of pulsars: Polar gaps, sparks and coherent microwave radiation. *Astrophys. J.*, 196:51–72, 1975.

[11] J. Arons and J.J. Barnard. Wave propagation in pulsar magnetospheres: Dispersion relations and normal modes of plasmas in superstrong magnetic fields. *Astrophys. J.*, 302:120–137, 1986.

[12] A. Ray and G. Benford. Electron-positron cascade in pulsar outer gaps. *Phys. Rev. D*, 23:2142–2150, 1981.

[13] A.F. Cheng and M.A. Ruderman. Bunching mechanism for coherent curvature radiation in pulsar magnetospheres. *Astrophys. J.*, 212:800–806, 1977.

[14] E. et al Asseo. A non-linear radio pulsar emission mechanism. *Mon. Not. R. astron. Soc.*, 247:529–548, 1990.

[15] A.P. Lightman and D.L. Band. Relativistic thermal plasmas: Radiation mechanisms. *Astrophys. J.*, 251:713–726, 1981.

[16] A.P. Lightman. *Positron-Electron Pairs in Astrophysics, AIP Conference Proceedings No 101*, pages 359–367 (ed. M.L. Burns, A.K. Harding and R. Ramaty). AIP, 1983.

[17] A.P. Lightman. Relativistic thermal plasmas: Pair processes and equilibria. *Astrophys. J.*, 253:842–858, 1982.

[18] F. Takahara and M. Kusunose. *Positron-Electron Pairs in Astrophysics, AIP Conference Proceedings No 101*, pages 400–404 (ed. M.L. Burns, A.K. Harding and R. Ramaty). AIP, 1983.

[19] K.A. Holcomb and T. Tajima. General-relativistic plasma physics in the early universe. *Phys. Rev. D*, 40:3809–3818, 1989.

[20] T. Tajima and T. Taniuti. Non-linear interaction of photons and phonons in electron-positron plasmas. *Phys. Rev. A*, 42:3587–3602, 1990.

[21] P.C. Clemmow. *Electrodynamics of Particles and Plasmas.* Addison-Wesley, 1990.

[22] N.A. Krall and A.W. Trivelpiece. *Principles of Plasma Physics.* McGraw-Hill, 1973.

[23] P. Lorrain and D.P. Corson. *Electromagnetic Fields and Waves.* Freeman, 1970.

[24] D.C. Montgomery and D.A. Tidman. *Plasma Kinetic Theory.* McGraw-Hill, 1964.

[25] R.J. Briggs. *Electron-Stream Interaction with Plasmas.* MIT, 1964.

[26] P.A. Sturrock. *Plasma Physics.* Cambridge University Press, 1994.

[27] B. Buti. Relativistic effects on plasma oscillations and two-stream instability. *Phys. Fluids*, 6:89–99, 1963.

[28] I.S. Gradshteyn and Ryzik I.M. *Table of Integrals, Series and Products.* London Academic Press, 1980.

[29] K.F. Riley. *Mathematical Methods for the Physical Sciences.* Cambridge University Press, 1974.

[30] W.H. et al Press. *Numerical Recipes in FORTRAN The Art of Scientific Computing.* Cambridge University Press, 1992.

[31] R.A. Cairns. *Plasma Physics.* Blackie, 1985.

[32] I.B. Bernstein. Waves in a plasma in a magnetic field. *Phys. Rev.*, 109:10–21, 1958.

[33] F.W. Crawford. A review of cyclotron harmonic phenomena in plasmas. *Nuclear Fusion*, 5:73–84, 1965.

[34] E. Butkov. *Mathematical Physics.* Addison-Wesley, 1968.

[35] T.H. Stix. *Waves in Plasmas.* AIP, 1992.

[36] Laing E.W. *Plasma Physics.* Sussex University Press, 1976.

[37] P.J. Davis and P. Rabinowitz. *Numerical Integration.* Blaisdell, 1967.